

APPLICATION OF SURFACE-ENHANCED RAMAN SCATTERING  
(SERS) METHOD FOR GENETIC ANALYSES

A THESIS SUBMITTED TO  
THE GRADUATE SCHOOL OF NATURAL AND APPLIED SCIENCES  
OF  
MIDDLE EAST TECHNICAL UNIVERSITY

BY

SEHER KARABIÇAK

IN PARTIAL FULFILLMENT OF THE REQUIREMENTS  
FOR  
THE DEGREE OF DOCTOR OF PHILOSOPHY  
IN  
CHEMISTRY

MARCH 2011

Approval of the Thesis;

**APPLICATION OF SURFACE-ENHANCED RAMAN SCATTERING (SERS)  
METHOD FOR GENETIC ANALYSES**

Submitted by **SEHER KARABIÇAK** in a partial fulfillment of the requirements for  
the degree of **Doctor of Philosophy in Chemistry Department, Middle East  
Technical University** by

Prof. Dr. Canan Özgen  
Dean, Graduate School of **Natural and Applied Sciences** \_\_\_\_\_

Prof. Dr. İlker Özkan  
Head of Department, **Chemistry** \_\_\_\_\_

Prof. Dr. Mürvet Volkan  
Supervisor, **Chemistry Department, METU** \_\_\_\_\_

Prof. Dr. Semra Kocabıyık  
Co-Supervisor, **Biology Department, METU** \_\_\_\_\_

**Examining Committee Members:**

Prof. Dr. O. Yavuz Ataman  
Chemistry Department, METU \_\_\_\_\_

Prof. Dr. Mürvet Volkan  
Chemistry Department, METU \_\_\_\_\_

Prof. Dr. Macit Özenbaş  
Metallurgical and Materials Engineering, METU \_\_\_\_\_

Prof. Dr. Meral Yücel  
Biology Department, METU \_\_\_\_\_

Prof. Dr. Bekir Salih  
Chemistry Department, Hacettepe University \_\_\_\_\_

**Date: 15.03.2011**

**I hereby declare that all information in this document has been obtained and presented in accordance with academic rules and ethical conduct. I also declare that, as required by these rules and conduct, I have fully cited and referenced all material and results that are not original to this work.**

Name, Last name: Seher Karabıçak

Signature

## ABSTRACT

### APPLICATION OF SURFACE-ENHANCED RAMAN SCATTERING (SERS) METHOD FOR GENETIC ANALYSES

Karabıçak, Seher

Ph.D., Department of Chemistry

Supervisor: Prof. Dr. Mürvet Volkan

Co-Supervisor: Prof. Dr. Semra Kocabıyık

March 2011, 150 pages

Raman spectroscopy offers much better spectral selectivity but its usage has been limited by its poor sensitivity. The discovery of surface-enhanced Raman scattering (SERS) effect, which results in increased sensitivities of up to  $10^8$ -fold for some compounds, has eliminated this drawback.

A new SERS active substrate was developed in this study. Silver nanoparticle-doped polyvinyl alcohol (PVA) coated SERS substrate prepared through chemical and electrochemical reduction of silver particles dispersed in the polymer matrix. Performances of the substrates were evaluated with some biologically important compounds.

The specific detection of DNA has gained significance in recent years since increasingly DNA sequences of different organisms are being assigned. Such sequence knowledge can be employed for identification of the genes of microorganisms or diseases. In this study, specific proteasome gene sequences were

detected both label free spectrophotometric detection and SERS detection. In label free spectrophotometric detection, proteasome gene probe and complementary target gene sequence were attached to the gold nanoparticles separately. Then, the target and probe oligonucleotide-modified gold solutions were mixed for hybridization and the shift in the surface plasmon absorption band of gold nanoparticles were followed.

SERS detection of specific nucleic acid sequences are mainly based on hybridization of DNA targets to complementary probe sequences, which are labelled with SERS active dyes. In this study, to show correlation between circulating proteasome levels and disease state we suggest a Raman spectroscopic technique that uses SERGen probes. This novel approach deals with specific detection of elevated or decreased levels of proteasome genes' transcription in patients as an alternative to available enzyme activity measurement methods. First, SERGen probes were prepared using SERS active labels and specific proteasome gene sequences. Then DNA targets to complementary SERGen probe sequences were hybridized and SERS active label peak was followed.

**Keywords:** Surface-Enhanced Raman Scattering (SERS), SERGen probes, DNA, Ubiquitin-proteasome system (UPS).

ÖZ

YÜZEYDE-GÜÇLENDİRİLMİŞ RAMAN SAÇILMASI (YGRS) METODUNUN  
GENETİK ANALİZLER İÇİN UYGULAMASI

Karabıçak, Seher

Doktora, Kimya Bölümü

Tez Yöneticisi: Prof. Dr. Mürvet Volkan

Ortak Tez Yöneticisi: Prof. Dr. Semra Kocabıyık

Mart 2011, 150 sayfa

Raman spektrometresi çok iyi spektral seçicilik sağlar fakat duyarlılığının düşük olması nedeni ile kullanımını çok kısıtlı kalmıştır. Yüzeyde güçlendirilmiş Raman saçılması (YGRS) etkisinin keşfedilmesi pek çok madde için duyarlılığın  $10^8$  kat artmasını sağlayarak bu olumsuzluğu gidermiştir.

Bu çalışmada yeni bir YGRS aktif substrat geliştirildi. Polivinilalkol (PVA) içerisine hapsedilmiş gümüş nano parçacıkla kaplı YGRS substrat, polimer matriks içerisindeki gümüşlerin hem kimyasal hem de elektrokimyasal olarak indirgenmesiyle hazırlandı. Bu substratların performansları biyolojik açıdan önemli birtakım bileşikler ile değerlendirildi.

Son yıllarda spesifik DNA tanımlaması büyük önem kazanmıştır; çünkü artan bir şekilde farklı organizmaların DNA dizileri saptanmaktadır. Dizin bilgisi mikroorganizma ya da hastalık genlerinin tanımlanması için kullanılabilir. Bu çalışmada, spesifik proteazom gen dizileri hem boya kullanılmadan spektrofotometrik olarak hem de YGRS ile belirlendi. Spektrofotometrik yöntemde, proteazom gen prob ve eşleniği olan hedef dizisi ayrı ayrı altın nano parçacığa tutturuldu. Daha sonra, hedef ve prob oligonükleotid ile modifiye edilmiş altın nanoparçacıkları karıştırılarak hibridizasyon yapıldı ve altın nanoparçacıkların yüzey plazmon absorpsiyon bantlarındaki kayma takip edildi.

Spesifik nükleik asit dizilerinin YGRS ile belirlenmesi hedef DNA ların eşleniği olan YGRS aktif boya ile etiketlenmiş prob dizinleri ile hibridizasyonuna dayanır. Bu çalışmada, proteazom düzeyleri ve hastalık durumu arasındaki ilişkiyi göstermek için YGRS gen problemlerinin kullanıldığı bir Raman spektroskopik yöntem öneriyoruz. Bu yeni yaklaşım, enzim aktivitesi ölçüm yöntemlerine alternatif olarak, hastalardaki artan ya da azalan proteazom gen transkripsiyon düzeylerinin tayini ile ilgilidir. İlk olarak, YGRS gen problemler, YGRS aktif boyalar ve spesifik proteazom gen dizileri kullanılarak hazırlandı. Daha sonra hedef DNA ile eşleniği olan YGRS gen prob dizinleri hibridize edilerek, SERS aktif pik takip edildi.

**Anahtar Kelimeler:** Yüzeyde-Güçlendirilmiş Raman Spektroskopisi (YGRS), Yüzeyde-Güçlendirilmiş Raman Gen Problemleri, DNA, Übikülin-proteazom sistem (UPS).

To My Family



## ACKNOWLEDGMENTS

I would like to express my sincere appreciation to my supervisor Prof. Dr. Mürvet Volkan for her great support, trust, continuous guidance, help and encouragement throughout this study. I learned from her many things, as well as science, especially to be patient.

I would like to express my sincere thanks to my co-advisor Prof. Dr. Semra Kocabıyık for her excellent help, support and endless guidance. I learned from her everything how to study with DNA.

I would like to thank to Prof. Dr. O. Yavuz Ataman and Prof. Dr. Macit Özenbaş for their perception as PhD committee members.

I would like to thank Prof. Dr. Ahmet M. Önal for his help and advice in experiments related with electrochemistry.

I would like to thank Prof. Dr. Necati Özkan for his help and valuable comments about zeta potential results. Also, I would like to thank Dr. İbrahim Çam for the zeta potential measurements.

I would like to thank to Prof. Dr. Ayhan S. Demir who let us to use autoclave and his helpful students, especially Farah, Betül, İlke and Peruze for using it.

I would like to Prof. Dr. Mehmet Parlak for his help of the gold film surface preparation.

I also wish to express my deepful thanks to my friend Murat Kaya for his warm friendship, continuous help and encouragement.

I also give my thanks to my friends Bahar Köksel, Rukiye Sancı, Tacettin Öztürk, Dilek Ünal, Gülfem Aygar, Tuğba Nur Aslan and Seda Kibar for their help and friendship.

Thanks are also extended to all the members of analytical chemistry research group.

I also wish to thank to my office coordinator Sema Atlıhan and my chief Dilara Özşuca for permission to make PhD experiments. And also I would like to thank my colleague Hasan Akçay and Nilgün Kadem Oğuz for their friendship and moral support.

Finally, my special appreciation and gratitude is devoted to my father, my mother and my sister for their trust, patience and moral support, which makes everything possible. I am very lucky to have such a good family. I also wish to thank my little nephew Ege for his help drawing the figures. I love him so much.

## TABLE OF CONTENT

ABSTRACT .....	iv
ÖZ .....	vi
ACKNOWLEDGMENTS .....	ix
TABLE OF CONTENT .....	xi
LIST OF TABLES .....	xv
LIST OF FIGURES .....	xvi
LIST OF ABBREVIATIONS .....	xxvi
CHAPTERS .....	1
INTRODUCTION .....	1
1.1 Raman Scattering .....	2
1.2 Surface-Enhanced Raman Scattering (SERS).....	5
1.2.1 Mechanisms of SERS.....	6
1.2.1.1 Electromagnetic Enhancement.....	6
1.2.1.1.1 Surface Plasmons.....	8
1.2.1.2 Chemical Enhancement.....	9
1.2.2 SERS Substrates.....	10
1.3 SERS Applications.....	12
1.3.1 Biological Applications.....	13
1.3.1.1 DNA Detection.....	13
1.3.1.2 Proteasomes.....	17
2 EXPERIMENTAL .....	23
2.1 Chemicals and DNA Oligonucleotides .....	23
2.2 Instrumentation .....	24
2.2.1 Raman Spectrometer .....	24
2.2.2 UV-VIS Spectrometer.....	24
2.2.3 Potentiostat–Galvanostat.....	25
2.2.4 Field Emission Scanning Electron Microscopy (FE-SEM).....	25

2.2.5	ZETA Potential and Mobility Measurement System.....	25
2.2.6	Spin Coater.....	25
2.2.7	Centrifuge.....	25
2.3	Procedures.....	26
2.3.1	Preparation of SERS-active Substrate.....	26
2.3.1.1	Silver Nanoparticle-Doped Polyvinyl Alcohol Coated (PVA-Ag) Substrate.....	26
2.3.2	Detection of Archaea and Human Proteosome Gene Sequences.....	27
2.3.2.1	Gold Colloid Preparation.....	27
2.3.2.2	Gold Substrate Preparation.....	28
2.3.2.3	Silver Colloid Preparation.....	28
2.3.2.4	Label Free Spectrophotometric Detection of Archaea Proteosome Gene Sequence.....	29
2.3.2.4.1	5'-Oligonucleotide-Modified Gold Probe and Target Nanoparticles Preparation.....	29
2.3.2.4.2	Hybridization of Oligonucleotide-Linked Gold Nanoparticle Probes with Targets in the Solution System.....	30
2.3.2.5	SERS Detection of Archaea and Human Proteosome Gene Sequences.....	31
2.3.2.5.1	Preparation of SERGen Probes.....	31
2.3.2.5.1.1	Covalent Labeling of Oligonucleotide Primers with BCB... 31	
2.3.2.5.1.2	Noncovalent Labeling of Oligonucleotide Primers with BCB.....	33
2.3.2.5.1.3	SERS Measurements of SERGen Probes.....	34
2.3.2.5.1.3.1	Zeta Potential Measurements of Unlabelled Oligonucleotides and Electrostatically labeled Oligonucleotides.....	35
2.3.2.5.2	Immobilization of SERGen Probes onto the Gold Surface Under the Hybridization Conditions.....	35
2.3.2.5.3	Immobilization of SERGen Probes onto the Gold Surface After the Decanethiol Treatment Under the Hybridization Conditions.....	35
2.3.2.5.4	Hybridization Experiments.....	36
2.3.2.5.5	Hybridization of Target and Probe Containing Single Base and Double Base Mismatches.....	38
2.3.2.5.6	Quantitative Study.....	39
3	RESULTS AND DISCUSSION.....	40

3.1	Silver Nanoparticle-Doped Polyvinyl Alcohol Coated (PVA-Ag) Substrate .....	40
3.1.1	SERS Measurement of Benzoic Acid on PVA-Ag Substrate Prepared Through Both Chemical and Electrochemical Reduction.....	43
3.1.2	SERS Measurement of p-Amino Benzoic Acid (PABA) on PVA-Ag Substrate.....	46
3.1.3	SERS Measurement of Pyridine on PVA-Ag Substrate .....	48
3.1.4	SERS Measurement of Dopamine on PVA-Ag Substrate .....	49
3.2	Detection of Archaea and Human Proteasome Gene Sequences.....	50
3.2.1	Characterization of Gold Colloid.....	50
3.2.2	Characterization of Gold Substrate .....	51
3.2.3	Characterization of Silver Colloid .....	52
3.2.4	Label Free Spectrophotometric Detection of Archaea Proteasome Gene Sequence .....	53
3.2.4.1	Characterization of 5'-Oligonucleotide-Modified Gold Probe and Target Nanoparticles.....	53
3.2.4.2	Hybridization of Oligonucleotide-Modified Gold Nanoparticle Probes with Targets in the Solution System.....	56
3.2.5	SERS Detection of Archaea and Human Proteasome Gene Sequences.....	59
3.2.5.1	Characterization of SERGen Probes.....	59
3.2.5.1.1	Covalent Labeling of Oligonucleotide Primers with BCB.....	62
3.2.5.1.2	Noncovalent Labeling of Oligonucleotide Primers with BCB..	64
3.2.5.1.2.1	Zeta Potential Measurements of Unlabelled Oligonucleotides and Electrostatically labeled Oligonucleotides.....	71
3.2.5.2	Characterization of SERGen Probes onto the Gold surface.....	73
3.2.5.3	Characterization of SERGen Probes Attached onto Gold surface under the Hybridization Conditions After the Decanethiol Treatment.....	74
3.2.5.4	Hybridization Experiments.....	78
3.2.5.4.1	Hybridization Experiment using The Probe Based on Archaea Proteasome Gene Sequence without Spacer.....	79
3.2.5.4.2	Hybridization Experiments using Archaea Proteasome Gene Based Probe in the Presence of the Spacer decanethiol.....	81

3.2.5.4.3	Hybridization Experiments using Archaea Proteasome Gene Sequence Based Probe with Other Spacers (11-Mercapto-1- undecanol and 10 T oligo).....	86
3.2.5.4.4	Hybridization Experiments using Human Proteasome Gene Sequence with Based Target DNA with 10 T oligo.....	92
3.2.5.4.5	Hybridization Experiments using Target and Probe Oligos Based on Human Proteasome Gene Sequence.....	95
3.2.5.4.6	Effect of Pre-Heating of Oligo Probe on Hybridization.....	101
3.2.5.5	The Effect of Different Temperatures on Hybridization.....	102
3.2.5.6	Hybridization of with Probes Containing Single and Double Base Mismatches.....	106
3.2.5.6.1	SERS Results of Hybridization with of Archaea Proteasome Gene Specific Single-Mismatch Probe.....	107
3.2.5.6.2	SERS Results of Hybridization with of Human Proteasome Gene Specific Single-Mismatch Probe.....	111
3.2.5.6.3	SERS Results of Hybridization with of Human Proteasome Gene Specific Double-Mismatch Probe.....	115
3.2.5.7	Quantitative Study Results for Human Proteasome Gene Sequence.....	119
4	CONCLUSIONS.....	121
	APPENDIX.....	133
	VITA.....	150

## LIST OF TABLES

### TABLES

<b>Table 1</b> Oligonucleotide Sequences .....	29
<b>Table 2</b> Oligonucleotide Sequences and Spacers .....	36
<b>Table 3</b> Oligonucleotide Sequences and Spacer.....	38
<b>Table 4</b> Oligonucleotide Sequences and Spacer.....	39
<b>Table 5</b> Average peak intensities observed at 580 nm for all temperatures.....	110
<b>Table 6</b> Average peak intensities observed at 580 nm for all temperatures.....	114
<b>Table 7</b> Average peak intensities observed at 580 nm for all temperatures.....	118
<b>Table 8</b> SERS intensity at 580 nm for different concentrations of SERGen probes. .....	119

## LIST OF FIGURES

### FIGURES

<b>Figure 1</b> (A) Schematic diagram of various interactions of a molecule with monochromatic light. (B) Molecular energy diagram of Rayleigh and Raman Scattering (Stokes and anti-Stokes). .....	3
<b>Figure 2</b> a) Fluorescence spectrum b) Raman spectrum.....	4
<b>Figure 3</b> A schematic representation of surface-enhanced Raman scattering. Molecules (blue dots) are attached to metal nanoparticles (orange balls). .....	5
<b>Figure 4</b> Illustration of the conduction electrons into collective oscillation by electromagnetic radiation.....	7
<b>Figure 5</b> Schematic illustration of the interaction of polarized light and gold nanospheres .....	8
<b>Figure 6</b> Variation of surface plasmon absorption of spherical gold nanoparticles depending on particle size. The UV-vis absorption spectra of colloidal gold solutions with diameters between 9 and 99 nm display that the absorption maximum red-shifts with increasing particle size.....	9
<b>Figure 7</b> Energy level diagram for a molecule adsorbed on a metal surface. The occupied and unoccupied molecular orbitals are expanded into resonances by their interaction with the metal states; orbital occupancy is designated by the Fermi energy. Possible charge transfer excitations are displayed. ....	10
<b>Figure 8</b> A schematic representation of the structure of a nucleotide.....	14
<b>Figure 9</b> Purine and pyrimidine bases structures. ....	14
<b>Figure 10</b> Schematic drawings of DNA double helix. ....	15
<b>Figure 11</b> A schematic diagram of the proteasome 20S core particle viewed from one side.....	17
<b>Figure 12</b> Schematic diagram of the 20S core protease (CP) and the 26S proteasome. ....	18
<b>Figure 13</b> The ubiquitin-proteasome pathway. ....	20



<b>Figure 14</b> Schematic representation of silver nanoparticle-doped polyvinyl alcohol coated (PVA-Ag) substrate. ....	26
<b>Figure 15</b> Schematic representation of electrochemical reduction of PVA-Ag substrate.....	27
<b>Figure 16</b> Schematic representation of 5'-oligonucleotide-modified gold probe and target nanoparticles preparation. ....	30
<b>Figure 17</b> Hybridization of oligonucleotide-modified gold nanoparticle probes with targets in the solution system. ....	31
<b>Figure 18</b> Chemical reaction for BCB labeling of DNA covalently. ....	32
<b>Figure 19</b> Schematic representation of covalent labeling of DNA with BCB. ....	33
<b>Figure 20</b> Schematic representation of noncovalent labeling of DNA with BCB. ...	33
<b>Figure 21</b> The picture of SERS microscope.....	34
<b>Figure 22</b> The variation of the relative SERS intensities of BA ( $10^{-2}$ M) acquired with PVA-Ag SERS-active substrates having various $\text{AgNO}_3$ to PVA weight ratios (Rw) A) 0.08; B) 0.16; C) 0.24; D) 0.36.....	42
<b>Figure 23</b> SERS spectrum of $10^{-3}$ M aqueous solution of BA acquired with PVA-Ag substrate ( $\text{AgNO}_3$ to PVA ratio was 0.24, chemical reduction).....	44
<b>Figure 24</b> SERS spectrum of $10^{-3}$ M aqueous solution of BA acquired with PVA-Ag substrate ( $\text{AgNO}_3$ to PVA ratio was 0.24, electrochemical reduction).....	45
<b>Figure 25</b> SERS spectra of different concentrations of BA solution acquired with PVA-Ag substrate (electrochemical reduction). ....	45
<b>Figure 26</b> Schematic representation of PVA-Ag coated ITO after the electrochemical reduction.....	46
<b>Figure 27</b> SERS spectrum of $10^{-4}$ M aqueous solution of PABA acquired with PVA-Ag substrate.....	47
<b>Figure 28</b> SERS spectrum of $10^{-1}$ M aqueous solution of pyridine acquired with PVA-Ag substrate. ....	49
<b>Figure 29</b> Structure of catechol. ....	49
<b>Figure 30</b> SERS spectrum of $10^{-4}$ M aqueous solution of dopamine acquired with PVA-Ag substrate. ....	50
<b>Figure 31</b> Absorbance spectrum for gold colloid has a $\lambda_{\text{max}}$ at 520 nm. ....	51
<b>Figure 32</b> FE-SEM image of gold nanoparticles deposited on silanized glass slide. 52	

<b>Figure 33</b> Absorption spectrum for silver colloid has a $\lambda_{\max}$ at 440 nm.....	53
<b>Figure 34</b> A) Schematic representation of preparation of 5'-oligonucleotide-modified gold probe and target nanoparticles. UV-vis spectra for B) gold nanoparticles C) gold nanoparticles functionalized with target and probe oligonucleotides. ....	55
<b>Figure 35</b> A) Schematic representation of hybridization. UV-vis spectra for B) gold nanoparticles functionalized with target and probe oligonucleotides, C) gold nanoparticles modified with target oligonucleotide after treatment with gold nanoparticles modified complementary probe DNA at 60 °C for 5 min. ....	57
<b>Figure 36</b> UV-vis spectra for thermal dissociation of polynucleotide aggregate at A) 75 °C, B) 100 °C .....	58
<b>Figure 37</b> SERS spectrum of $10^{-6}$ M BCB solution on silver colloid in dry condition. ....	60
<b>Figure 38</b> SERS spectrum of $10^{-6}$ M CFV solution on silver colloid in dry condition. ....	60
<b>Figure 39</b> SERS spectrum of $10^{-6}$ M CV solution on silver colloid in dry condition. ....	61
<b>Figure 40</b> SERS spectrum of $10^{-5}$ M FITC solution on silver colloid in dry condition. ....	62
<b>Figure 41</b> SERS spectrum of BCB labeled DNA probe solution acquired by using silver colloid in wet condition. Labeling was done covalently.....	63
<b>Figure 42</b> SERS spectrum of BCB labeled DNA probe solution acquired by using silver colloid in dry condition. Labeling was done covalently. ....	63
<b>Figure 43</b> The chemical structure of BCB .....	64
<b>Figure 44</b> SERS spectrum of BCB labeled DNA probe solution acquired by using silver colloid in wet condition. Labeling was done electrostatically in 18 h. at 50 °C. ....	65
<b>Figure 45</b> SERS spectrum of BCB labeled DNA probe solution acquired by using silver colloid in dry condition. Labeling was done electrostatically in 18 h. at 50 °C. ....	65
<b>Figure 46</b> SERS spectrum of BCB labeled DNA probe solution acquired by using silver colloid in dry condition. Labeling was done electrostatically at room temperature for 4 hours. ....	66

<b>Figure 47</b> SERS spectra of BCB labeled DNA probe solution acquired by using silver colloid in dry condition from five different points. Labeling was done electrostatically at room temperature for 4 hours and then labeled DNA incubated at hybridization conditions at room temperature. ....	67
<b>Figure 48</b> SERS spectra of BCB labeled DNA probe solution acquired by using silver colloid in dry condition from five different points. Labeling was done electrostatically at room temperature for 4 hours and then labeled DNA incubated at hybridization conditions at 65 °C. ....	68
<b>Figure 49</b> SERS spectrum of CFV labeled DNA probe solution acquired by using silver colloid in dry condition. Labeling was done electrostatically at room temperature for 4 h. ....	69
<b>Figure 50</b> SERS spectrum of CV labeled DNA probe solution acquired by using silver colloid in dry condition. Labeling was done electrostatically at room temperature for 4 h. ....	69
<b>Figure 51</b> The chemical structure of FITC.....	70
<b>Figure 52</b> SERS spectrum of FITC labeled DNA probe solution acquired by using silver colloid in dry condition. Labeling was done electrostatically at room temperature for 4 h. ....	70
<b>Figure 53</b> Zeta potential distribution of DNA.....	71
<b>Figure 54</b> Schematic representation of immobilization of SERGen probes onto the gold surface under the hybridization conditions: 300 µL 10 mM phosphate buffer solution (pH 7) and 150 µL 2 M NaCl solution for 90 min. at 25 °C. ....	73
<b>Figure 55</b> SERS spectra of only SERGen probe on the gold surface with silver colloid in dry condition. SERGen probe was designed based on the archaea proteasome gene sequence. The numbers are representing the locations at which the SERS measurements were done. The colors are coding the signal obtained from that particular point on the gold surface.....	74
<b>Figure 56</b> Schematic representation of expected binding of SERGen probes onto the gold surface after the decanethiol treatment under the hybridization conditions. ....	75
<b>Figure 57</b> SERS spectra of SERGen probe on the gold surface with silver colloid in dry condition when decanethiol is used as spacer. SERGen probe was designed using archaea proteasome gene sequence. The numbers are representing the locations at	

which the SERS measurements were done. The colors are coding the signal obtained from that particular point on the gold surface. .... 76

**Figure 58** Schematic representation of SERGen probes onto the gold surface after the decanethiol treatment under the hybridization conditions washing with hybridization buffer in a shaker. SERGen probe was designed using archaea proteasome gene sequence. .... 77

**Figure 59** SERS spectra of SERGen probe on the gold surface with silver colloid in dry condition: A) after 10 min. shake wash, B) after 20 min. shake wash, C) after 30 min. shake wash. .... 78

**Figure 60** Schematic representation of hybridization without spacer possible bindings are shown. .... 80

**Figure 61** SERS spectra of BCB-labeled DNA after the hybridization onto the gold surface with silver colloid in dry condition in the absence of a spacer. SERGen probe was designed using archaea proteasome gene sequence. The numbers are representing the locations at which the SERS measurements were done. The colors are coding the signal obtained from that particular point on the gold surface. .... 81

**Figure 62** Schematic representation of hybridization with various spacers (i.e., decanethiol, mercaptoundecanol and 10T oligo). .... 82

**Figure 63** SERS spectra of BCB-labeled DNA after hybridization onto the gold surface with silver colloid in dry condition when decanethiol was used as spacer. SERGen probe was designed using archaea proteasome gene sequence. The numbers are representing the locations at which the SERS measurements were done. The colors are coding the signal obtained from that particular point on the gold surface.. .... 83

**Figure 64** Schematic representation of thiol modified short and long oligonucleotides behavior onto the gold surface. .... 84

**Figure 65** Schematic representation of control hybridization experiment by use of a non-complementary SERGen probe with spacer. Spacer used in this experiment was decanethiol. .... 85

**Figure 66** SERS spectra of BCB-labeled DNA after the hybridization control experiment onto the gold surface with silver colloid in dry condition. SERGen probe

was designed using archaea proteasome gene sequence having same sequence as the target DNA. Spacer used in this experiment was decanethiol. .... 86

**Figure 67** SERS spectra of BCB-labeled DNA after hybridization onto the gold surface with silver colloid in dry condition. SERGen probe was designed using archaea proteasome gene sequence. The numbers are representing the locations at which the SERS measurements were done. The colors are coding the signal obtained from that particular point on the gold surface. Spacer used in this experiment was 11-mercapto-1-undecanol..... 87

**Figure 68** SERS spectra of BCB-labeled DNA after the hybridization control experiment onto the gold surface with silver colloid in dry condition. SERGen probe was designed using archaea proteasome gene sequence having same sequence as the target DNA. Spacer used in this experiment was 11-mercapto-1-undecanol. .... 88

**Figure 69** SERS spectra of BCB-labeled DNA after hybridization onto the gold surface with silver colloid in dry condition. SERGen probe was designed using archaea proteasome gene sequence. The numbers are representing the locations at which the SERS measurements were done. The colors are coding the signal obtained from that particular point on the gold surface. Spacer used in this experiment was 10T. .... 89

**Figure 70** SERS spectrum of BCB-labeled DNA obtained in the control hybridization experiment onto the gold surface with silver colloid in dry condition. SERGen probe was designed using archaea proteasome gene sequence having same sequence as the target DNA. The numbers are representing the locations at which the SERS measurements were done. The colors are coding the signal obtained from that particular point on the gold surface. Spacer used in this experiment was 10T..... 90

**Figure 71** Schematic representation of test hybridization using 10T as spacer. .... 91

**Figure 72** Schematic representation of control hybridization experiment using 10T as spacer. .... 91

**Figure 73** SERS spectra of BCB-labeled DNA after hybridization onto the gold surface with silver colloid in dry condition. SERGen probe was designed using human proteasome gene sequence. The numbers are representing the locations at which the SERS measurements were done. The colors are coding the signal obtained

from that particular point on the gold surface. Spacer used in this experiment was 10T. ....	93
<b>Figure 74</b> SERS spectra of BCB-labeled DNA in the control hybridization experiment onto the gold surface with silver colloid in dry condition. SERGen probe was designed using human proteasome gene sequence. The numbers are representing the locations at which the SERS measurements were done. The colors are coding the signal obtained from that particular point on the gold surface. Spacer used in this experiment was 10T. ....	94
<b>Figure 75</b> SERS spectra of BCB-labeled DNA after hybridization onto the gold surface with silver colloid in dry condition. SERGen probe was designed using human proteasome gene sequence. The numbers are representing the locations at which the SERS measurements were done. The colors are coding the signal obtained from that particular point on the gold surface. Spacer used in this experiment was 10T. ....	95
<b>Figure 76</b> SERS spectra of BCB-labeled DNA after hybridization onto the gold surface with silver colloid in dry condition. SERGen probe was designed using human proteasome gene sequence. The numbers are representing the locations at which the SERS measurements were done. The colors are coding the signal obtained from that particular point on the gold surface. Spacer used in this experiment was decanethiol. ....	96
<b>Figure 77</b> SERS spectra of BCB-labeled DNA in the control hybridization experiment onto the gold surface with silver colloid in dry condition. SERGen probe was designed using human proteasome gene sequence. Spacer used in this experiment was decanethiol. ....	97
<b>Figure 78</b> SERS spectra of BCB-labeled DNA after hybridization onto the gold surface with silver colloid in dry condition. SERGen probe was designed using human proteasome gene sequence. The numbers are representing the locations at which the SERS measurements were done. The colors are coding the signal obtained from that particular point on the gold surface. Spacer used in this experiment was 11-mercapto-1-undecanol. ....	98
<b>Figure 79</b> SERS spectra of BCB-labeled DNA in the control hybridization experiment onto the gold surface with silver colloid in dry condition. SERGen probe	

was designed using human proteasome gene sequence. Spacer used in this experiment was 11-mercapto-1-undecanol. .... 99

**Figure 80** SERS spectra of three BCB-labeled DNA after hybridization onto the gold film with silver colloid in dry condition (A, B, C). SERGen probe was designed using human proteasome gene sequence. The numbers are representing the locations at which the SERS measurements were done. The colors are coding the signal obtained from that particular point on the gold film. Spacer used in this experiment was 11-mercapto-1-undecanol. .... 100

**Figure 81** SERS spectra of BCB-labeled DNA after hybridization onto the gold surface with silver colloid in dry condition. SERGen probe was designed using human proteasome gene sequence. The numbers are representing the locations at which the SERS measurements were done. The colors are coding the signal obtained from that particular point on the gold surface. Spacer used in this experiment was 11-mercapto-1-undecanol. .... 101

**Figure 82** Schematic representation of hybridization at different annealing temperatures. .... 102

**Figure 83** SERS spectra of BCB-labeled DNA after the hybridization at A) 25 °C B) 35 °C onto the gold surface with silver colloid in dry condition. SERGen probe was designed using human proteasome gene sequence. The numbers are representing the locations at which the SERS measurements were done. The colors are coding the signal obtained from that particular point on the gold surface. Spacer used in this experiment was 11-mercapto-1-undecanol. .... 103

**Figure 84** SERS spectra of BCB-labeled DNA after the hybridization at A) 45 °C B) 55 °C onto the gold surface with silver colloid in dry condition. SERGen probe was designed using human proteasome gene sequence. The numbers are representing the locations at which the SERS measurements were done. The colors are coding the signal obtained from that particular point on the gold surface. Spacer used in this experiment was 11-mercapto-1-undecanol. .... 104

**Figure 85** SERS spectra of BCB-labeled DNA after the hybridization at 65 °C onto the gold surface with silver colloid in dry condition. SERGen probe was designed using human proteasome gene sequence. The numbers are representing the locations at which the SERS measurements were done. The colors are coding the signal

obtained from that particular point on the gold surface. Spacer used in this experiment was 11-mercapto-1-undecanol. ....	105
<b>Figure 86</b> Schematic representation of hybridization mismatch experiments. Spacer was 11-mercapto-1-undecanol. ....	106
<b>Figure 87</b> SERS spectra of BCB-labeled DNA after the hybridization at A) 25 °C B) 35 °C onto the gold surface with silver colloid in dry condition. SERGen probe was designed using archaea proteasome gene sequence. The numbers are representing the locations at which the SERS measurements were done. The colors are coding the signal obtained from that particular point on the gold surface. Spacer used in this experiment was 11-mercapto-1-undecanol. ....	108
<b>Figure 88</b> SERS spectra of BCB-labeled DNA after the hybridization at A) 45 °C B) 55 °C onto the gold surface with silver colloid in dry condition. SERGen probe was designed using archaea proteasome gene sequence. The numbers are representing the locations at which the SERS measurements were done. The colors are coding the signal obtained from that particular point on the gold surface. Spacer used in this experiment was 11-mercapto-1-undecanol. ....	109
<b>Figure 89</b> SERS spectra of BCB-labeled DNA after the hybridization at 65 °C onto the gold surface with silver colloid in dry condition. SERGen probe was designed using archaea proteasome gene sequence. The numbers are representing the locations at which the SERS measurements were done. The colors are coding the signal obtained from that particular point on the gold surface. Spacer used in this experiment was 11-mercapto-1-undecanol. ....	110
<b>Figure 90</b> SERS spectra of BCB-labeled DNA after the hybridization at A) 25 °C B) 35 °C onto the gold surface with silver colloid in dry condition. SERGen probe was designed using human proteasome gene sequence. The numbers are representing the locations at which the SERS measurements were done. The colors are coding the signal obtained from that particular point on the gold surface. Spacer used in this experiment was 11-mercapto-1-undecanol. ....	112
<b>Figure 91</b> SERS spectra of BCB-labeled DNA after the hybridization at A) 45 °C B) 55 °C onto the gold surface with silver colloid in dry condition. SERGen probe was designed using human proteasome gene sequence. The numbers are representing the locations at which the SERS measurements were done. The colors are coding the	



signal obtained from that particular point on the gold surface. Spacer used in this experiment was 11-mercapto-1-undecanol. .... 113

**Figure 92** SERS spectra of BCB-labeled DNA after the hybridization at 65 °C onto the gold surface with silver colloid in dry condition. SERGen probe was designed using human proteasome gene sequence. The numbers are representing the locations at which the SERS measurements were done. The colors are coding the signal obtained from that particular point on the gold surface. Spacer used in this experiment was 11-mercapto-1-undecanol. .... 114

**Figure 93** SERS spectra of BCB-labeled DNA after the hybridization at A) 25 °C B) 35 °C onto the gold surface with silver colloid in dry condition. SERGen probe was designed using human proteasome gene sequence (double base mismatch). The numbers are representing the locations at which the SERS measurements were done. The colors are coding the signal obtained from that particular point on the gold surface. Spacer used in this experiment was 11-mercapto-1-undecanol..... 116

**Figure 94** SERS spectra of BCB-labeled DNA after the hybridization at A) 45 °C B) 55 °C onto the gold surface with silver colloid in dry condition. SERGen probe was designed using human proteasome gene sequence. The numbers are representing the locations at which the SERS measurements were done. The colors are coding the signal obtained from that particular point on the gold surface. Spacer used in this experiment was 11-mercapto-1-undecanol. .... 117

**Figure 95** SERS spectra of BCB-labeled DNA after the hybridization at 65 °C onto the gold surface with silver colloid in dry condition. SERGen probe was designed using human proteasome gene sequence. The numbers are representing the locations at which the SERS measurements were done. The colors are coding the signal obtained from that particular point on the gold surface. Spacer used in this experiment was 11-mercapto-1-undecanol ..... 118

**Figure 96** The graph of SERGen probes concentrations to SERS intensities at 580 nm..... 120

## LIST OF ABRREVIATIONS

A	Adenine
BA	Benzoic Acid
BCB	Brilliant Cresyl Blue
bp	Base pair
C	Cytosine
CFV	Cresyl Fast Violet
CV	Crystal Violet
DNA	Deoxyribonucleic Acid
FITC	Fluorescein Isothiocyanate
G	Guanine
SPR	Surface Plasmon Resonance
PABA	Para-amino Benzoic Acid
PVA	Polyvinyl Alcohol
SAM	Self-Assembled Monolayer
SERS	Surface-Enhanced Raman Scattering
ss-DNA	Single stranded DNA
T	Thymine
UPS	Ubiquitin-Proteasome System

## CHAPTER 1

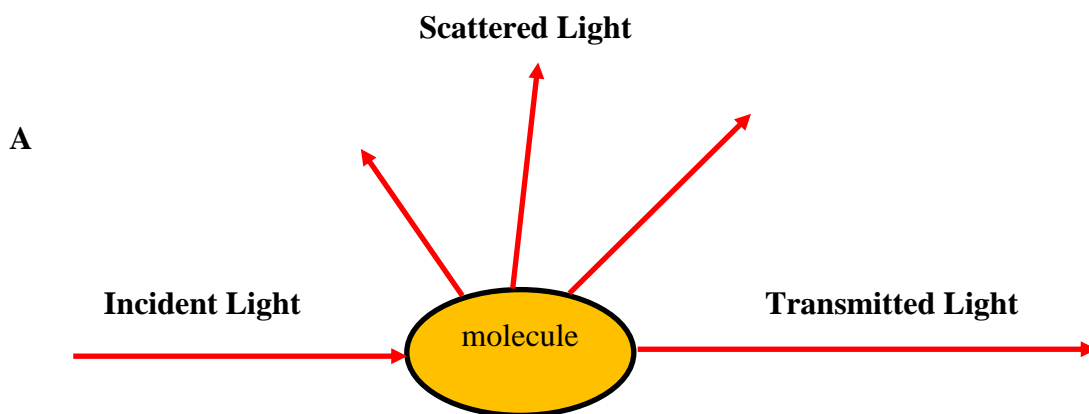
### INTRODUCTION

In 1928, when Sir Chandrasekhra Venkata Raman explored the phenomenon that bears his name, primitive instrumentation was available. He used sunlight as the source, a telescope as the collector and the detector was his eyes (**Ferraro, Nakamoto, & Brown, 2003**). The introduction of laser light sources was a milestone in the history of Raman spectroscopy and resulted in significantly increased scattering signals. Raman effect has attracted attention both a basic investigation point of view and an effective spectroscopic technique for many practical applications (**Kneipp, Kneipp, Itzkan, Dasari, & Feld, 1999**).

Raman spectroscopy is a spectroscopic technique related with vibrational transitions that provide very narrow spectral features characteristic of the examined sample (**Vo-Dinh, 2003**).

## 1.1 Raman Scattering

Raman scattering is a process between a photon and a molecule. Incident photons are scattered from a molecule elastically, called Rayleigh scattering or inelastically, called Raman scattering (see Figure 1). When the photons are scattered inelastically, the frequency shifts by the energy of its characteristic molecular vibrations. Frequency-shifted scattered photons could have higher or lower energy relative to the incoming photons. In the former one, photons lose energy by exciting a vibration and the scattered light seems at a lower frequency, called the Stokes scattering. In the latter one, photons gain energy from the molecular vibrations by interacting with a molecule in an excited vibrational state, and the scattered light seems at higher frequency, called anti-Stokes scattering (**Kneipp, Kneipp, Itzkan, & Dasari, 2002**).



B

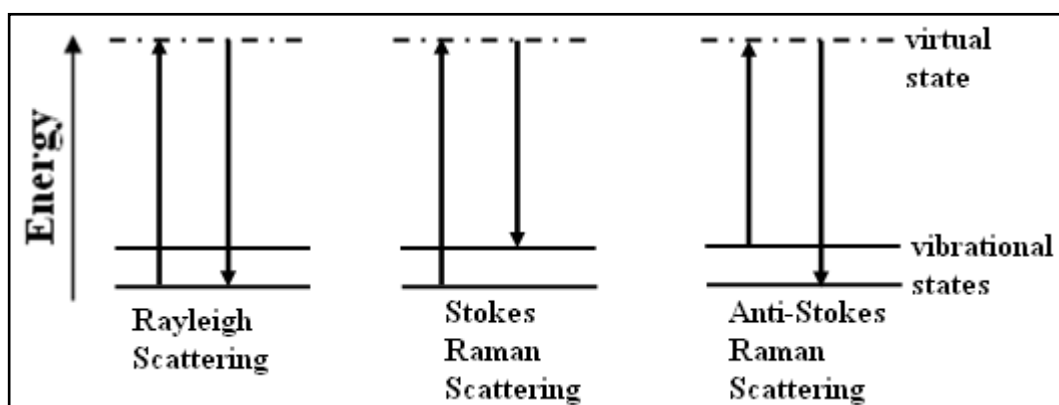


**Figure 1** (A) Schematic diagram of various interactions of a molecule with monochromatic light. (B) Molecular energy diagram of Rayleigh and Raman Scattering (Stokes and anti-Stokes).

Typical fluorescence and Raman Spectra are shown in Figure 2. Fluorescence spectra are relatively ‘broad bands’ and do not give structural information about the molecule. On the other hand, the Raman effect deals with vibrational levels of the molecule, which depend on the types of atom and their bond strengths and arrangements in a specific molecule. Consequently, Raman spectra supply structural ‘fingerprints’ of the molecules.

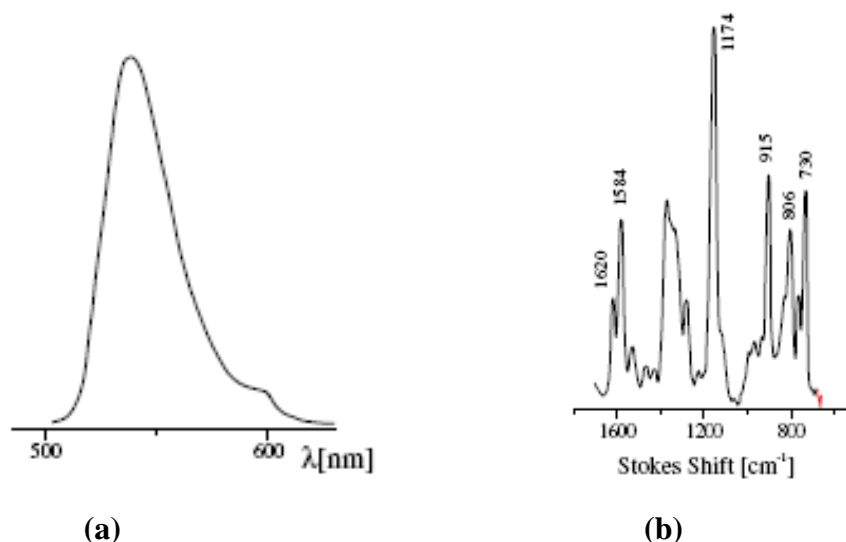


**Figure 2** a) Fluorescence spectrum b) Raman spectrum (Kneipp, Kneipp, Itzkan, & Dasari, 2002).

On the other hand, for many decades, Raman spectroscopy has not been considered as a useful analytical tool owing to the small normal Raman scattering cross-section of many molecules (**Kudelski, 2008**). Raman signals in higher intensity and lower detection limits can be obtained using surface-enhanced Raman scattering (SERS) method. SERS provides very large enhancements in the effective Raman cross-section of molecules. In comparison to infrared absorption and normal Raman scattering spectroscopies, SERS has the advantages of application in aqueous media and the sensitivity adequate for trace level detection. SERS has the distinct advantages such as low detection limit, real-time response, both qualitative and quantitative analysis abilities, a high degree of specificity, and simultaneous multi-component detection (**Yonzon, Stuart, Zhang, McFarland, Haynes, & Van Duyne, 2005**).

## 1.2 Surface-Enhanced Raman Scattering (SERS)

Surface-enhanced Raman scattering (SERS) takes place when molecules have been adsorbed onto specially prepared metallic surfaces with their surface roughnesses on the 10 to 100 nm scale. Raman scattering is enhanced by  $10^6$  by adsorbing Ag and Au surfaces. In some cases, enhancements of  $10^{12}$  to  $10^{14}$  are possible when the single molecules are being studied (Doering, Piotti, Natan, & Freeman, 2007).

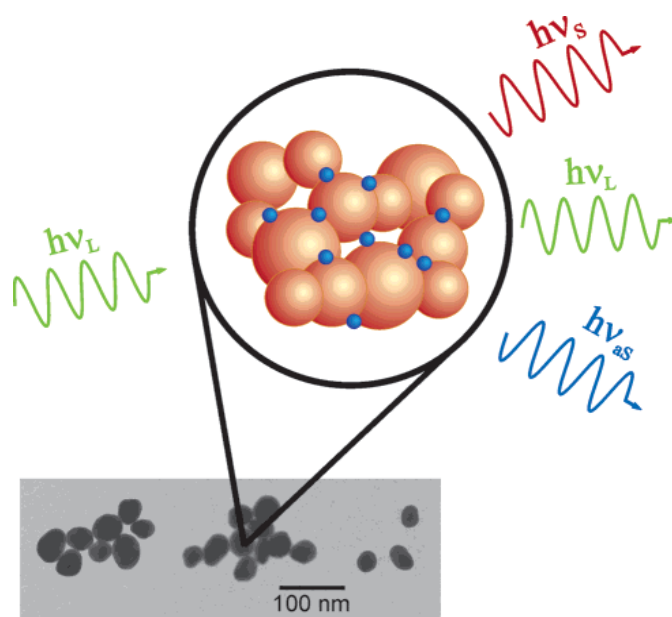


**Figure 3** A schematic representation of surface-enhanced Raman scattering. Molecules (blue dots) are attached to metal nanoparticles (orange balls) (Kneipp, Kneipp, & Kneipp, 2006).

SERS was discovered, though not perceived as such, by Fleischmann *et al.* (Fleischmann, Hendra, & McQuilla, 1974) in 1974, who achieved intense Raman scattering from pyridine adsorbed on electrochemically roughened silver electrodes. According to Fleischmann, this enhancement was arisen from the increased surface area formed by the electrochemical roughening, leading to increased the number of

adsorbed molecules (**Campion & Kambhampati, 1998**). Jeanmaire and Van Duyne (**Jeanmaire & Van Duyne, 1977**) and Albrecht and Creighton (**Albrecht & Creighton, 1977**) recognized independently that intense Raman scattering could not be accounted for simply by the increase in surface area by displaying that intense SERS signals could be acquired with electrode surfaces roughened too slightly for the rise in surface area to exceed a factor of 10 (**Moskovits, 1985**). Jeanmaire and Van Duyne proposed electromagnetic enhancement whereas Albrecht and Creighton explained with chemical enhancement (**Campion & Kambhampati, 1998**).

### **1.2.1 Mechanisms of SERS**

Although SERS is an extensively application method, the mechanism inducing to the enhancement is not completely understood yet. The enhancement mechanisms are roughly classified as electromagnetic effect and chemical effect (**Vo-Dinh, 2003**).

#### **1.2.1.1 Electromagnetic Enhancement**

To comprehend the electromagnetic enhancement, the size, shape and material of the nanoscale roughness features must be considered. The resonant frequency of the conduction electrons in a metallic nanostructure depends on these characteristics. When the electromagnetic radiation with the same frequency is incident upon the nanostructure, the electric field of the radiation forces the conduction electrons into collective oscillation (Figure 4) (**Haynes, McFarland, & Van Duyne, 2005**).



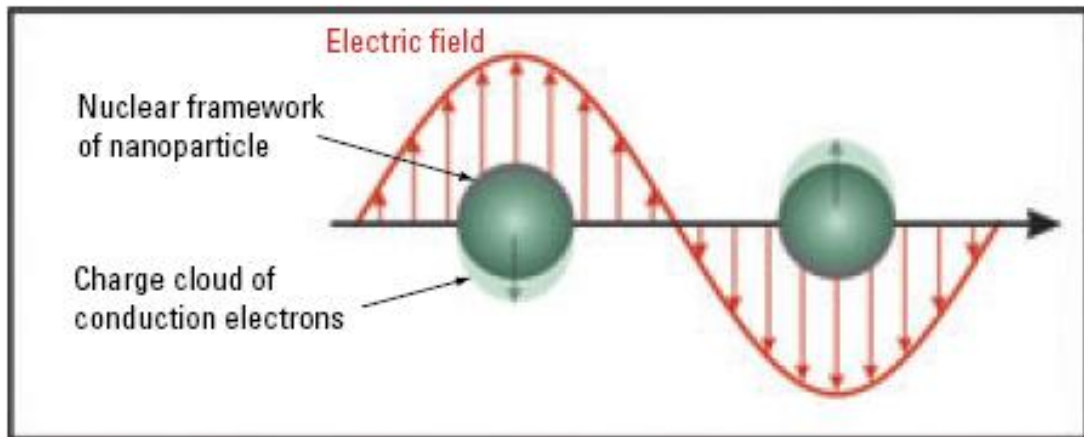


**Figure 4** Illustration of the conduction electrons into collective oscillation by electromagnetic radiation (Haynes, McFarland, & Van Duyne, 2005).

The electromagnetic contribution of the SERS enhancement is arising from the electromagnetic field enhancement that occurs by the plasmon excitation through the incident laser light on the metal surface (Hering, et al., 2008). Collective excitation of the electrons on the metal surface, called a surface plasmon. The excited surface plasmons cause an electromagnetic field in nanostructured surfaces, which extends from the metal surface, where the sample is located (Moskovits, 1985).

Since surface plasmons have to be excited by the incident laser radiation, the excitation wavelength for a SERS experiment must be adjusted to the plasmon wavelength of the respective metal and also to the nanostructure of the metal surface, which also has an influence on the plasmon resonance wavelength. Therefore, SERS excitation lines involve mainly the visible spectral region up to the near infrared (NIR) between 450 and 1064 nm. With these laser wavelengths, the surface plasmons of metals such as silver and gold, which are extensively used as SERS-active substrates, can be excited (Tian, Yang, Ren, & Wu, 2006).

### 1.2.1.1.1 Surface Plasmons

Dipole oscillations of the free electrons with respect to the ionic core of a spherical nanoparticle occur surface plasmon absorption (**Link & El-Sayed, 2003**). Interaction of a net charge difference on the nanoparticle surface with an electric field which concludes a polarization of the electrons with respect to the ionic core of a nanoparticle (see Figure 5).

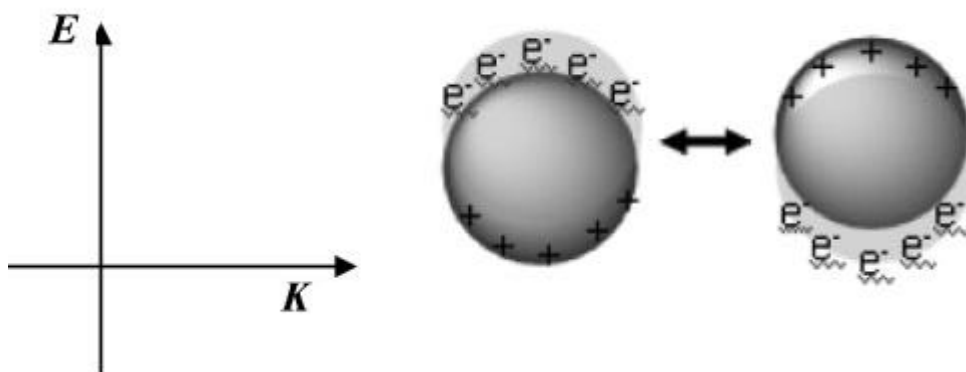


**Figure 5** Schematic illustration of the interaction of polarized light and gold nanospheres (Huang, Neretina, & El-Sayed, 2009)

The SPR oscillation leads to a strong absorption of light, as seen in the UV–vis region, which is the origin brilliant colors of the colloidal solution as explained by Mie theory. The SPR band depends on the particle size, shape, structure, the dielectric properties of the metal, and the surrounding medium, because these factors influences the electron charge density on the particle surface (**Link & El-Sayed, 2003**). Spherical gold, silver, and copper nanoparticles exhibit a strong SPR band in the visible region whereas other metals exhibit broad and weak bands in the UV region (**Creighton & Eadon, 1991**).

Increasing particle size causes SPR band to red shift as the bandwidth increases (**Link & El-Sayed, 2003**). Physically, the light cannot polarize the nanoparticles homogeneously for larger particles. Link and El-Sayed (**Link & El-Sayed, 1999**)

have shown that when the nanoparticles are larger than 20 nm, the bandwidth increases with the increasing of the nanoparticle size.

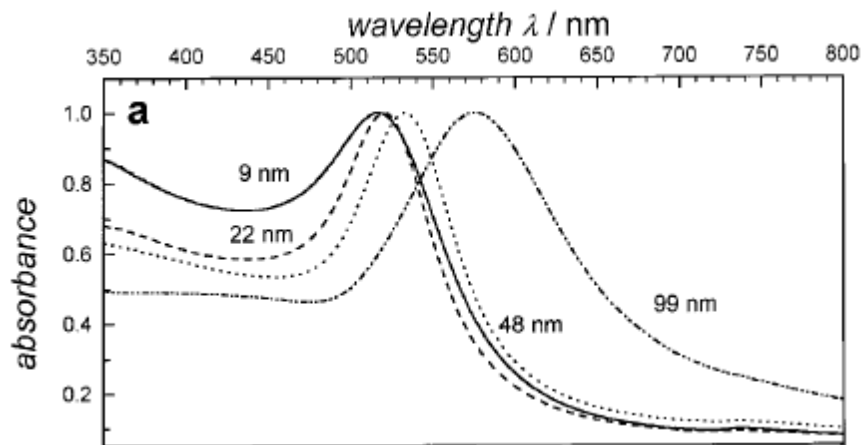


**Figure 6** Variation of surface plasmon absorption of spherical gold nanoparticles depending on particle size. The UV-vis absorption spectra of colloidal gold solutions with diameters between 9 and 99 nm display that the absorption maximum red-shifts with increasing particle size (**Link & El-Sayed, 1999**).

### 1.2.1.2 Chemical Enhancement

Chemical enhancement is based on a charge transfer process between the adsorbed analyte and the metal surface. Consequently, vibrations included in the charge transfer process are enhanced, which is similar to the resonance enhancement (**Otto, 1982**).

The highest occupied molecular orbital (HOMO) and lowest unoccupied molecular orbital (LUMO) of the adsorbed analyte are symmetrically regulated in energy with respect to the Fermi level of the metal (Figure 7). In this instance charge transfer excitations (either from the metal to the analyte or vice versa) can take place at about half the energy of the intrinsic intramolecular excitations of the adsorbate. Molecules mostly studied by SERS typically have their lowest-lying electronic excitations in the

near ultraviolet region which would put the charge transfer excitations of this model in the visible region of the spectrum (**Campion & Kambhampati, 1998**).

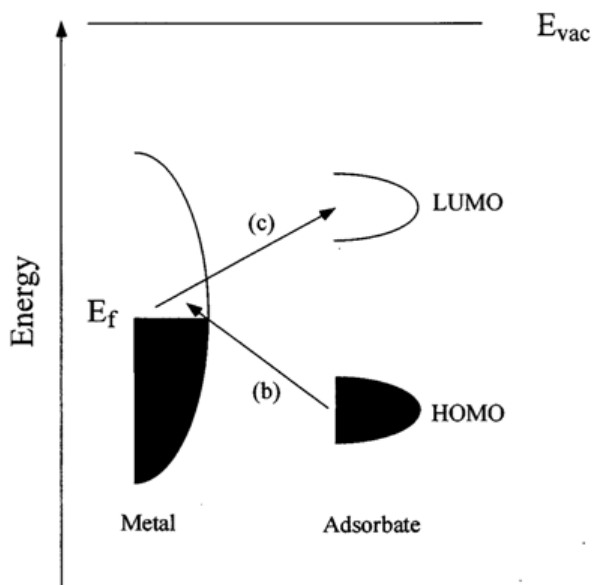


**Figure 7** Energy level diagram for a molecule adsorbed on a metal surface. The occupied and unoccupied molecular orbitals are expanded into resonances by their interaction with the metal states; orbital occupancy is designated by the Fermi energy. Possible charge transfer excitations are displayed (**Campion & Kambhampati, 1998**).

### 1.2.2 SERS Substrates

The first SERS-active substrate is a roughened metal electrode and it served as the basis for extensive theoretical studies. Afterwards, metal colloids gained prevalent use in SERS studies due to easy preparation by chemical means with mostly used reagents. Whereas the popularity of metal colloids has kept since the early 1980s, alternative media, like metal nanoparticle films and nanostructured probes, have been evolved for a broad variety of applications with improved reproducibility. In an attempt to simplify production of solid SERS probes, materials have been mechanically roughened to cause the SERS effect. Many of these technologies have been the basis of ultimately improved innovative probes, like silver-nanoparticle-

embedded polymers, in situ photoreduced sols, and a variety of fiber-optic-based SERS probes **(Vo-Dinh, 2003)**.

A silver nanoparticle-doped polyvinyl alcohol (PVA) coated SERS substrate prepared through the chemical reduction of silver particles dispersed in the polymer matrix has been reported for the detection of biologically important compounds: benzoic acid (BA), p-amino benzoic acid (PABA), pyridine and dopamine **(Karabiçak, Kaya, Vo-Dinh, & Volkan, 2008)**.

Kurokawa *et al.* have reported silver doped acetate and nafion polymer membranes through counter diffusion method to develop a SERS active substrate **(Kurokawaa & Imaib, 1991)**. Wang *et al.* have reported a silver-doped polycarbonate film prepared by chemical reduction. The performances of the substrates were investigated with different chemicals **(Wang & Li, 1997)**. Bell *et al.* have displayed that surface-enhanced resonance Raman active media can be prepared by isolating nanoparticles from Ag and Au sols in swelling polymer matrix, such as polycarbophil polymer **(Bell & Spence, 2001)**. Giesfeldt *et al.* have reported composites prepared via physical vapor deposition of gold metal onto pliable polydimethylsiloxane (PDMS) polymer as a SERS active substrate **(Giesfeldt, Connatser, De Jesu' s, Dutta, & Sepaniak, 2005)**. Yu *et al.* **(Yu, Lin, Lin, Chang, & Yang, 2007)** and Lin *et al.* **(Lin & Yang, 2005)** prepared SERS active substrates doped silver nanoparticles into polyvinyl alcohol-Poly( $\gamma$ -glutamic acid) polymer blend membranes.

Recently, a combination of electrochemical triangular-wave oxidation/reduction cycles and argon plasma treatment used to prepare SERS active substrates. In this technique, SERS effect increases roughening the substrate through electrochemical cycles **(Wang & Chen, 2008) (Wang C.-C. , 2008)**. Tourwe *et al.* prepared SERS-active electrodes applying a roughening procedure for electrodes. The desired roughness was acquired with ex-situ from a halide-free electrolyte solution via the electrodeposition of silver in a potentiostatic double potential step **(Tourwe' & Hubin, 2006)**. Liu *et al.* prepared SERS active silver substrates using

electrochemical oxidation-reduction cycles method. Substrates were modified with TiO<sub>2</sub> nanoparticles to develop the corresponding SERS performances (**Liu, Yu, & Hsu, 2008**). Sauer *et al.* have reported preparation of SERS active silver film electrodes via electrocrystalization of silver. They demonstrated that the electrodeposition of a sufficiently large amount of silver on silver films at high over potentials brings about excellent substrates for SERS measurements (**Sauer, Nickel, & Schneider, 2000**).

### **1.3 SERS Applications**

Surface-enhanced Raman spectroscopy has attained particular importance in fields including surface sciences, electrochemistry, analytical chemistry, biological and biomedical sciences, and forensic science (**Ren, Liu, Lian, Yang, & Tian, 2007**).

SERS was applied on amino acids and peptides, on purine and pyrimidine bases, but also on ‘large’ molecules such as proteins, DNA and RNA. SERS experiments were also performed on many ‘intrinsically coloured’ biomolecules such as chlorophylls and other pigments, as well as from larger molecules including chromophores such as the haem-containing proteins (**Kneipp, Kneipp, Itzkan, & Dasari, 2002**).

Medical applications of SERS involve detection of stimulating drugs (**Bell, Fido, Sirimuthu, Speers, Peters, & Cosbey, 2007**) and selective analysis of antitumour drug interaction with DNA (**Chourpa, Lei, Dubois, Manfait, & Sockalingum, 2008**).

SERS technique has been also carried out to study biophysically interesting processes. For instance, SERS can be utilized to monitor transport through membranes. The results display that SERS can discriminate between the movement of different molecules across a membrane and to observe different interfacial arrival times and concentration growth rates in the accepting (colloidal silver) solution (**Wood, Sutton, Beezer, Creighton, Davis, & Mitchell, 1997**). SERS offers also an

interesting approach for studying charge transfer processes, for example in aminothiophenol, which has been widely searched on gold and silver coated substrates **(Zhou, Li, Fan, Zhang, & Zheng, 2006)**.

### **1.3.1 Biological Applications**

Surface-enhanced Raman scattering (SERS) is a powerful technique for analyzing biological samples as it provides a rapid and nondestructive analytical ability and in some instances, it gives structural information about molecules in aqueous environments **(Hudson & Chumanov, 2009)**.

Raman scattering phenomenon provides the basis for SERS performing both quantitative and qualitative molecular information about biological molecules **(Hering, et al., 2008)**. As opposed to IR spectroscopy, the Raman scattering cross-section of water molecules is small, allowing vibrational information to be acquired from biological samples in their native aqueous environment and their efficient detection and distinction from the background. Low detection limits, narrow spectral bandwidths, the capability to quench fluorescence, and using with or without optical labels make SERS a good choice for DNA or RNA analysis **(Barhoumi, Zhang, Tam, & Halas, 2008) (Vo-Dinh, 2008)**.

#### **1.3.1.1 DNA Detection**

The specific detection of DNA has gained significance in recent years since increasingly DNA sequences of different organisms are being assigned. Such sequence knowledge can be employed for the identification of the genus or species of microorganisms, diseases, or even a single individual **(Hering, et al., 2008)**.

DNA is the abbreviation of deoxyribonucleic acid. DNA is a long polymer made from repeating units called nucleotides. It stores and expresses all the information necessary for building and maintaining life. The number of nucleotides in a DNA molecule is in the millions that are linked together. Nucleotides are the monomer

units of DNA. Each nucleotide contains of a 5-carbon sugar (pentose), a nitrogen involving base attached to the sugar, and a phosphate group as shown in Figure 8.

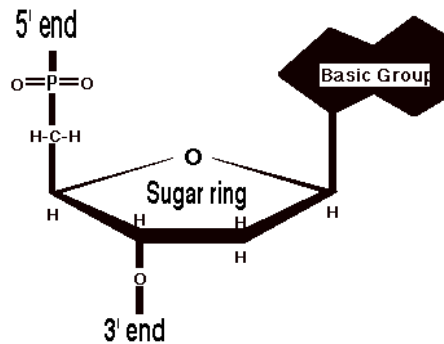


**Figure 8** A schematic representation of the structure of a nucleotide.

There are four different kinds of nucleotides found in DNA, differing only in the nitrogenous base. These bases can be either purines or pyrimidines. Purines are double-ringed molecules while pyrimidines are single-ringed molecules. The bases adenine, guanine, cytosine, and thymine are abbreviated as A, G, C, and T respectively. Adenine and guanine are purines. Cytosine and thymine are pyrimidines (**Darnell, Lodish, & Baltimore, 1990**).

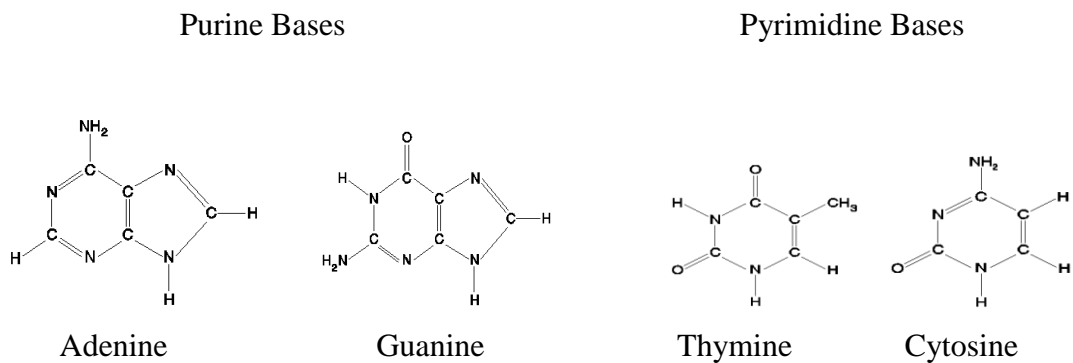


**Figure 9** Purine and pyrimidine bases structures.

In 1953, the 3D structure of DNA double helix was described by Watson and Crick (Watson & Crick, 1953). DNA double helix consists of two DNA strands winding around each other as shown in Figure 10.



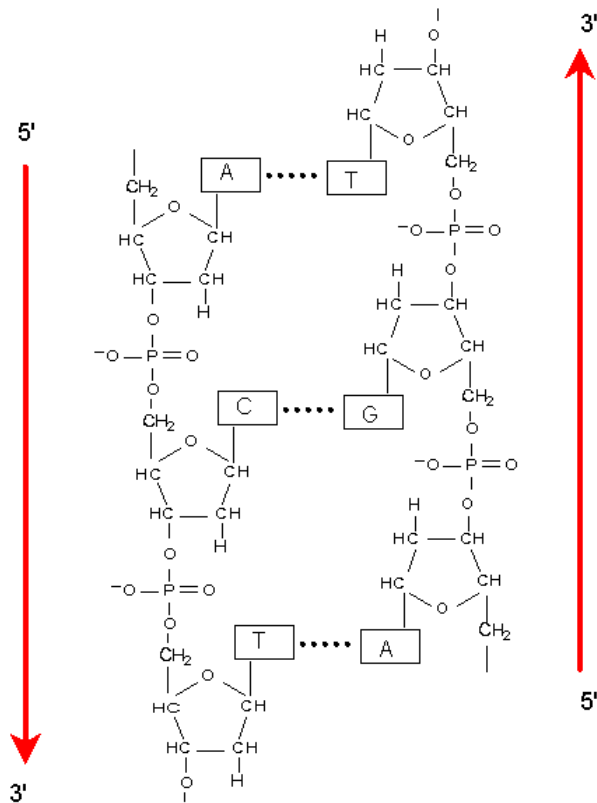
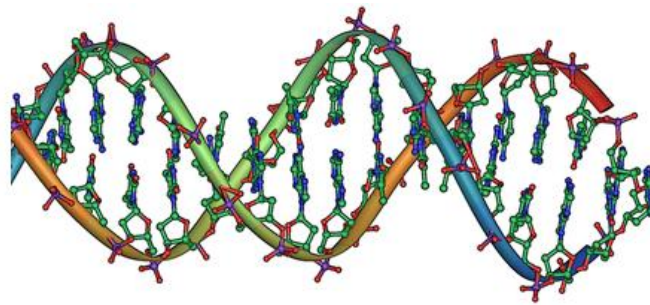


**Figure 10** Schematic drawings of DNA double helix.

The directions from 5' to 3' of the two strands are opposite. The two strands are held together by hydrogen bonding and hydrophobic interactions. Within the DNA double helix, A forms 2 hydrogen bonds with T on the opposite strand, and G forms 3 hydrogen bonds with C on the opposite strand. This base-pair complementarity is assigned by the structure, dimension, and chemical composition of the bases. Base-pairs stack on top of one another layer by layer because of the planarity of both the bases and the base-pairs. Hydrophobic and van der Waals forces between adjacent

base pairs in the stack contribute dramatically to the overall stability of the double helix (**Darnell, Lodish, & Baltimore, 1990**).

SERS detection of specific nucleic acid sequences are mainly based on hybridization of DNA targets (e.g., gene sequences, bacteria, viral DNA) to complementary probe sequences, which are labelled with SERS active dyes. This method enables a very high degree of accuracy in identifying DNA sequences (**Vo-Dinh, 2003**).

Vo-Dinh *et al.* reported SERS detection of specific nucleic acid sequences with the use of labeled DNA as gene probes (**Vo-Dinh, Allain, & Stokes, 2002**). They have been detected DNA fragments of the human immunodeficiency virus (HIV) (**Isola, Stokes, & Vo-Dinh, 1998**) and breast cancer (BRCA1) gene detection (**Vo-Dinh, Allain, & Stokes, 2002**). In these studies, firstly, a SERS active dye was attached to the oligonucleotide of a HIV and BRCA 1 gene sequences, called SERGen probes. Hybridization were performed to detect DNA sequences of interest. BRCA 1 and HIV capture probes were immobilized on the supported material, and then, dye labelled SERGen probes were added. After the washing, SERS detection of hybridized probes were made adding silver colloid. SERS spectrum of the dye have been provided detection of hybridization of the labeled probe BRCA 1 DNA and HIV DNA.

Cao *et al.* also reported SERS detection of DNA. To detect DNA targets, they used gold nanoparticle probes labeled with oligonucleotide and SERS active dyes, which on the underlying chip in microarray format. However, existence of gold nanoparticles could not be permitted SERS detection. According to authors, packing of nanoparticles on the surface was not enough to form an electromagnetic field enhancement. SERS signals were obtained after the additional of silver deposition process (**Cao, Jin, & Mirkin, 2002**).

Graham *et al.* have demonstrated sufficient sensitivity for single-molecule DNA detection by using surface-enhanced resonance Raman scattering (SERRS) (**Thompson, Enright, Faulds, Smith, & Graham, 2008**). They have dedected

fluorophore-labeled DNA adsorbed onto colloidal silver particles and examined over a range of concentrations ( $\sim 10^{-11}$ - $10^{-7}$  M) (Stokes, Macaskill, Lundahl, Smith, Faulds, & Graham, 2007).

### 1.3.1.2 Proteasomes

The proteasome is a very large protein complex in the cells of all eukaryotes, archaea, and in some bacteria (Peters, Franke, & Kleinschmidt, 1994). These large multimeric proteases play crucial role in the protein quality control, clearance of misfolded proteins and processing by partial proteolysis and preparation of peptides for immune presentation. 20 S proteasome is comprised 28 individual  $\alpha$ - and  $\beta$ -subunits, which are arranged in four rings, with each ring consisted of either seven  $\alpha$ - or seven  $\beta$ -subunits. The two inner rings of the proteasome contain the  $\beta$ -subunits, which possess the catalytically active proteolytic sites. The  $\alpha$ -rings function as docking platform and serve as a template for proper folding and assembly of  $\beta$ -subunit precursors.

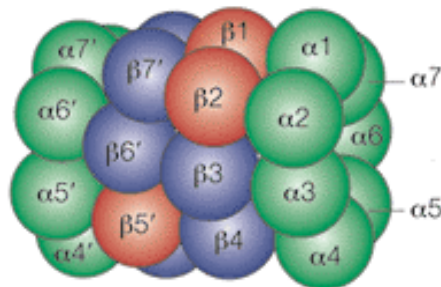


**Figure 11** A schematic diagram of the proteasome 20S core particle viewed from one side (Kloetzel, 2001).

The proteasome subcomponents are commonly characterized and named to by their Svedberg sedimentation coefficient (denoted S). The most widespread form of the proteasome is 26S proteasome, which is about 2000 kilodaltons (kDa) in molecular mass and involves one 20S core particle structure and two 19S regulatory caps (Keller, Hanni, & Markesbery, 2000). The core is hollow and supplies an enclosed

cavity in which proteins are degraded; openings at the two ends of the core enable the target protein to enter. Each end of the core particle capped by a 19S regulatory subunit that consists of multiple ATPase active sites and ubiquitin binding sites; it is this structure that identifies polyubiquitinated proteins and transfers these proteins to the catalytic core (Wang & Maldonado, 2006).

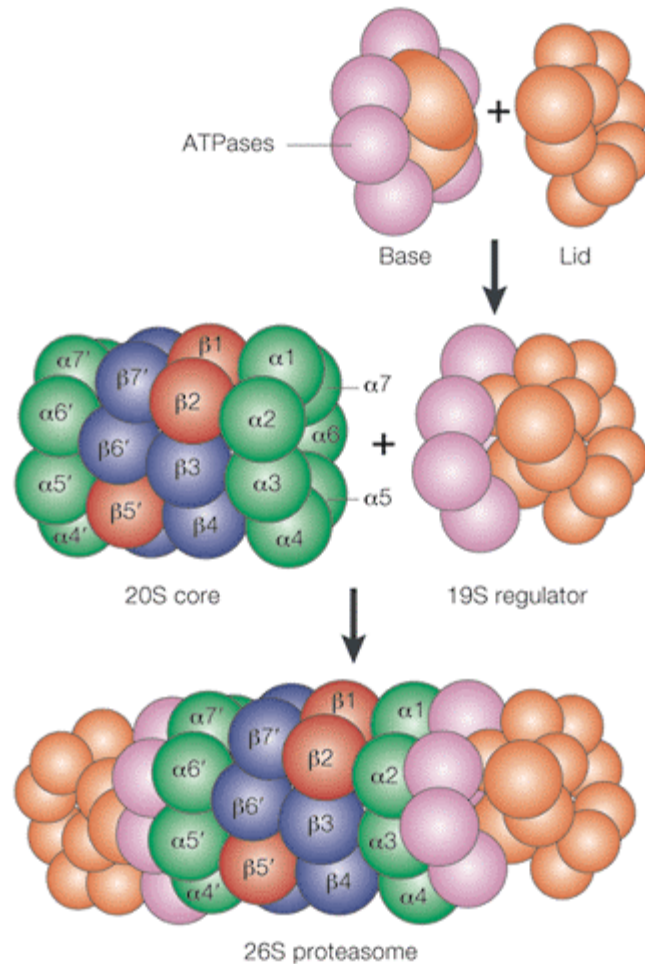


**Figure 12** Schematic diagram of the 20S core protease (CP) and the 26S proteasome (Kloetzel, 2001).

In eucaryotes, removal of denatured, misfolded, damaged or improperly translated proteins, as well as the regulated proteolysis of intracellular proteins such as cell-cycle regulators, oncogenes, tumour suppressors and transcription factors occurs through ATP dependent ubiquitin-proteasome pathway (UPS) (Wang &

**Maldonado, 2006)**. Ciechanover (**Ciechanover, 2005**), Hershko (**Hershko, 2005**) and Rose (**Rose, 2005**) for the discovery of the function of ubiquitin received Nobel Prize in Chemistry at 2004. In addition to ubiquitinated proteins, the proteasome has been demonstrated in several cellular functions, containing differentiation (**Bowerman & Kurz, 2006**), proliferation, apoptosis (**Naujokat & Hoffmann, 2002**), gene transcription (**Collins & Tansey, 2006**), signal transduction (**Taylor & Jobin, 2005**), metabolic regulation (**Asher, Bercovich, Tsvetkov, Shaul, & Kahana, 2005**), immune surveillance (**Strehl, Seifert, Krüger, Heink, Kuckelkorn, & Kloetzel, 2005**) and many others (**Sakai, Sawada, & Sawada, 2004**).

Ubiquitin proteasome system mediated protein degradation takes place in two discrete and consecutive steps. In the first step, the protein substrate is tagged by multiple ubiquitin molecules covalently to generate the polyubiquitin chain that serves as a recognition marker to the ubiquitin receptor subunit in the 19S complex of 26S proteasome complex. In the second step, the 26S proteasome complex, which induces subsequent release of free and reusable ubiquitin, degrades the tagged to short peptides. The second process is interceded by ubiquitin recycling enzymes such as isopeptidases, also known as ubiquitin-specific proteases (UBPs) and deubiquitinating enzymes (DUBs).

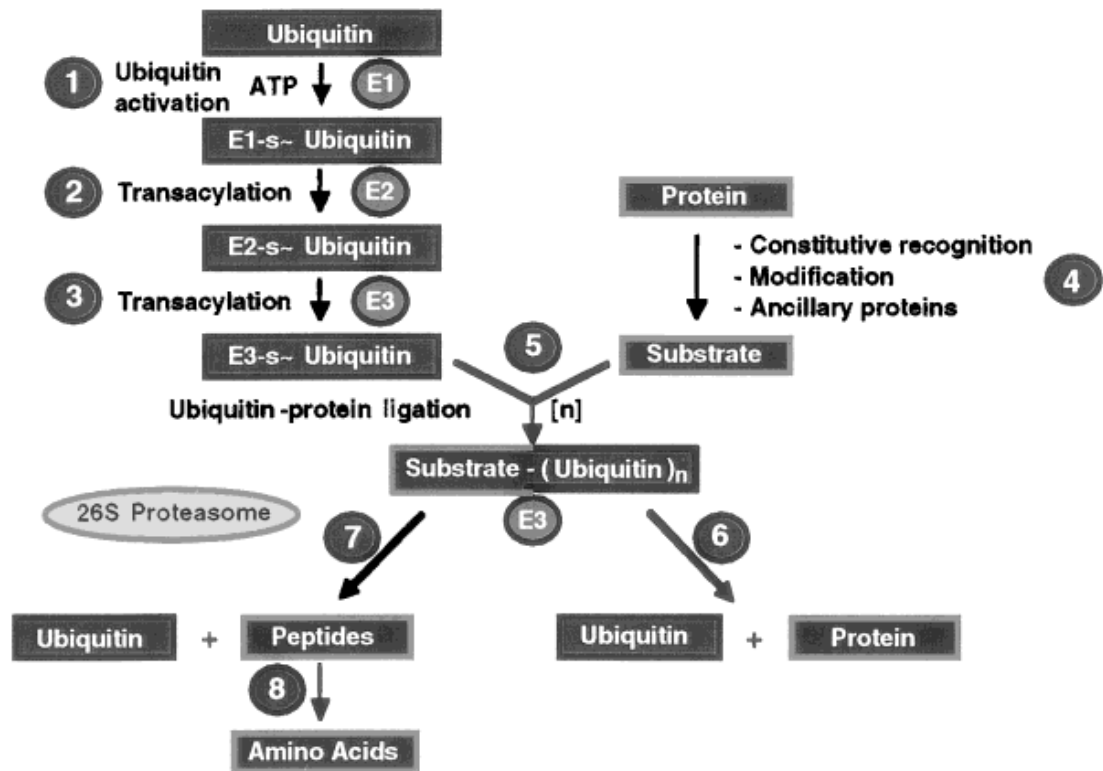


**Figure 13** The ubiquitin-proteasome pathway (Ciechanover, Orian, & Schwartz, 2000).

Conjugation of ubiquitin, 76 amino acids in size, to the protein substrate proceeds by way of three-step cascade mechanism. Firstly, ubiquitin-activating enzyme, E1, activates ubiquitin to a high energy of thiol ester intermediate. Then ubiquitin is transferred, via transacylation, to a member of the ubiquitin-carrier proteins family of enzymes, E2 (ubiquitin-conjugating enzyme - UBC). A high energy of ubiquitin intermediate, E2-S, forms. From E2 activated ubiquitin can be transferred via transacylation to a member of the ubiquitin-protein ligases family of enzymes, E3. A high energy of ubiquitin intermediate, E3-S, forms in these situations. In the fourth step, conversion of a cellular protein into a substrate of the ubiquitin system happens. In the next step, the protein substrate associates with E3 and transfers activated ubiquitin moieties to generate a polyubiquitin chain anchored to an  $\epsilon$ -NH<sub>2</sub> group of a Lys residue of the substrate. In the sixth step, ubiquitin moieties “mistakenly” attached to a protein not destined for degradation are removed via the activity of isopeptidases. In the seventh step, the ubiquitin-tagged substrate is degraded by the

26S proteasome complex. In steps 6 and 7, free and reusable ubiquitin is released. In the last step, peptidase-mediated degradation of peptides released by the proteasome to free amino acids (**Ciechanover, Orian, & Schwartz, 2000**).

Since UPS system is essential for eucaryotic cells, any alteration (**Dahlmann, 2007**) to its components has potential pathological consequences. Age-related decrease in proteasome activity weakens cellular capacity to remove oxidatively modified proteins and favours the development of neurodegenerative and cardiac diseases. On the otherhand, up-regulation of proteasome activity is observed in muscle wasting conditions including sepsis, cachexia and uraemia. Meanwhile, enhanced presence of immunoproteasomes in aging brain and muscle tissue might be due to a persistent inflammatory defence and anti-stress mechanism, whereas in cancer cells, their down-regulation reflects a means by which to escape immune surveillance. Hence, induction of apoptosis by selective proteasome inhibitors is a potential treatment strategy for misfolded protein disorders while broad-spectrum proteasome inhibitor drugs are designed to target cancer (**Vij, 2011**). In contrast, for other diseases such as muscle wasting and neurodegeneration the use of proteasome-activating or -modulating compounds could be more effective (**Richardson, Mitsiades, Hideshima, & Anderson, 2006**). Therefore, recently, the UPS has been recognized as an exciting novel therapeutic target for the treatment of many neurodegenerative disorders, cancers, viral infections and cardiac dysfunction (**Paul, 2008**). An array of synthetic and natural inhibitors of the proteolytic sites on the proteasome has been developed as therapeutic agents. Currently there are some inhibitors either approved or in clinical trials for the treatment of multiple cancers and strokes (**Tsukamoto & Yokosawa, 2006**). The first proteasome inhibitor used for clinical trials was bortezomib. Recently, bortezomib (PS-341) got Food and Drug Administration (FDA) approval for the use in multiple myeloma and is being evaluated for the treatment of solid tumors (**Nawrocki, et al., 2005**) (**Papandreou & Logothetis, 2004**). Preclinical studies have indicated that bortezomib, a dipeptidyl boronic acid, is a discriminating and potent inhibitor of the 26S proteasome that lessens proliferation, causes apoptosis, enhances the activity of chemotherapy and radiation, and reverses chemoresistance in a variety of hematologic and solid malignancy models both in vitro and in vivo (**Adams, 2004**).

Thus, proteasomes are often overexpressed in cancer cells; abnormally high expression of proteasomes having been found in human leukaemia cells, renal cancer cells and in breast cancer cell lines. In patients suffering from auto-immune diseases, malignant myelo-proliferative syndromes, multiple myeloma, acute and chronic lymphatic leukaemia, solid tumour, sepsis or trauma, the concentration of circulating proteasome has been found to be elevated. On the other hand, in age-related decrease in the expression of proteasomes is related to pathologies such as neurodegenerative and cardiac diseases. Thus, detection of increased or decreased level of proteasome activity is an important data to correlate with the disease state, and may have prognostic significance as well. Proteasome (enzyme activity) levels have been measured by enzyme-linked immunosorbent assay (ELISA) techniques in cell lysates, serum or plasma samples and there are a number of such kits commercially available.

In this study with a novel approach to correlate between circulating proteasome levels and disease state, we suggest a Raman spectroscopic technique that uses oligo SERS probes. This approach deals with specific detection of elevated or decreased levels of proteasome genes' transcription in patients as an alternative to available enzyme activity measurement methods.



## CHAPTER 2

### EXPERIMENTAL

#### 2.1 Chemicals and DNA Oligonucleotides

All chemicals and solvents used throughout this study were of reagent grade. Benzoic acid (Merck), p- amino benzoic acid (Merck), pyridine (Fisher), dopamine (Pharma), polyvinylalcohol (PVA) (MW: 88 000), 1-ethyl-3-(3-dimethylaminopropyl)carbodiimide (EDC), imidazole, dithiothreitol (DTT), chlorogoldric acid (HAuCl<sub>4</sub>), trisodium citrate, 3-aminopropyltriethoxysilane (APTS), brilliant cresyl blue (BCB), cresyl fast violet (CFV), crystal violet (CV), fluorescein isothiocyanate (FITC), 1-decanethiol, 11-mercapto-1-undecanol, tetrabutyl ammonium tetrafluoroborate (Sigma-Aldrich) were used without further purification.

All of the nucleic acid probes, target DNA oligonucleotides and oligo T spacer were purchased from Alpha DNA (Canada) and used without further purification. Nucleic acid sequences of the probes were designed considering the universally conserved domains of archaeal proteasome  $\beta$ -subunit and human proteasome beta peptide 7. The base sequences corresponding to the three nucleic acid probes were 5'-SH- CTG TGC CCG AAT CCC ATG (archaea proteasome gene sequence), 5'- CTG TGC CCG AAT CCC ATG (archaea proteasome gene sequence), 5'- GGC CCG AGA ATC CAC (human proteasome gene sequence), respectively. The base sequences of

the complementary targets DNA were 5'-SH-GAAGAGGCTCATGGGATTCGGGCACAGAGTATATAAGACATATGATCC (archaea proteasome gene sequence), 5'-SH-GAA GAG GCT CAT GGG ATT CGG GCA CAG (archaea proteasome gene sequence), 5'-SH- TTTTTTTTTT GCA GTG GAT TCT CGG GCC (human proteasome gene sequence) respectively. The base sequences of single and double base mismatched DNA, mismatched bases are underlined, were 5'- CTGTGCCCCGACTCCCATG (archaea proteasome gene sequence) , 5'- GGC CCG AGC ATC CAC (human proteasome gene sequence), 5'- GGC CCG GA A ATC CAC (human proteasome gene sequence). The base sequence of oligo T spacer was 5'-SH- TTTTTTTTTT.

All of the equipments and buffer solutions were sterilized in autoclave before the experiments.

## **2.2 Instrumentation**

### **2.2.1 Raman Spectrometer**

Jobin Yvon LabRam confocal microscopy Raman spectrometer with a charge-coupled device (CCD) detector and a holographic notch filter was used. The spectrograph was equipped with a 1800-grooves/mm grating and all measurements were carried out with a 200- $\mu$ m entrance slit. SERS excitation was supplied by 632.8 nm radiation from a He-Ne laser with a total power of 20 mW.

### **2.2.2 UV-VIS Spectrometer**

Absorbance measurements of oligonucleotides and gold nanoparticles were performed using a Cary 100 Bio UV-Visible spectrophotometer.

### **2.2.3 Potentiostat–Galvanostat**

Electroanalytical studies were performed using a Gamry PCI4/300 potentiostat–galvanostat.

### **2.2.4 Field Emission Scanning Electron Microscopy (FE-SEM)**

Shape and size characterization of gold nanoparticles were performed using a Quanta 400 F field emission scanning electron microscopy (FE-SEM) from FEI Company at METU central laboratory.

### **2.2.5 ZETA Potential and Mobility Measurement System**

Zeta potential of oligonucleotides and dye labelled oligonucleotides were measured at room temperature with a MALVERN Nano ZS90 Zetasizer at METU central laboratory.

### **2.2.6 Spin Coater**

To prepare SERS-active substrates Chematt Tecnology Spin-Coater KW-4A was used.

### **2.2.7 Centrifuge**

Sigma 2-16 model with a maximum capacity of 14000 rpm was used to centrifuge processes.

## 2.3 Procedures

### 2.3.1 Preparation of SERS-active Substrate

#### 2.3.1.1 Silver Nanoparticle-Doped Polyvinyl Alcohol Coated (PVA-Ag) Substrate

Glass microscope slides ( $20 \times 20$  mm) and indium tin oxide (ITO) glasses (Delta Tech.  $8-12 \Omega$ ,  $7 \text{ mm} \times 50 \text{ mm}$ ) were cleaned in ethanol several times. 5% (w/w) polyvinyl alcohol aqueous solution was prepared. After a homogeneous solution was obtained, different amounts of  $\text{AgNO}_3$  were added to 6 mL of this solution. This mixture was stirred at room temperature for 24 hours.  $150 \mu\text{L}$  of PVA- $\text{AgNO}_3$  solution was conveyed to the surface of the glass plate with care to ensure that the whole surface of the glass was covered. The plate was then spun at 2000 rpm for 20 s using a spinning device in order to disperse the PVA-Ag composite on the glass and ITO glass surfaces uniformly. The PVA-Ag coated plates were then dried overnight at  $60^\circ \text{C}$  and afterwards dried at  $100^\circ \text{C}$  for two hours.

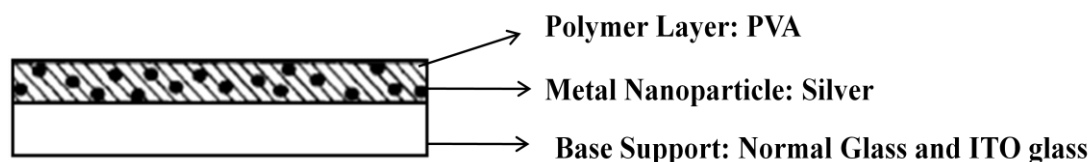


**Figure 14** Schematic representation of silver nanoparticle-doped polyvinyl alcohol coated (PVA-Ag) substrate.

Silver (I) ion was reduced to metallic silver by using chemical and electrochemical reduction. In chemical reduction, the dried glass substrates were dipped into 4% (w/w)  $\text{FeSO}_4 \cdot 7\text{H}_2\text{O}$  solution for 30 s for chemical reduction of  $\text{Ag}^+$  ions to silver metal nanoparticles, and then dried in an oven at  $100^\circ \text{C}$  for 15 minutes (**Karabiçak, Kaya, Vo-Dinh, & Volkan, 2008**).

For electrochemical reduction, half of the indium tin oxide glass coated by PVA-Ag substrate dipped into the electrochemical cell containing electrolyte solution of 0.1 M tetrabutyl ammonium tetrafluoroborate and -0.3 V potential was applied to reduce silver ion to metallic silver (Figure 15).

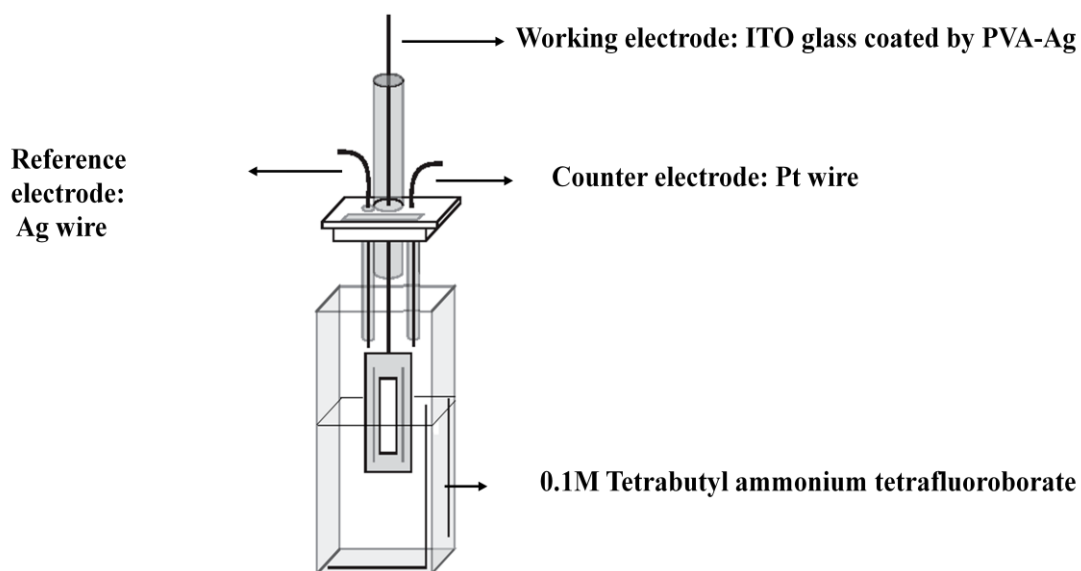


**Figure 15** Schematic representation of electrochemical reduction of PVA-Ag substrate.

## 2.3.2 Detection of Archaea and Human Proteosome Gene Sequences

### 2.3.2.1 Gold Colloid Preparation

Gold colloid was prepared by citrate reduction of  $\text{HAuCl}_4$  as described before (Grabar, Freeman, Hommer, & Natan, 1995). In a beaker, 50 mL of 1 mM  $\text{HAuCl}_4$  was brought to boil with vigorous stirring. Addition of 5 mL of 38.8 mM sodium citrate to the vortex of the solution rapidly resulted in a color change from pale yellow to deep red. Boiling was run on for 10 min.; the heating mantle was closed, and stirring was run on for an additional 15 min.

### **2.3.2.2 Gold Substrate Preparation**

Microscope slides were cut into square strips approximately 2.0 x 2.0 cm. The slides were cleaned by sequential sonication for 15 min. each in dilute nitric acid, ethanol and distilled water and finally dried in an oven before use. The slides were firstly immersed into %1 (v/v) 3-aminopropyltriethoxysilane (APTS) solution for 30 min. for silanization of the glass surface. After immersion, the slides were rinsed with deionized water several times. Then, silanized slides were immersed in gold colloid solution which was prepared by citrate reduction of  $\text{HAuCl}_4$  as described before **(Grabar, Freeman, Hommer, & Natan, 1995)**. After 72 hours, the slides were taken out and washed with deionized water to remove unbounded gold nanoparticles. Thus prepared gold nanoparticle coated surfaces are called as “gold substrate”.

### **2.3.2.3 Silver Colloid Preparation**

Silver colloid was prepared using a modified Lee and Meisel procedure **(Lee & Meisel, 1982)**. 9 mg  $\text{AgNO}_3$  were dissolved in 50 mL of deionized water and brought to boiling with rapid stirring. A solution of 1 mL of 1% sodium citrate was added into this solution and the contents were boiled for 30 min.; the heating mantle was closed, and stirring was applied for an additional 15 min.

### 2.3.2.4 Label Free Spectrophotometric Detection of Archaea Proteosome Gene Sequence

#### 2.3.2.4.1 5'-Oligonucleotide-Modified Gold Probe and Target Nanoparticles Preparation

Table 1 lists oligonucleotide sequences used in this experiment.

**Table 1** Oligonucleotide Sequences

Description	Oligonucleotide Sequence
<u>Archaea proteasome gene sequences</u>	
Target	SH-5'-GAAGAGGCT <b>CATGGGATTCGGGCACAG</b> AGTATATAAGACATATGATCC
Probe	SH-5'- <b>CTGTGCCCGAATCCCATG</b>

Note: Complementary bases are written in red color.

The 5'-thiol modified, single-stranded probe and target DNA molecules were bound to the gold nanoparticles separately following the procedure of Mirkin and workers (Storhoff, Elghanian, Mucic, Mirkin, & Letsinger, 1998). Prior to the functionalization of gold nanoparticles, the possible disulfide formation on the oligonucleotides was cleaved by treating the oligonucleotides with 0.1 M dithiothreitol (DTT) in phosphate buffer (0.18 M, pH 8) for 1 h (typically, 10 OD of DNA and 40  $\mu$ L DTT). Optical density (OD) of 1 at a wavelength of 260 nm corresponds to a concentration of 50  $\mu$ g/mL for double-stranded DNA. The cleaved oligonucleotides were purified using mini quick spin oligo columns (Sephadex G-25 medium, DNA grade, Roche Applied Science). Before applying the new spin column for the purification of the DNA, it was first vigorously inverted several times. Then, the top cap was removed from the column and the bottom tip was snapped off. The column was placed in a sterile 1.5 mL microcentrifuge tube and centrifuged at 1000 x g for 1 min at room temperature. The eluted buffer was discarded from the collection tube. While keeping the column upright, 300  $\mu$ L sterile distilled water was applied to the center of the column bed and centrifuged at 1000 x g for 2 min at room

temperature. The eluted buffer was discarded from the collection tube. The prepared column was placed in a clean, sterile 1.5 mL microcentrifuge tube. The sample was applied to the center of the column bed very slowly and carefully. Then the tube was centrifuged at 1000x g (speed) for 4 min. at room temperature in the microcentrifuge. The eluate in the second collection tube was saved. It contains the purified nucleic acid.

Freshly cleaved 2.25 OD oligonucleotides were added to 4.5 mL of aqueous solution gold nanoparticles and incubated at room temperature for 16 h. Then, the solutions were diluted with 10 mM phosphate buffer (pH 7) containing 0.1 M NaCl, up to 9 mL. After standing for 40 h, the solutions were centrifuged 25 min. at 14000 rpm to remove excess reagents. Following removal of the supernatant, the red oily precipitates were washed with 0.1 M NaCl, 10 mM phosphate buffer (pH 7) solution, recentrifuged, and redispersed in a 4.5 mL 10 mM phosphate buffer containing 0.3 M NaCl, (pH 7) (Figure 16).

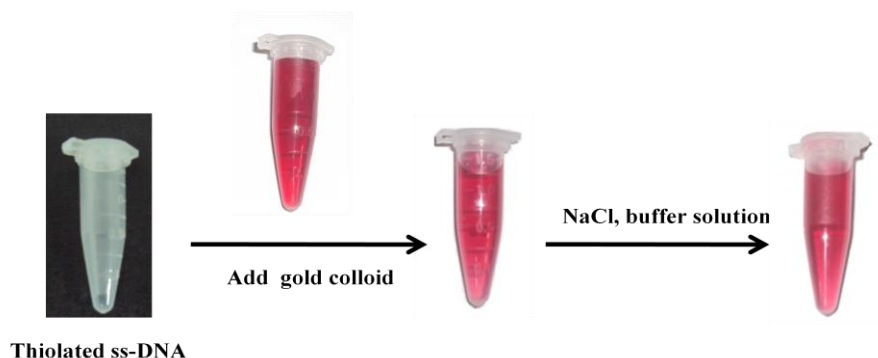


**Figure 16** Schematic representation of 5'-oligonucleotide-modified gold probe and target nanoparticles preparation.

#### 2.3.2.4.2 Hybridization of Oligonucleotide-Linked Gold Nanoparticle Probes with Targets in the Solution System

The target DNA was mixed with complementary probe DNA, each being modified with gold nanoparticles, in equal concentration. Then, the solution was heated to



60°C for 5 min. and then allowed to cool to room temperature. Approximately 2-3 h later, full precipitation had occurred and the solution was diluted to 3 mL with a 10 mM phosphate buffer (pH 7) containing 0.3 M NaCl solution (Figure 17).

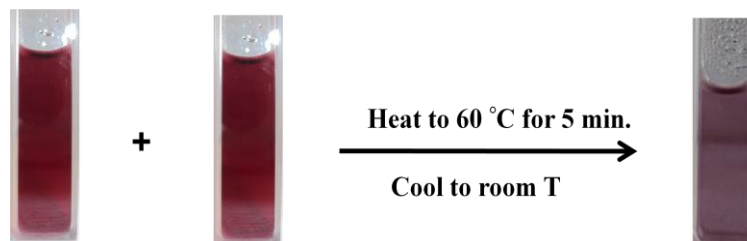


**Figure 17** Hybridization of oligonucleotide-modified gold nanoparticle probes with targets in the solution system.

### 2.3.2.5 SERS Detection of Archaea and Human Proteasome Gene Sequences

#### 2.3.2.5.1 Preparation of SERGen Probes

Brilliant cresyl blue (BCB), cresyl fast violet (CFV), crystal violet (CV) and fluorescein isothiocyanate (FITC) were used as SERS-active labels. The probe sequences were 5'- GGC CCG AGA ATC CAC (human proteasome gene sequence) and 5'- CTG TGC CCG AAT CCC ATG (archaea proteasome gene sequence).

##### 2.3.2.5.1.1 Covalent Labeling of Oligonucleotide Primers with BCB

In the covalent attachment of BCB to the oligonucleotide, the traditional method described by Chu *et al.* (Chu & Orgel, 1983) was used with minor modification (Vo-Dinh, Stokes, Griffin, Volkan, Kim, & Simon, 1999). Firstly, 2.25  $\mu$ L (0.5 OD) ss-DNA primer was converted to 5'-phosphoroimidazolide intermediates with 0.5 M 1-ethyl-3,3-dimethylaminopropyl carbodiimide in 20  $\mu$ L of 0.1 M imidazole (pH 6.0) by incubation at 50 °C for 3 h. The 5'-phosphorimidazolides were then reacted with the 0.02 M 20  $\mu$ L BCB for 18 h at 50 °C. Unreacted label was removed

from the reaction mixture by gel filtration on mini Quick Spin Oligo Columns (Figure 18,19).

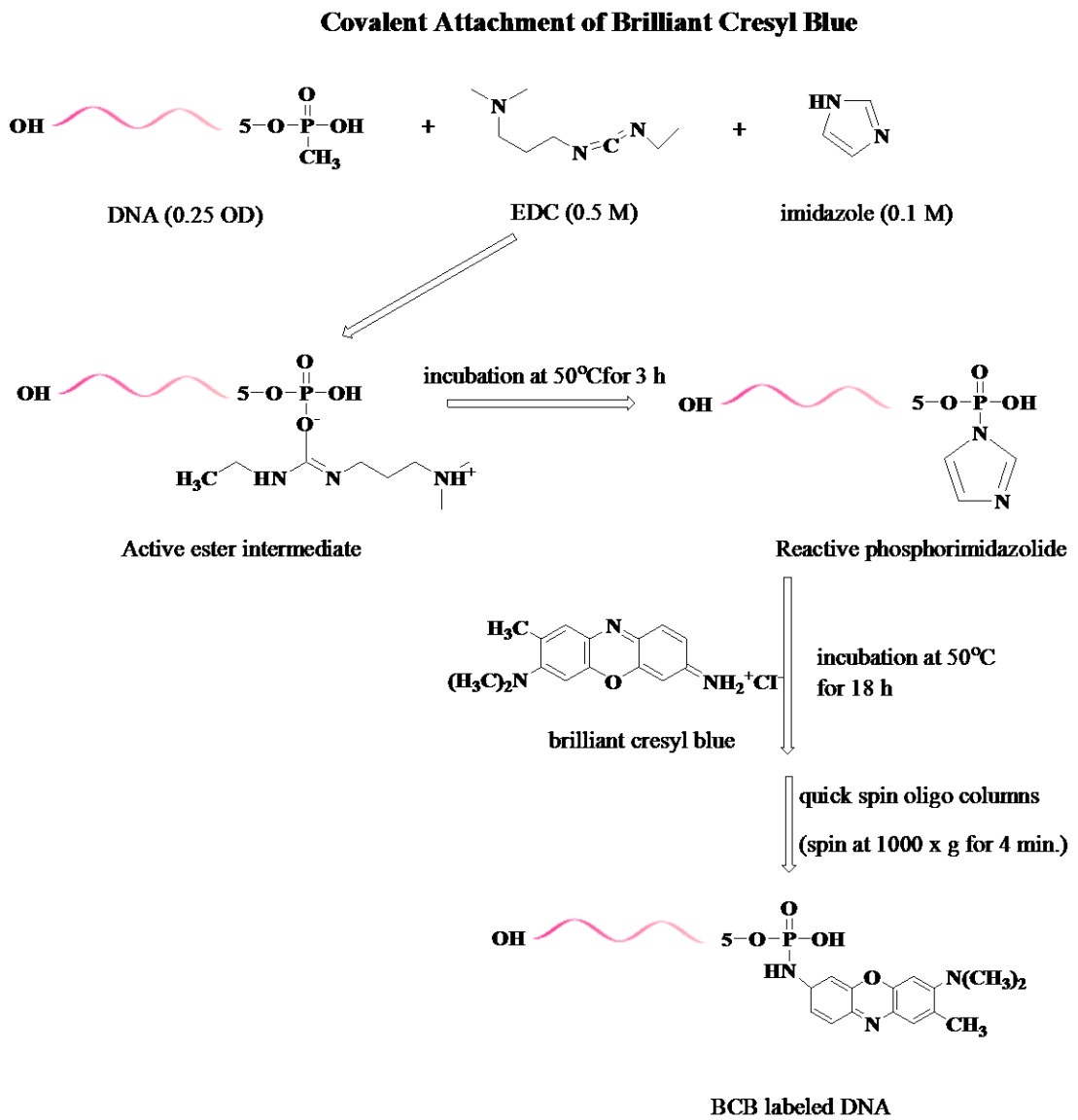


**Figure 18** Chemical reaction for BCB labeling of DNA covalently.

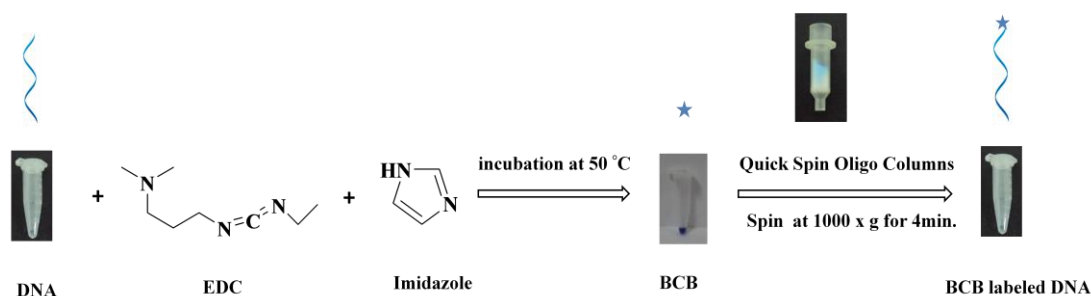


**Figure 19** Schematic representation of covalent labeling of DNA with BCB.

### 2.3.2.5.1.2 Noncovalent Labeling of Oligonucleotide Primers with BCB

In the electrostatic attachment of cationic dyes, BCB, CFV and CV, to the oligonucleotide, dye solution of  $20 \mu\text{L } 10^{-3} \text{ M}$  was added to the  $2.25 \mu\text{L}$  (0.5 OD) oligonucleotide and incubated at  $50^\circ\text{C}$  for 18 h. Unreacted label was removed from the reaction mixture by gel filtration on mini Quick Spin Oligo Columns (Figure 20).



**Figure 20** Schematic representation of noncovalent labeling of DNA with BCB.

Also this experiment was repeated at room temperature and with shorter incubation times for BCB.

For attachment of the neutral dye, FITC, to the oligonucleotide, dye solution of 20  $\mu\text{L}$   $10^{-3}$  M was added to the 2.25  $\mu\text{L}$  (0.5 OD) oligonucleotide and incubated at room temperature for 4 h. Unreacted label was removed from the reaction mixture by gel filtration on mini Quick Spin Oligo Columns.

#### **2.3.2.5.1.3 SERS Measurements of SERGen Probes**

The SERS spectra of BCB labeled oligonucleotides were measured utilizing silver nanoparticles as substrate either in wet or dry conditions. Wet means, SERS spectrum was recorded as soon as the droplet of silver colloid and BCB labeled oligonucleotides mixture were placed on the surface of glass plate (Figure 21). If the droplet of silver colloid and BCB labeled oligonucleotide mixture was dried before taking the SERS spectrum it was called as dry condition.

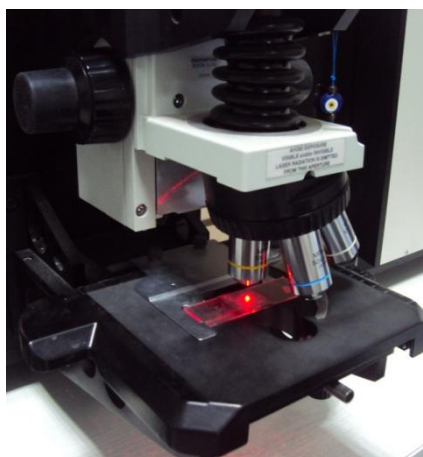


**Figure 21** The picture of SERS microscope.

#### **2.3.2.5.1.3.1 Zeta Potential Measurements of Unlabelled Oligonucleotides and Electrostatically labeled Oligonucleotides**

Zeta potentials of unlabelled oligonucleotide and electrostatically labeled oligonucleotides with BCB and FITC were measured (3 measurements per sample) with a MALVERN Nano ZS90 Zetasizer. Oligonucleotides were diluted to a concentration of 8.1  $\mu\text{M}$  in phosphate buffer (10 mM, pH 7.0) for the measurement of Zeta potentials.

#### **2.3.2.5.2 Immobilization of SERGen Probes onto the Gold Surface Under the Hybridization Conditions**

Electrostatically labeled SERGen probes were immobilized onto the gold surface under the hybridization conditions. SERGen probes (1  $\mu\text{M}$ ) were added onto the clean gold substrate in a mixture of 300  $\mu\text{L}$  10 mM phosphate buffer solution (pH 7) and 150  $\mu\text{L}$  2 M NaCl solution for 90 min. at room temperature. Following incubation, substrate rinsed with hybridization buffer solution three times.

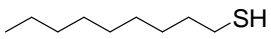
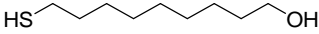
#### **2.3.2.5.3 Immobilization of SERGen Probes onto the Gold Surface After the Decanethiol Treatment Under the Hybridization Conditions**

The gold substrate (2.0 x 2.0 cm) was exposed to the aqueous solution of 1 mM 500  $\mu\text{L}$  decanethiol for 1 h. Then, substrate was washed with sterile water and SERGen probe was added onto the gold substrate in a mixture of 300  $\mu\text{L}$  10 mM phosphate buffer solution (pH 7) and 150  $\mu\text{L}$  2 M NaCl solution for 90 min. at room temperature. Following incubation, substrate was rinsed with hybridization buffer solution three times.

### 2.3.2.5.4 Hybridization Experiments

Table 2 lists oligonucleotide sequences used in this experiment.

**Table 2** Oligonucleotide Sequences and Spacers

Description	Oligonucleotide Sequences
<u>Archaea proteasome gene sequences</u>	
Target sequence	SH-5'-GAAGAGGCTCATGGGATTCGGGCACAG
Probe sequence	5'- CTGTGCCCGAATCCCATG
Noncomplementary sequence used as controls	5'- GAAGAGGCTCATGGGATTCGGGCACAG
<u>Human proteasome gene sequences</u>	
Target sequence	SH- 5'- TTTTTTTTTT GCA GTG GAT TCT CGG GCC
Probe sequence	5'- GGC CCG AGA ATC CAC
Noncomplementary sequence used as controls	5'- GCA GTG GAT TCT CGG GCC
Spacers	
Decanethiol	
11-mercapto-1-undecanol	
10 T Oligo	SH- 5'- TTTTTTTTTT

Note: Complementary bases are written in red color.

In hybridization, DNA targets refer to immobilized single strand DNA having unknown sequences and DNA probes refer to complimentary sequences of the unknown fraction of the target that will be captured. Hybridization experiments were performed with and without spacers. In all experiments, firstly, thiolated DNA targets were treated with the 0.1 M dithiothreitol (DTT) in phosphate buffer (0.18 M, pH 8) for 1 h (typically, 10 OD of DNA and 40  $\mu$ L DTT) to cleave the disulfide functionality on the oligonucleotides. The cleaved oligonucleotides were purified using mini quick spin oligo columns (Sephadex G-25 medium, DNA grade, Roche Applied Science). Freshly cleaved thiolated DNA targets (1  $\mu$ M) were added onto the clean gold substrates in 500  $\mu$ L 1 M phosphate buffer solution (pH 7) for 4 h. Then, gold substrates were washed with sterile water to remove unbound targets. SERGen probes (1  $\mu$ M) were added onto the gold substrate in 300  $\mu$ L 10 mM

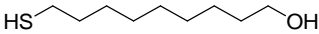
phosphate buffer solution (pH 7) and 150  $\mu\text{L}$  2 M NaCl solution for 90 min. at room temperature in the absence of spacer. When spacer was used, first, freshly cleaved thiolated DNA targets (1  $\mu\text{M}$ ) were added onto the clean gold substrates in 500  $\mu\text{L}$  1 M phosphate buffer solution (pH 7) for 4 h. Then, gold substrates were washed with sterile water to remove unbound targets. Then, gold substrates were exposed to the aqueous solution of 1mM 500  $\mu\text{L}$  spacer solution for 1 h. Subsequent to the substrate washing with sterile water, for hybridization, SERGen probes (1  $\mu\text{M}$ ) were added onto the gold substrate in 300  $\mu\text{L}$  10 mM phosphate buffer solution (pH 7) and 150  $\mu\text{L}$  2 M NaCl solution and incubated at 25 and 65 $^{\circ}\text{C}$  for 90 min. Before analysis, all substrates were washed by shaking with hybridization buffer solution and sterile water respectively, then silver colloid was added onto the surfaces to record SERS spectra.

As a negative control in hybridization, the non-complementary sequence, which has the same sequence as the immobilized target DNA without the HS- attachment at the 5' end, was labeled with BCB in the same way as the SERGen probe. Hybridization was performed as described before.

### 2.3.2.5.5 Hybridization of Target and Probe Containing Single Base and Double Base Mismatches

Oligonucleotide sequences and spacer used in these experiments are listed in Table 3.

**Table 3** Oligonucleotide Sequences and Spacer

Description	Oligonucleotide Sequences
<u>Archaea Proteasome Gene Sequences</u>	
Target sequence	SH-5'- GAAGAGGCTCATGGGATTCGGGCACAG
Probe sequence	5'- CTGTGCCCGA <b>C</b> TCCCATG
<u>Human Proteasome Gene Sequences</u>	
Target sequence	SH- 5'- TTTTTTTTTT GCA GTG GAT <b>T</b> CTCGG GCC
Probe sequence:	
Single Base Mismatch	5'- GGC CCG AG <b>C</b> ATC CAC
Double Base Mismatch	5'- GGC CCG <b>GA</b> A ATC CAC
Spacer	
11-mercapto-1-undecanol	HS  OH

Note: Mismatched bases are underlined and written in bold or in blue color.

Hybridization experiments were carried out with single and double mismatch probes according to the procedure given in the previous section (2.3.2.5.4 Hybridization Experiments)

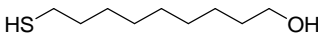


### 2.3.2.5.6 Quantitative Study

Oligonucleotide sequences used in these experiments are listed in Table 4.

**Table 4** Oligonucleotide Sequences and Spacer

---

<u>Human Proteasome Gene Sequence</u>	
Target sequence	SH- 5'- TTTTTTTTTT GCA GTG GAT TCT CGG GCC
Probe sequence	5'- GGC CCG AGA ATC CAC
Spacer	
11-mercapto-1-undecanol	

---

Note: Complementary bases are written in red color.

To make quantitative analysis, target concentration was kept fixed at 5  $\mu\text{M}$  and SERGen probes were prepared by increasing concentration stepwise from 0.5 to 5  $\mu\text{M}$ . Freshly cleaved thiolated DNA targets (1  $\mu\text{M}$ ) were added onto the clean gold substrates in 500  $\mu\text{L}$  1 M phosphate buffer solution (pH 7) for 4 h. Then, gold substrates were washed with sterile water to remove unbound targets. They were exposed to the aqueous solution of 500  $\mu\text{L}$  spacer solution for 1 h. Then, substrate was washed with sterile water. For hybridization, SERGen probes (0.5, 1, 2, 3, 4 and 5  $\mu\text{M}$ ) were added onto gold substrate in a mixture of 300  $\mu\text{L}$  10 mM phosphate buffer solution (pH 7) and 150  $\mu\text{L}$  2 M NaCl solution for 90 min. 55  $^{\circ}\text{C}$ . Before analysis, all substrates were washed by shaking with hybridization buffer solution and sterile water respectively, then silver colloid was added onto the surfaces to record SERS spectra.

## CHAPTER 3

### RESULTS AND DISCUSSION

#### 3.1 Silver Nanoparticle-Doped Polyvinyl Alcohol Coated (PVA-Ag) Substrate

The spin coating technique was chosen to produce thin and homogeneous coatings. The concentration of aqueous PVA solution was adjusted firstly due to the high viscosity of the PVA solution. From the experimental studies, it was found that 5 g PVA per 95 g of water (5 % w/w) were found sheer enough for spin coating. After the spin coating, the PVA-AgNO<sub>3</sub> solution-coated glass plates were colorless. The color of the substrates subsequently turned into yellow with time and became red following the drying step. It is proposed that (Hirai, Nakao, & Toshima, 1979) (Ho & Dalrymple, 1994) silver nitrate is dispersed in the PVA matrix in molecular form and Ag<sup>+</sup> is stabilized via coordination with the oxygen atoms in the preparation of PVA-AgNO<sub>3</sub> solution. However, the color change could be a sign of the formation of mono dispersed silver particles (Yen, 1996). Silver ions are usually reduced to metallic silver by chemical reduction (Krkljes, Nedeljkovic, & Kacarevic-Popovic, 2007) (Badr & Mahmoud, 2006) (Badr & Mahmoud, 2006) (Khanna, Singh, Charan, Subbarao, V.V.V.S., & Gokhale, 2005) (Mbhele, Salemane, Sittert, Djokovic, & Luyt, 2003) (Chou & Ren, 2000), electrochemical reduction (Liu, Yu, & Hsu, 2008) (Sauer, Nickel, & Schneider, 2000) and photoreduction (Gaddy,

**Korchev, McLain, & Slaten, 2004) (Gaddy, McLain, Steigerwalt, Broughton, Slaten, & Mills, 2001).**

Silver reduction can be made using various reducing agents. In this study, for chemical reduction, an aqueous solution of  $\text{FeSO}_4 \cdot 7\text{H}_2\text{O}$  (4% w/w) (**Volkan, Stokes, & Vo-Dinh, 1999**) which has been previously used in our studies, was employed as a reducing agent. The substrates were dipped horizontally into this solution and pulled out whenever the color of the coating turned into light gray (ca in 30s). The formation of the gray color can be ascribed to the clustering of silver particles in the water domain of the PVA-Ag nanocomposite throughout the diffusion period (**Yen, 1996**). The reduction time is kept at minimum because otherwise some of the silver clusters might be leached into the solution. A typical immersion time for reduction silver was 30 seconds. It is notable that PVA is a water soluble polymer. Consequently, coating was coming off when the substrates were dipped into  $\text{FeSO}_4 \cdot 7\text{H}_2\text{O}$  solution. In many studies (**Liang, Engert, & Kiefer, 1993**), particularly in PVA membrane preparations (**Ho & Dalrymple, 1994**), usually a cross-linking process is applied to avoid the dissolution of PVA. However we succeeded to overcome dissolution of the coating in the time period necessary for the reduction (ca 30s) simply by drying the plates overnight at  $60^\circ\text{C}$  after coating.

The most crucial parameter that needs to be investigated was the effect of concentration of  $\text{AgNO}_3$  in aqueous PVA solution. Substrates with different  $\text{AgNO}_3$  to PVA (5% w/w aqueous solution) weight ratios ( $R_w$ ) were prepared. The SERS activities of these substrates were investigated using  $10^{-2}$  M benzoic acid (BA) solution. The intense peak observed at  $1003\text{ cm}^{-1}$  was attributed to the ring-stretching vibration of the phenyl ring. Therefore, this peak was followed.

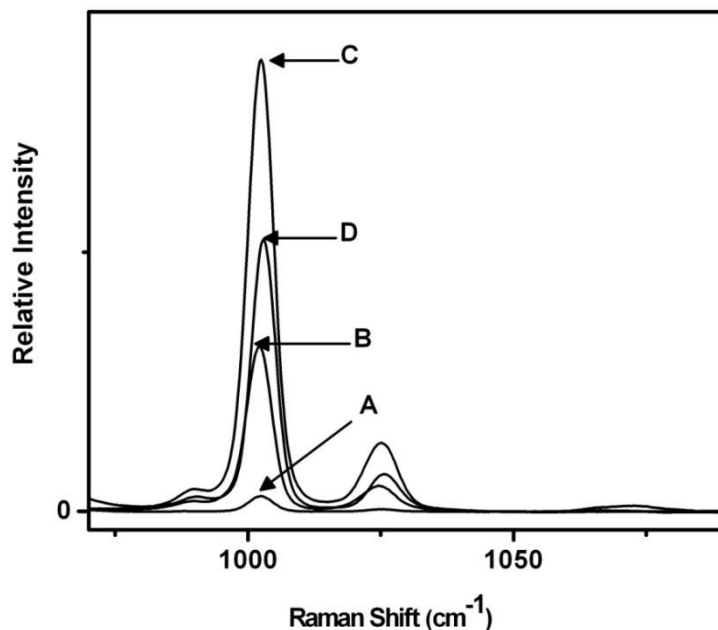


**Figure 22** The variation of the relative SERS intensities of BA ( $10^{-2}$  M) acquired with PVA-Ag SERS-active substrates having various  $\text{AgNO}_3$  to PVA weight ratios ( $R_w$ ) A) 0.08; B) 0.16; C) 0.24; D) 0.36.

As can be seen from the figure,  $\text{AgNO}_3$  to PVA (5 % w/w aqueous solution) weight ratio of 0.24 gives the substrate with the best SERS performance. When weight ratios of  $\text{AgNO}_3$  to PVA higher than 1, the intensity becomes zero. Silver island type structure (**Jennings, Aroca, Hor, & Loutfy, 1984**), which is appropriate for SERS enhancement, formed at the ratio of 0.24 that silver metals were most likely embedded into PVA matrix and separated from each other. On the other hand, a continuous metallic layer formation was observed at higher silver loadings on the surface. This fact was simply examined by two points conductance measurements. Conductivity was considered as a sign of continuous surface coverage by metallic silver particles. The surface that gave the best SERS enhancement (C in Figure 22) did not indicate any conductance while the ones, with which the SERS spectrum could not be obtained ( $R_w > 1$ ), showed metallic conductance designation that a continuous metal layer was formed on the surface. Thus, the weight ratio of 0.24 was adapted in the preparation of PVA- $\text{AgNO}_3$  solution in the following studies. It is necessary to accentuate that PVA-Ag nanocomposite coating provides a hydrophilic surface which is very advantageous for probing biological samples.

PVA-Ag coated ITO substrate was prepared using electrodeposition technique at optimized PVA and silver amounts (silver nitrate to PVA ratio is 0.24). In this technique, indium-tin oxide (ITO) coated by the PVA-Ag layer, silver wire and platinum wire were used as working electrode, reference electrode and counter electrode respectively. Half of the indium tin oxide glass coated by PVA-Ag substrate was dipped into the electrochemical cell and potential was applied to reduce silver ion to metallic silver. Reduction potential of silver was measured by scanning from -0.8V up to 0.8V and it was determined as -0.3 V. Although -400 mV was reported in the literature, the potential of enables to silver reduction (**Zhao, Shi, Wang, & Zhang, 2005**).

The performances of the SERS-active substrates obtained through both chemical and electrochemical reduction were evaluated with benzoic acid (BA) to make comparison between two substrates.

### **3.1.1 SERS Measurement of Benzoic Acid on PVA-Ag Substrate Prepared Through Both Chemical and Electrochemical Reduction**

Figure 23 shows the SERS spectrum of  $10^{-3}$  M aqueous BA solution obtained with the PVA- Ag substrates, chemical reduction, at optimized conditions.

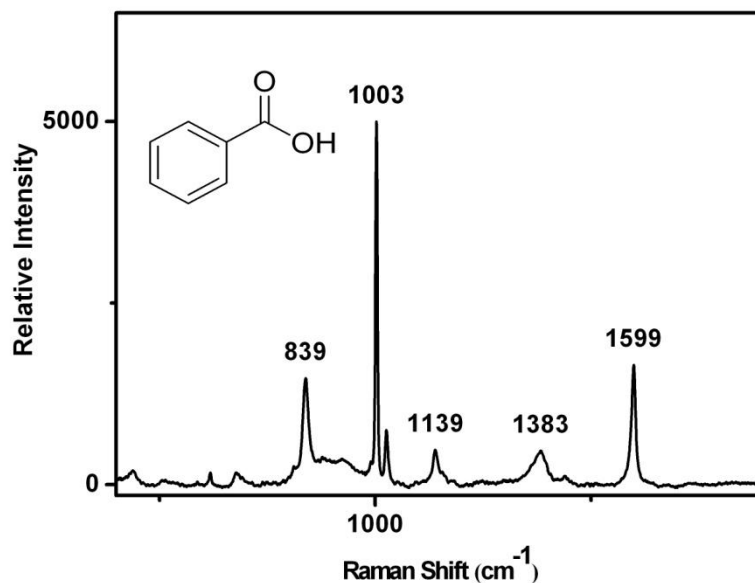


**Figure 23** SERS spectrum of  $10^{-3}$  M aqueous solution of BA acquired with PVA-Ag substrate ( $\text{AgNO}_3$  to PVA ratio was 0.24, chemical reduction).

According to the literature, the peak at  $998\text{ cm}^{-1}$  is arisen from the benzene ring stretching (Wang, Tang, & Ding, 2005), the band at  $1600\text{ cm}^{-1}$  and  $1140\text{ cm}^{-1}$  are arisen from the benzene ring vibration and C-H in-plane bending vibration, respectively (Li, Wang, & Cheng, 2001) and the symmetric vibration of  $\text{COO}^-$  ion takes place in the range of  $1440\text{-}1340\text{ cm}^{-1}$  (Dollish, Fateley, & Bentley, 1974). Therefore, the intense peak observed at  $1003\text{ cm}^{-1}$  was ascribed to the benzene ring-stretching. Whereas the peaks at  $1600\text{ cm}^{-1}$  and  $1141\text{ cm}^{-1}$  were attributed to the benzene ring vibration and C-H in-plane bending vibration, respectively, the small peak at  $1383\text{ cm}^{-1}$  was related to the  $\text{COO}^-$  ion vibration.

The SERS intensity of  $10^{-3}$  M aqueous BA solution at  $1000\text{ cm}^{-1}$  obtained with the electrochemically reduced PVA-Ag substrate (Figure 24) was six fold intense than that of the PVA- Ag substrates prepared by chemical reduction (Figure 23). SERS spectra of BA solutions at a concentration range of  $10^{-4}\text{-}10^{-6}$  M acquired with electrochemically reduced PVA-Ag substrate are presented in Figure 25. As can be seen from the Figure the most intense peak at  $1003\text{ cm}^{-1}$  is still observable at  $10^{-6}$  M

concentration. However, at this low concentration the back ground signal arised from PVA coating becomes predominant. Hence a new peak was observed at  $1700\text{ cm}^{-1}$  at low concentrations( $\sim$  below  $10^{-5}\text{M}$ ). It was assigned to the vibration of carbonyl residual acetate (**Badr & Mahmoud, 2006**).

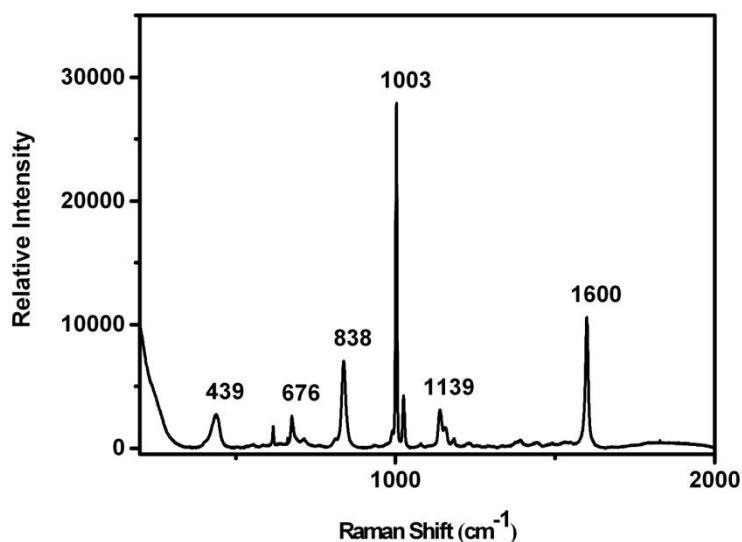


**Figure 24** SERS spectrum of  $10^{-3}$  M aqueous solution of BA acquired with PVA-Ag substrate ( $\text{AgNO}_3$  to PVA ratio was 0.24, electrochemical reduction).

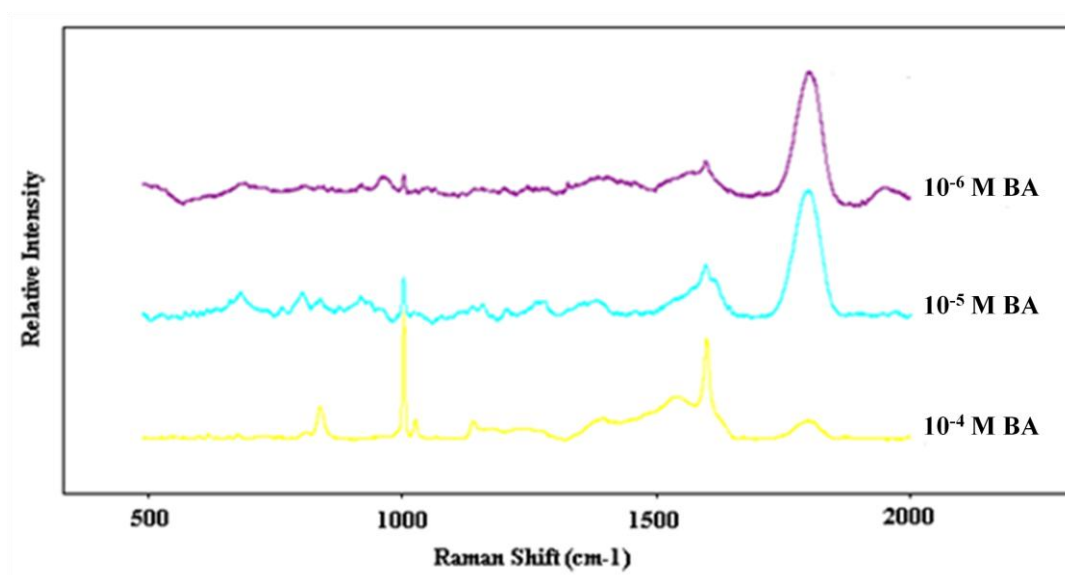


**Figure 25** SERS spectra of different concentrations of BA solution acquired with PVA-Ag substrate (electrochemical reduction).

The homogeneity of the surface coverage of the electrochemically prepared PVA-Ag substrates was examined visually and dark regions caused by the aggregation of silver nanoparticles at certain points of the surface were recognized by eye (Figure 26). Moreover, SERS studies have shown that high intensity SERS signals were acquired only from these dark spots.

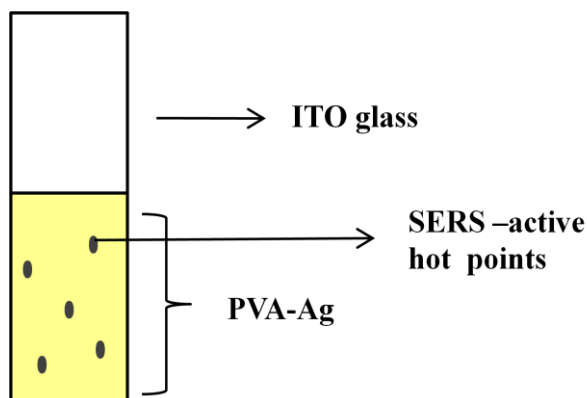


**Figure 26** Schematic representation of PVA-Ag coated ITO after the electrochemical reduction.

We decided to use PVA-Ag substrates prepared by chemical reduction due to the heterogeneity of the PVA-Ag coated ITO surface. Biologically important compounds frequently used in SERS studies, p-amino benzoic acid (PABA), pyridine and dopamine, were examined using SERS-active substrates obtained through chemical reduction.

### **3.1.2 SERS Measurement of p-Amino Benzoic Acid (PABA) on PVA-Ag Substrate**

The spectrum of  $10^{-4}$  M aqueous solution of PABA acquired with PVA-Ag substrate is shown in Figure 27. Previous literature values were employed to band assignments (Liang, Engert, & Kiefer, 1993) (Laserna, Torres, & Winefordner, 1987) (Suh, DiLella, & Moskovits, 1983) (Ibrahim, Oldham, Stokes, & Vo-Dinh, 1996). It has been admitted that, PABA molecules presume a flat position on the SERS active surface rather than “stand up”, binding through either the carboxylate or amine group



(Liang, Engert, & Kiefer, 1993) (Laserna, Torres, & Winefordner, 1987) (Ibrahim, Oldham, Stokes, & Vo-Dinh, 1996).

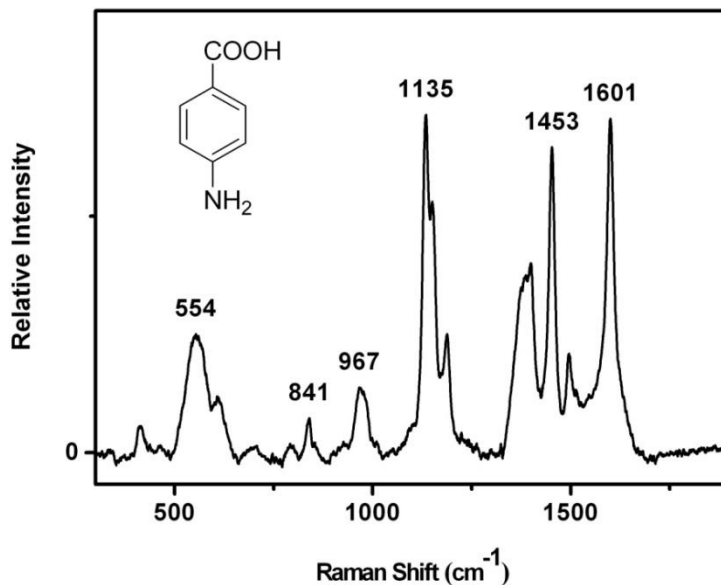


**Figure 27** SERS spectrum of  $10^{-4}$  M aqueous solution of PABA acquired with PVA-Ag substrate.

At high PABA concentrations, the molecules make hydrogen bonds between  $\text{NH}_2$  and  $\text{COO}^-$  groups. Hence, as the molecule bonded through the benzene ring of PABA, thus benzene ring vibrations,  $1515\text{ cm}^{-1}$ ,  $1452\text{ cm}^{-1}$  and  $1598\text{ cm}^{-1}$  are strongly displayed in the SERS spectrum (Suh, DiLella, & Moskovits, 1983). On the other hand, at low PABA concentrations, the adsorbed molecules isolated on the surface and then adsorbed by means of both the carboxyl and amino groups. Therefore, the vibrations arised from these groups are emphasized. The band at  $1389\text{ cm}^{-1}$  corresponds to the  $\text{COO}^-$  stretching and vibrations at  $1615\text{ cm}^{-1}$  and  $1452\text{ cm}^{-1}$  correspond to the benzene ring vibration and  $\text{NH}_2$  bending respectively (Liang, Engert, & Kiefer, 1993) (Laserna, Torres, & Winefordner, 1987) (Suh, DiLella, & Moskovits, 1983).

The most noticeable peaks observed in the SERS spectrum of PABA acquired with PVA-Ag substrates are  $1399\text{ cm}^{-1}$ ;  $1452\text{ cm}^{-1}$  and  $1503\text{ cm}^{-1}$ ;  $1135\text{ cm}^{-1}$ , and  $1600\text{ cm}^{-1}$ . These peaks correspond to the  $\text{COO}^-$  stretching,  $\text{NH}_2$  bending and benzene ring stretching vibrations, respectively and values closely match up those reported in the literature. Consequently, we conclude that PABA molecules are adsorbed through mainly  $\text{NH}_2$  and benzene groups to the PVA-Ag substrate. The adsorption of  $\text{COO}^-$  group on the substrate seems weak compared to that of the others.

### 3.1.3 SERS Measurement of Pyridine on PVA-Ag Substrate

Many workers have searched SERS spectra of pyridine (**Brolo, Irish, & Lipkowski, 1997**) (**Saito, 1993**) (**Temperini, Sala, Lacconi, Gioda, Macagno, & Arvia, 1988**) (**Zhang, Liu, He, & Xin, 1995**). Most of these SERS studies were conducted on silver (**Saito, 1993**) (**Temperini, Sala, Lacconi, Gioda, Macagno, & Arvia, 1988**) and gold (**Brolo, Irish, & Lipkowski, 1997**) electrodes. Intense SERS peaks for neutral pyridine is symmetric ( $1008\text{ cm}^{-1}$ ) and asymmetric ( $1038\text{ cm}^{-1}$ ) breathing vibrations of the ring (**Temperini, Sala, Lacconi, Gioda, Macagno, & Arvia, 1988**). It has been reported that (**Brolo, Irish, & Lipkowski, 1997**) pyridine adsorption on the surface occurs through nitrogen lone pairs (end-on configuration). Figure 28 represents the SERS spectrum of  $10^{-1}\text{ M}$  pyridine acquired by PVA-Ag substrate. As can be seen from the figure, the bands at  $1037\text{ cm}^{-1}$  and at  $1008\text{ cm}^{-1}$  correspond to the symmetric and asymmetric breathing vibrations of the pyridine ring respectively.

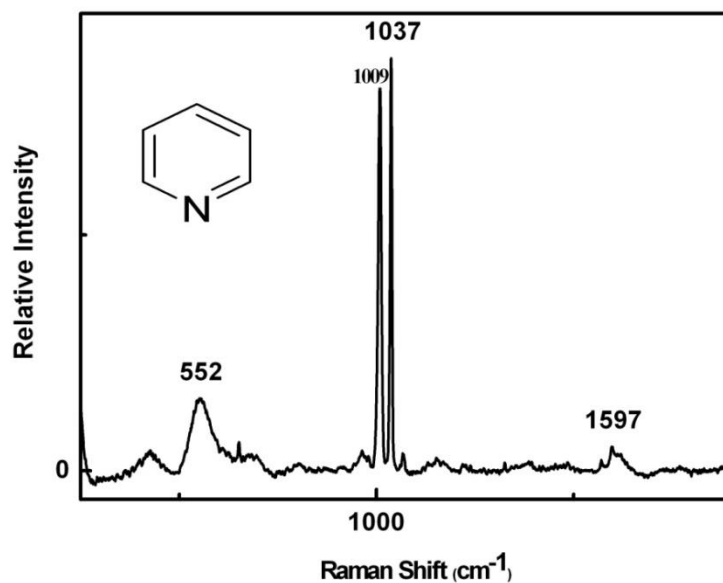
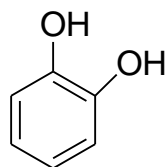


**Figure 28** SERS spectrum of  $10^{-1}$  M aqueous solution of pyridine acquired with PVA-Ag substrate.

### 3.1.4 SERS Measurement of Dopamine on PVA-Ag Substrate

The SERS spectrum of  $10^{-4}$  M solution of dopamine is shown in Figure 30. In the dopamine structure, 3,4-dihydroxyphenyl group is called catechol (**Wikipedia, 2010**).



Catechol

**Figure 29** Structure of catechol.

The most intense band around  $1480\text{ cm}^{-1}$  has arisen from the ring stretching vibration, contributed mainly by the stretching of the CO-CO bond. The band around  $1267\text{ cm}^{-1}$  was ascribed to the stretching of the catechol CO bond. The remaining

bands correspond to the various rings stretching vibrations (Salama, Stong, Neilands, & Spiro, 1978).

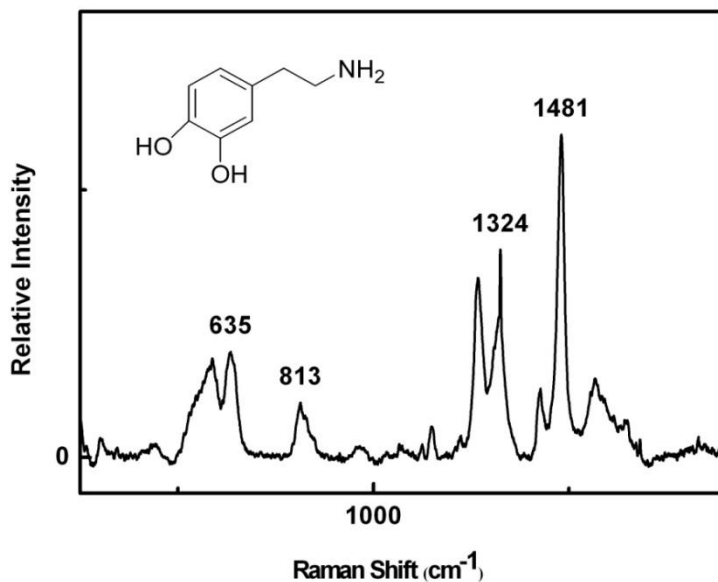


**Figure 30** SERS spectrum of  $10^{-4}$  M aqueous solution of dopamine acquired with PVA-Ag substrate.

## 3.2 Detection of Archaea and Human Proteosome Gene Sequences

### 3.2.1 Characterization of Gold Colloid

In this study, gold nanoparticles with 13 nm in diameter were chosen since they can be readily prepared with little deviation in size and show a sharp plasmon absorption band (Figure 31).

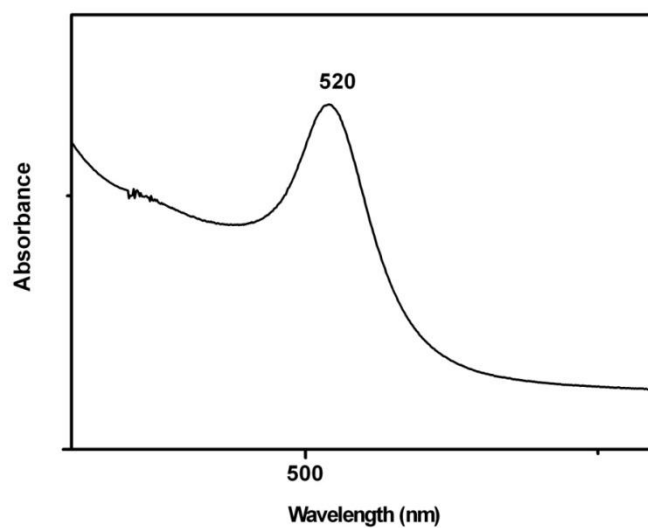


**Figure 31** Absorbance spectrum for gold colloid has a  $\lambda_{\text{max}}$  at 520 nm.

Absorption measurement was performed after 5-fold dilution of gold colloid with de-ionized water (0.0002 M). Maximum absorbance was observed at wavelength 520 nm. According to the literature, gold nanoparticles with size distribution of 9-22 nm display maximum absorption around 500-550 nm.

### 3.2.2 Characterization of Gold Substrate

The gold substrate was prepared as described in section 2.2.2.2. Morphological character of gold surface was demonstrated using FE-SEM microscopy. The monodisperse size distribution of gold nanoparticles with spherical shape are displayed in FE-SEM image (Figure 32).

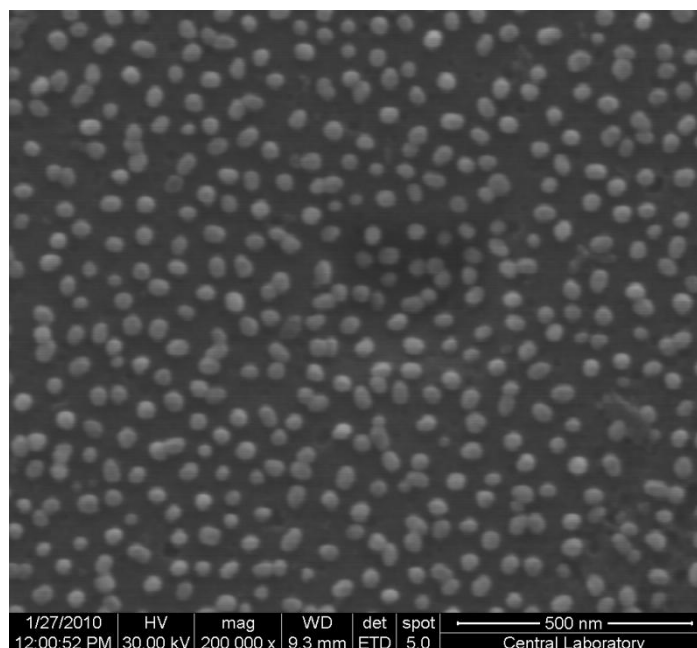


**Figure 32** FE-SEM image of gold nanoparticles deposited on silanized glass slide.

### **3.2.3 Characterization of Silver Colloid**

Silver colloid was prepared as described in section 2.2.2.3. Absorption measurement was performed after 5-fold dilution of silver colloid with de-ionized water. Maximum absorbance was observed at wavelength 440 nm (Figure 33). Spherical shape silver nanoparticles with size distribution of 60-80 nm display maximum absorption around 410-440 nm.

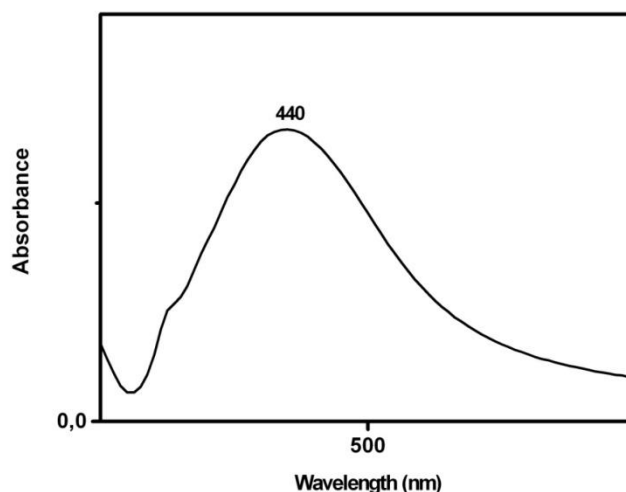


**Figure 33** Absorption spectrum for silver colloid has a  $\lambda_{\max}$  at 440 nm.

### **3.2.4 Label Free Spectrophotometric Detection of Archaea Proteosome Gene Sequence**

#### **3.2.4.1 Characterization of 5'-Oligonucleotide-Modified Gold Probe and Target Nanoparticles**

We detected specific archaea proteasome gene sequence by spectrophotometric method. In this method, firstly, archaea proteasome gene probe and complementary target gene sequences were attached to the gold nanoparticles separately. Then, the target and probe oligonucleotide-modified gold solutions were mixed for the hybridization and the shift in the surface plasmon absorption band of gold nanoparticles were followed.

5'-oligonucleotide modified gold probe and target nanoparticles were prepared as described in section 2.3.2.4.1. To attach of the oligonucleotides to the gold nanoparticle, 5'-end of the thiol modified gene sequences were used. The terminal sulfur atoms of thiolated DNA form disulfide bonds (DNA- C5-S-S-C5-DNA) in the

presence of oxygen which, prevents the attachment of DNA to the gold nanoparticles. Therefore, a reducing agent, DTT, was used to break the disulfide bonds, yielding DNA with the thiol group at the 5' end of the oligonucleotide (Green, Liu, Cohen, Köllensperger, & Cass, 2006). Oligonucleotides were expected to be attaching to gold nanoparticles from their thiol portion. However, they have other functional groups (amines, carbonyls) and negatively charged DNA backbone that would be involved in the attachment process (Figure 34 A). These secondary interactions between the oligonucleotide and the gold nanoparticle should be prevented for maximizing the number of surface-bound targets that are accessible for specific hybridization with complementary oligonucleotides.

Therefore, salt was added to weaken the electrostatic interaction between the oligonucleotide portion of the adsorbate and the positively charged nanoparticle surface. In other words, the salt provided electroneutral medium (Figure 34 A).

Gold nanoparticles display strong surface plasmon band in the UV-region. Therefore, the attachments of thiolated probe and target oligonucleotides to gold nanoparticles were confirmed by UV-Vis absorption. After thiolated DNA adsorption on gold nanoparticles, only a modest shift in the surface plasmon band from 520 (Figure 34 B) to 525 nm (Figure 34 C) was observed. The shift of surface plasmon band could arise from salt addition as an electrolyte. This addition caused charge screening effects on gold nanoparticles and a change in the dielectric constant of the medium. In addition, particle size distribution of DNA modified gold nanoparticles may be affected by centrifugation. Surface modification of gold nanoparticles with oligonucleotide induced decrease in intensity of plasmon band due to the decrease in particle concentration during the centrifugation steps.

This experiment was repeated several times and reproducible results were obtained.



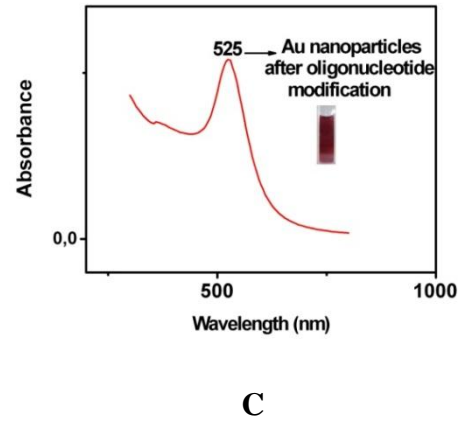
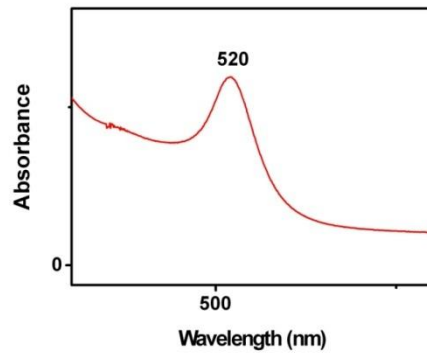
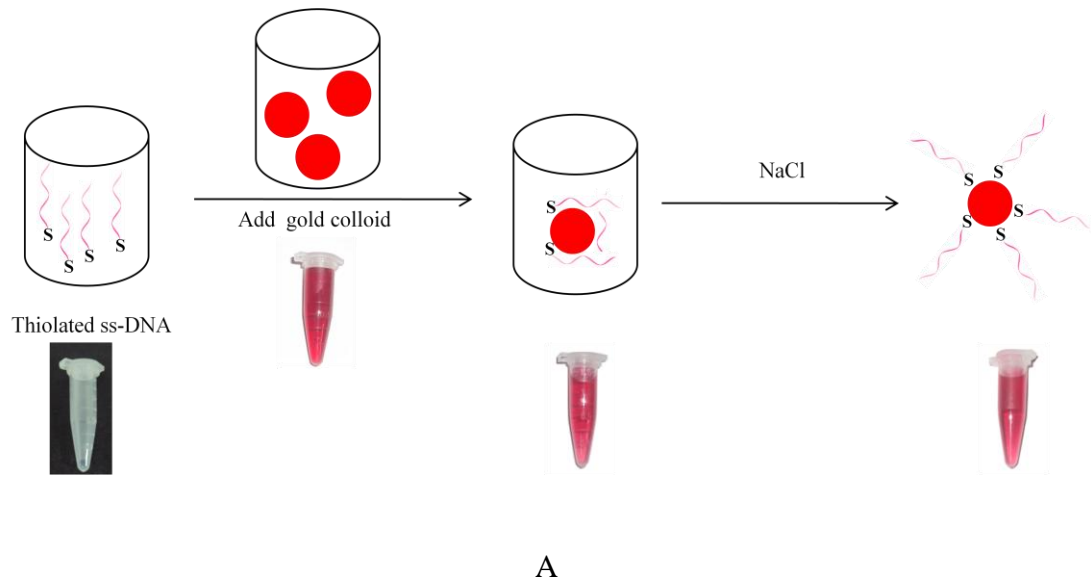


**Figure 34** A) Schematic representation of preparation of 5'-oligonucleotide-modified gold probe and target nanoparticles. UV-vis spectra for B) gold nanoparticles C) gold nanoparticles functionalized with target and probe oligonucleotides.

### **3.2.4.2 Hybridization of Oligonucleotide-Modified Gold Nanoparticle Probes with Targets in the Solution System**

When gold nanoparticles functionalized with single-stranded oligonucleotide as a probe are mixed with gold nanoparticles functionalized with a target of complementary DNA, aggregate formation occurs (**Park, Lee, Georganopoulou, & Mirkin, 2006**).

Prepared oligonucleotide-modified gold probe and target were hybridized to detection of gene sequence. Hybridization was performed as described in section 2.3.2.4.2. As a result of the hybridization experiment aggregate formation was observed (Figure 35 A). Hybridization induced the formation of a polymeric network of DNA-gold nanoparticles with a concomitant red-to-purple color change. The signal for colorimetric hybridization was conducted by the optical properties of the nanoparticles, which depend in part on their spacing within the polymeric network (Figure 35 C). In solution, monodisperse 13-nm diameter gold nanoparticles seemed red and showed a relatively narrow surface plasmon absorption band centered at 520 nm in the UV–vis region. On the contrary, a solution involving aggregated gold nanoparticles appeared purple in color, corresponding to a red shift in the surface plasmon resonance of the particles from 520 to 557 nm (554, 555, 560 nm).

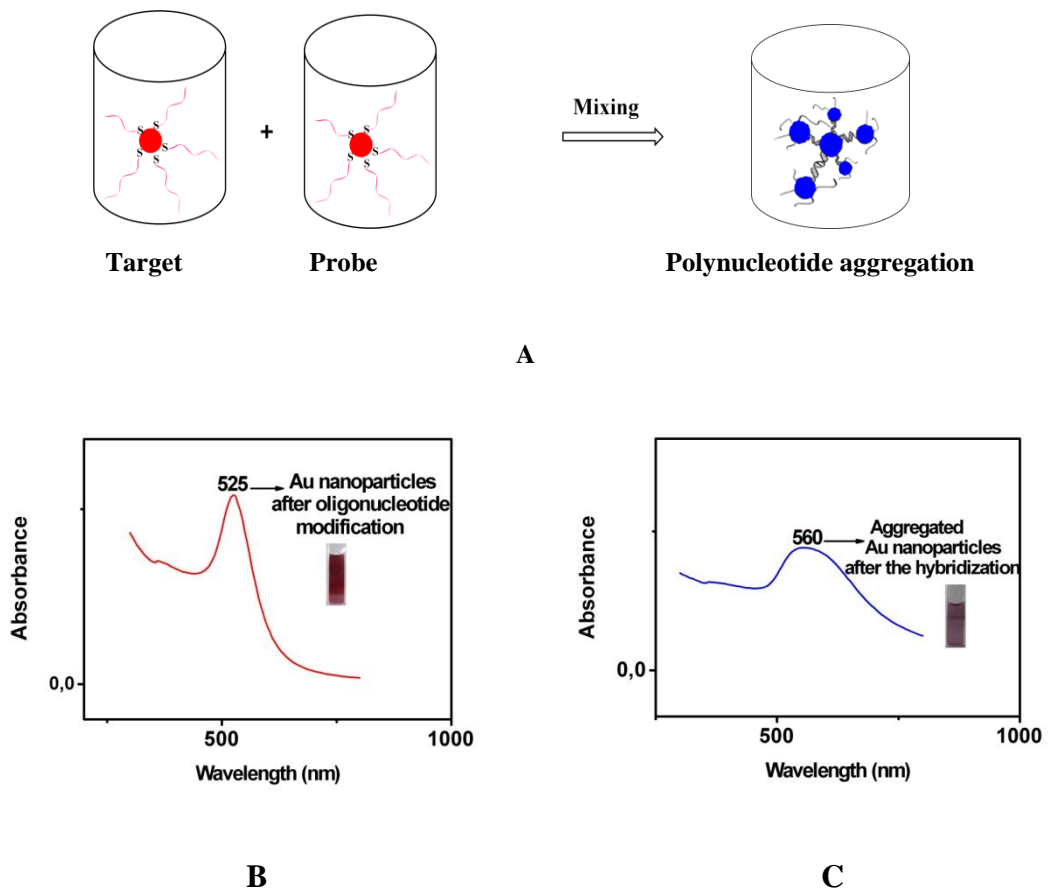
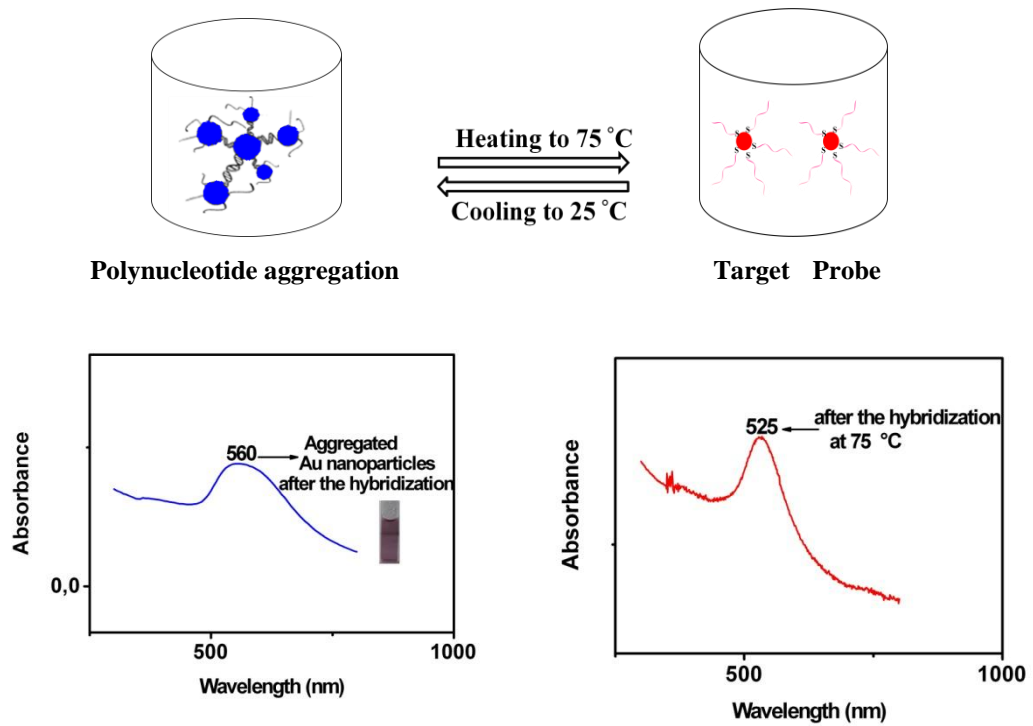
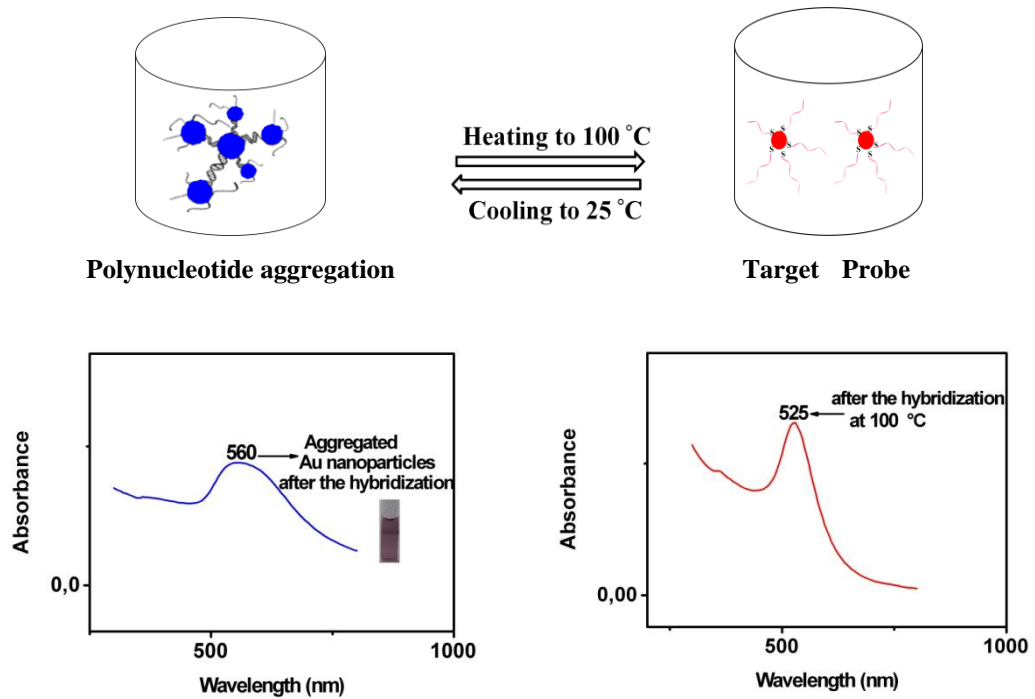


**Figure 35** A) Schematic representation of hybridization. UV-vis spectra for B) gold nanoparticles functionalized with target and probe oligonucleotides, C) gold nanoparticles modified with target oligonucleotide after treatment with gold nanoparticles modified complementary probe DNA at 60 °C for 5 min.

At room temperature, gold probe/target polynucleotides are aggregated. However, aggregation of gold probe/target polynucleotide is a reversible process. In other words, heating of the aggregated polynucleotide causes separation of gold probe and gold target oligonucleotide from each other. To investigate thermally dissociation of gold probe/target polynucleotide aggregate(s), the temperature was increased from 25 °C to 75 °C and 25 °C to 100 °C and the color of the solution was monitored (Figure 36).



A



B

**Figure 36** UV-vis spectra for thermal dissociation of polynucleotide aggregate at A) 75 °C, B) 100 °C.

The UV-Vis spectra of thermal dissociation of polynucleotide aggregates at 75 and 100 °C are shown in Figure 36 A, Figure 36 B respectively. As can be seen from these figures, the particles were reversibly dissociated inducing a blue shift in the surface plasmon absorbance to 525 nm, so, appearing red in color. As can be seen from these spectra, sharper plasmon band was obtained from polynucleotide aggregates heated to 100 °C compared to that of 75 °C due to the more complete dissociation of the aggregates.

### **3.2.5 SERS Detection of Archaea and Human Proteasome Gene Sequences**

#### **3.2.5.1 Characterization of SERGen Probes**

The SERS method includes SERS-active platforms and the surface-enhanced Raman gene (SERGen) probes that can be utilized to detect DNA targets via hybridization to DNA sequences complementary to these probes. Therefore labeled oligonucleotides are required for detection of nucleic acid sequences. Two-step labelling strategy was carried out in this study. First 5' phosphate group of DNA was activated which was subsequently to be modified with a dye. Brilliant cresyl blue (BCB), cresyl fast violet (CFV), crystal violet (CV) and fluorescein isothiocyanate (FITC) were used as Raman active labels. Their SERS spectra (Figure 37, 38, 39 and 40) were obtained and assignments of peak positions were done according to the literature. Silver nanoparticles were used as substrate.

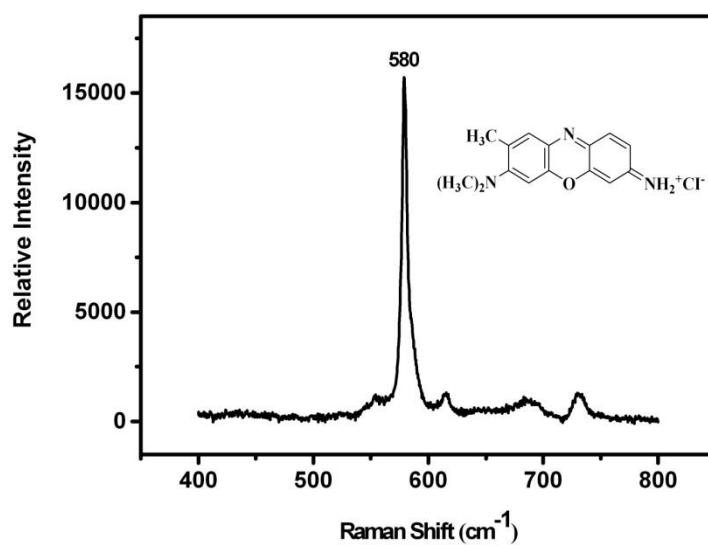


**Figure 37** SERS spectrum of  $10^{-6}$  M MCB solution on silver colloid in dry condition.

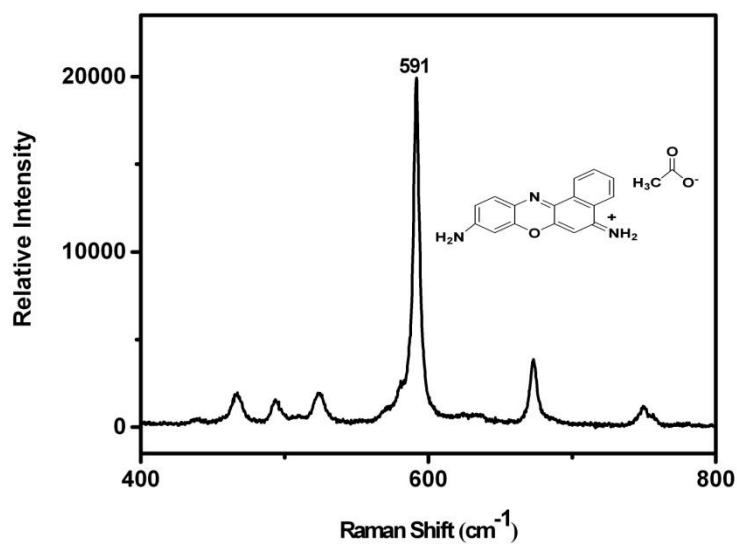


**Figure 38** SERS spectrum of  $10^{-6}$  M CFV solution on silver colloid in dry condition.

For the SERS spectra of BCB (Figure 37) and CFV (Figure 38) the intense bands observed at  $580\text{ cm}^{-1}$  and at  $590\text{ cm}^{-1}$  respectively were assigned to their benzene ring deformation modes. (Törnblom & Henriksson, 1997) (Vo-Dinh, Stokes, Griffin, Volkan, Kim, & Simon, 1999).

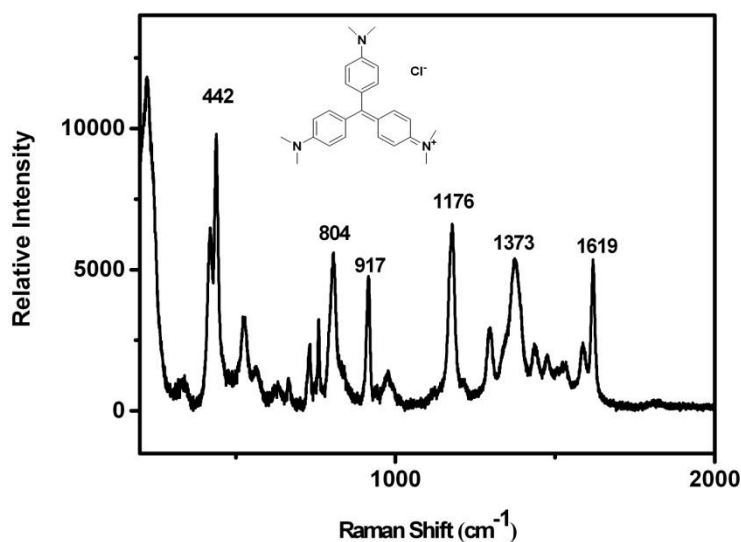


**Figure 39** SERS spectrum of  $10^{-6}$  M CV solution on silver colloid in dry condition.

According to the literature, the bands at  $795\text{ cm}^{-1}$ ,  $922\text{ cm}^{-1}$  and  $1170\text{ cm}^{-1}$  were arised from C–H out-of-plane bending, the ring skeletal vibration and C–H in-plane bending vibrations respectively for the SERS spectrum of CV. Therefore, in Figure 40, the peak at  $804\text{ cm}^{-1}$  was ascribed to the C–H out-of-plane bending. Whereas the peaks at  $917\text{ cm}^{-1}$  and  $1176\text{ cm}^{-1}$  were attributed to the ring skeletal vibration and C–H in-plane bending vibration, respectively (Volkan, Stokes, & Vo-Dinh, 1999).

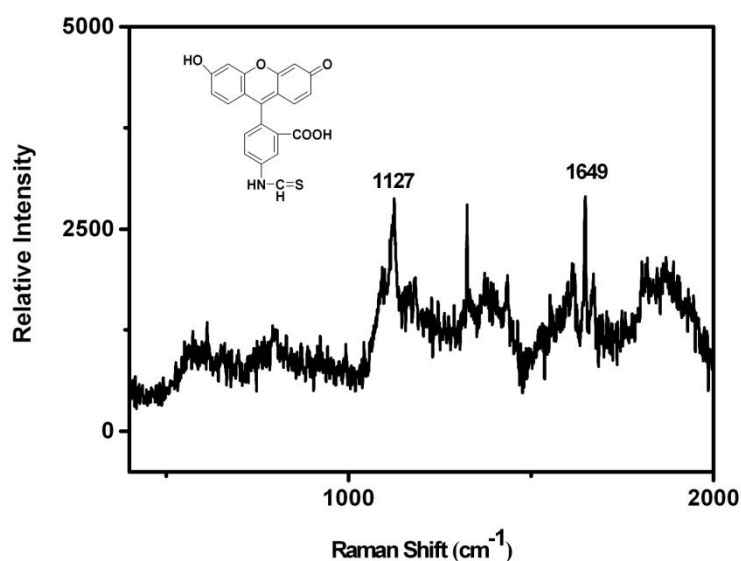


**Figure 40** SERS spectrum of  $10^{-5}$  M FITC solution on silver colloid in dry condition.

The benzene ring vibration and C-H in-plane bending vibration bands of FITC (Figure 40) were observed at around  $1600\text{ cm}^{-1}$  and  $1140\text{ cm}^{-1}$  respectively as stated in the literature (Li, Wang, & Cheng, 2001).

### 3.2.5.1.1 Covalent Labeling of Oligonucleotide Primers with BCB

In the covalent attachment of BCB to the oligonucleotide, EDC was used for the activation of 5' phosphate group. The chemical reaction for labeling of oligonucleotide with BCB is shown in Figure 18. Firstly, 5' phosphate group of oligonucleotide was converted to 5'-phosphoroimidazolide intermediates with solution of EDC in imidazole (pH 6.0). After incubation at  $50\text{ }^{\circ}\text{C}$  for 3 h., BCB was added and incubation was extended for another 18 h. BCB was attached through amine functional group to the oligonucleotide by replacing the leaving group. Unreacted BCB was removed from the reaction mixture by gel filtration on mini Quick Spin Oligo Columns.



The SERS spectra of BCB labeled oligonucleotides were recorded in wet (Figure 41) and dry (Figure 42) conditions as described in section 2.3.2.5.1.3.

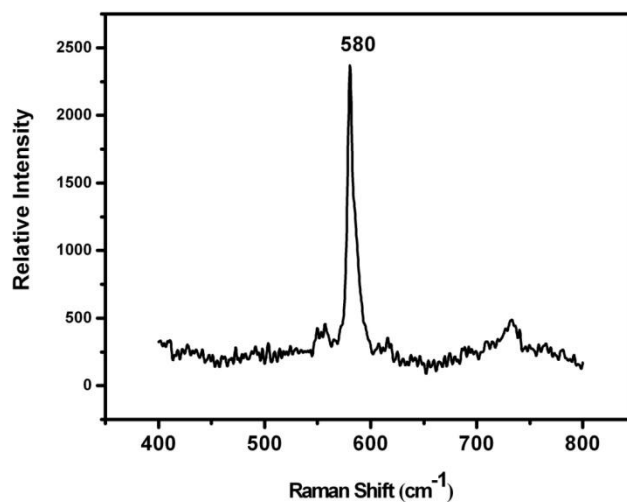


**Figure 41** SERS spectrum of BCB labeled DNA probe solution acquired by using silver colloid in wet condition. Labeling was done covalently.

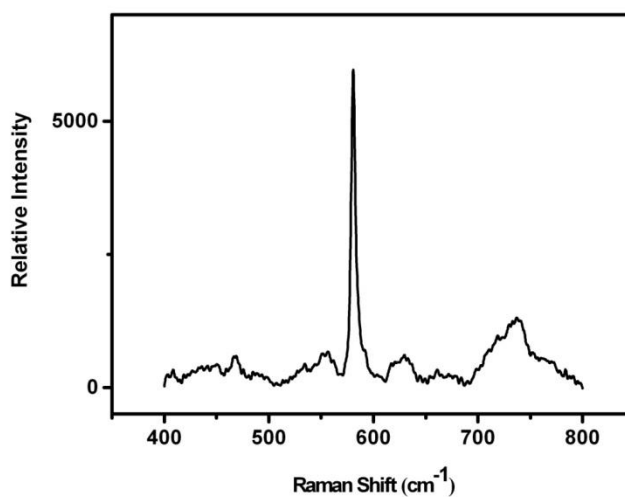


**Figure 42** SERS spectrum of BCB labeled DNA probe solution acquired by using silver colloid in dry condition. Labeling was done covalently.

The intense band at  $580\text{ cm}^{-1}$  is assigned to the benzene ring deformation mode of BCB. As can be deduced from the Figures 41 and 42, the SERS signal acquired from dried droplet was twice more intense than that of wet one. It needs to be pointed out that, this intense signal was obtained from the edges of the dry droplet due to the accumulation of the particles at the periphery of the droplet under the control of surface tension.

### 3.2.5.1.2 Noncovalent Labeling of Oligonucleotide Primers with BCB

Brilliant cresyl blue (BCB) is a kind of quinone-imide dye and positively charged in neutral solutions.

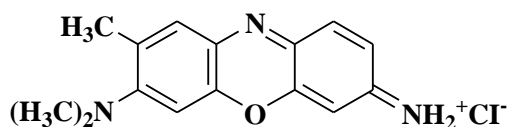


**Figure 43** The chemical structure of BCB

The noncovalent interaction between BCB and nucleic acids was accounted for the cumulative effect of electrostatic attraction and hydrophobic forces. Since BCB is a cationic dye that could bind to nucleic acids, anionic biomacromolecules, mainly through electrostatic way. Naturally, the pentaglucose may coordinate the BCB molecule and base hydrogens of DNA may participate in hydrogen bond formation with the nitrogen atoms in the BCB molecule (Wang, Zhao, Li, & Tong, 2000). Referring to the larger contribution of electrostatic attraction to noncovalent interactions, for cationic dyes electrostatic attachment and noncovalent attachment were used interchangeably.

Electrostatic attachment of BCB to the oligonucleotide was performed as described in section 2.3.2.5.1.2. The SERS spectra of BCB labeled oligonucleotides in wet and

dry conditions are shown in Figure 44 and 45 respectively. As can be seen from the Figures, these results are similar to covalent attachment of BCB to DNA.

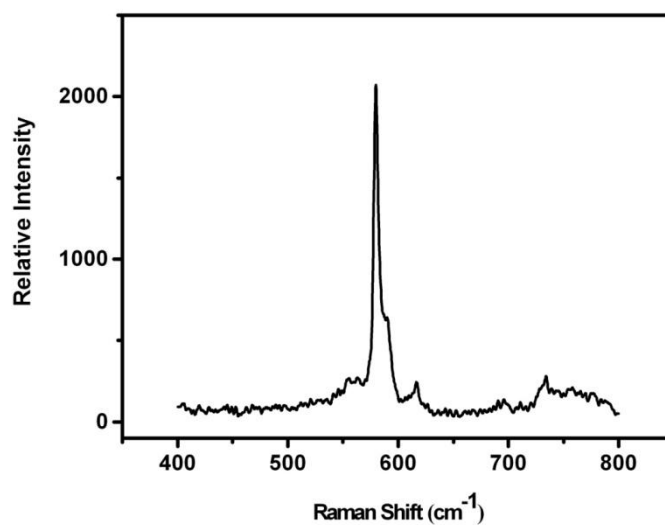


**Figure 44** SERS spectrum of BCB labeled DNA probe solution acquired by using silver colloid in wet condition. Labeling was done electrostatically in 18 h. at 50 °C.

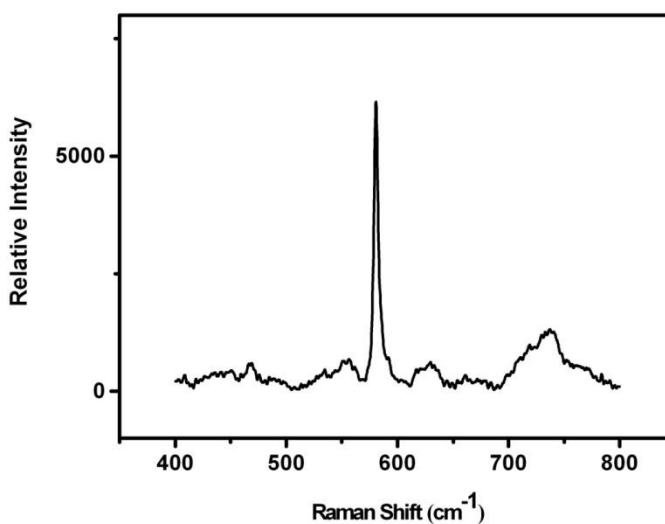


**Figure 45** SERS spectrum of BCB labeled DNA probe solution acquired by using silver colloid in dry condition. Labeling was done electrostatically in 18 h. at 50 °C.

The duration and the temperature of the electrostatic labeling process were reduced from 18 h to 4 h and 50 °C to room temperature. The SERS spectrum of BCB labeled oligonucleotide prepared electrostatically at room temperature and 4 h incubation time is shown in Figure 46.

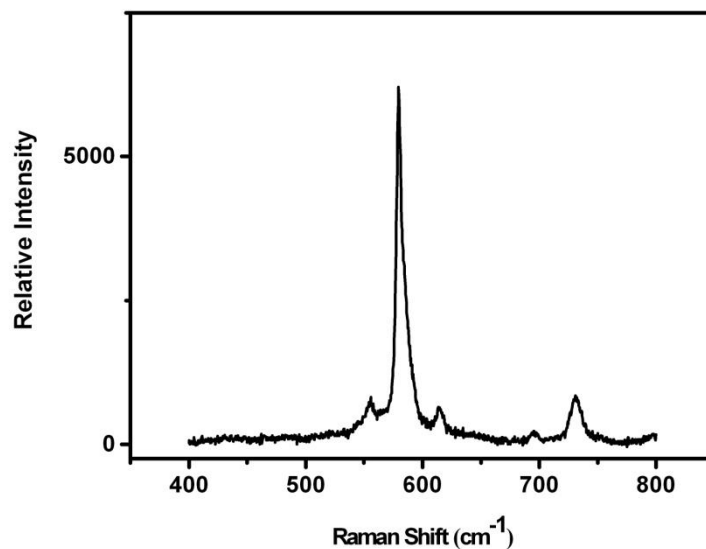


**Figure 46** SERS spectrum of BCB labeled DNA probe solution acquired by using silver colloid in dry condition. Labeling was done electrostatically at room temperature for 4 hours.

As can be seen from the Figure 46, BCB labeled DNA prepared at room temperature and 4 h incubation time gave similar SERS spectrum of the ones prepared at 50 °C and 18 h incubation time. Consequently, 4 h incubation at room temperature was decided to be used for electrostatic labeling of DNA with BCB.

Comparison of the Figures 41 and 42 and Figures 44 and 45 have shown that the SERS intensities of electrostatically labeled oligonucleotides are similar to the ones obtained from covalently labeled oligonucleotides. These outcomes illustrated that covalent and electrostatic attachment of the dyes onto the DNA strands were taking place simultaneously. Besides the strength of attachments in both cases were

adequate to render the labels stable through washing and gel filtration-centrifuging steps.

The effect of hybridization conditions on noncovalent attachment of BCB onto DNA was examined. Noncovalent labeling was carried out in a medium containing hybridization buffer (pH 7) and 1 M NaCl at room temperature and at 65 °C. Following 90 min incubation at room temperature, unreacted label was removed from the reaction mixture by gel filtration on mini Quick Spin Oligo Columns and the SERS spectrum of labeled DNA was measured (Figure 47, Figure 48).

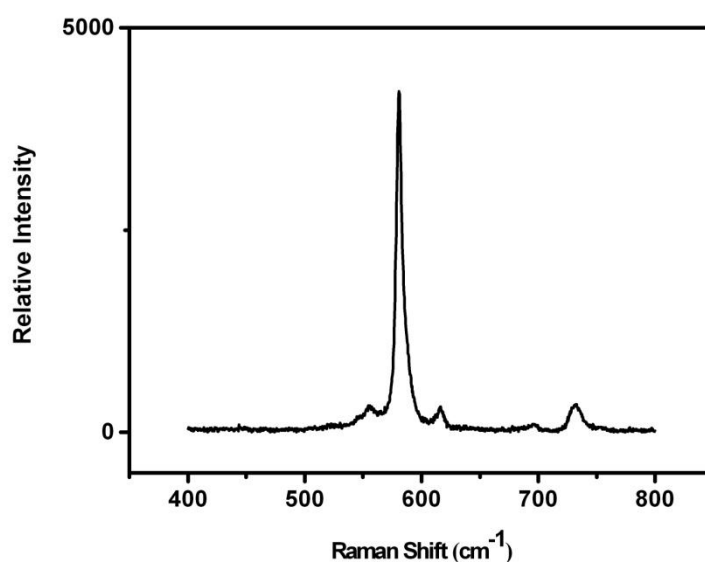


**Figure 47** SERS spectra of BCB labeled DNA probe solution acquired by using silver colloid in dry condition. Labeling was done electrostatically at room temperature for 4 hours and then labeled DNA incubated at hybridization conditions at room temperature.

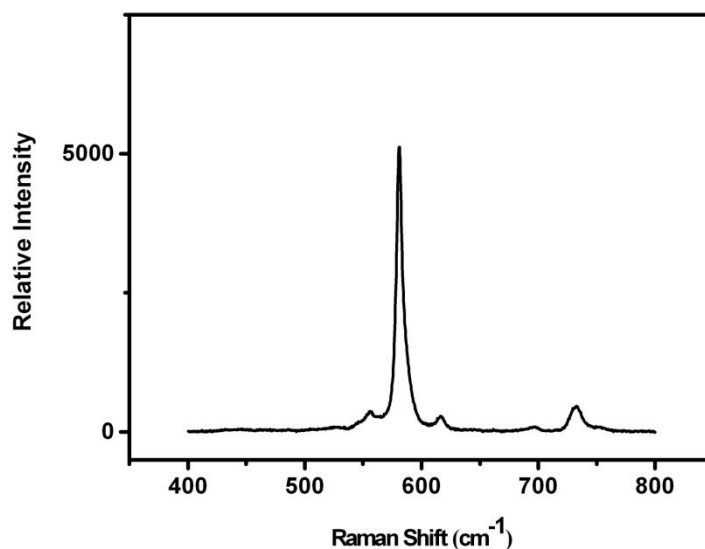


**Figure 48** SERS spectra of BCB labeled DNA probe solution acquired by using silver colloid in dry condition. Labeling was done electrostatically at room temperature for 4 hours and then labeled DNA incubated at hybridization conditions at 65 °C.

The results have shown that BCB labeling achieved through electrostatic attachment was strong enough to be stable even at very high ionic strength conditions used for hybridization.

After the success of electrostatic attachment of BCB on DNA, the labeling of other cationic dyes, cresyl fast violet (CFV) and crystal violet (CV) were also tried through electrostatic attraction. The SERS spectra of electrostatically labeled oligonucleotides with CFV and CV are shown in Figure 49 and 50.

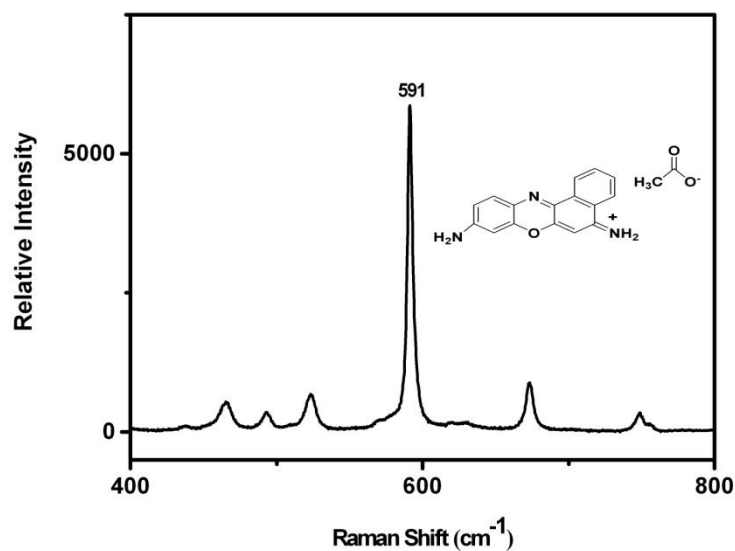


**Figure 49** SERS spectrum of CFV labeled DNA probe solution acquired by using silver colloid in dry condition. Labeling was done electrostatically at room temperature for 4 h.

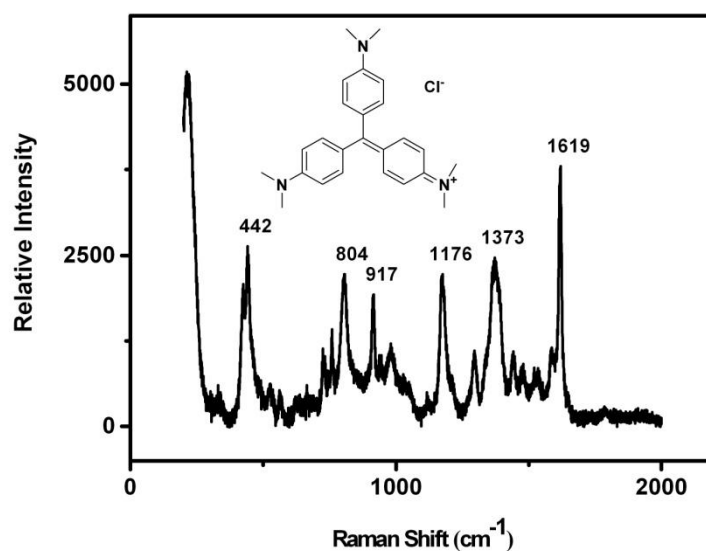


**Figure 50** SERS spectrum of CV labeled DNA probe solution acquired by using silver colloid in dry condition. Labeling was done electrostatically at room temperature for 4 h.

In addition to the cationic dyes one neutral dye FITC was used for labeling in the same manner as noncovalent (electrostatic) BCB labeling.

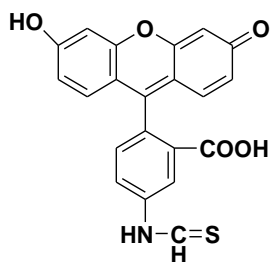


**Figure 51** The chemical structure of FITC

The SERS spectrum of FITC labeled oligonucleotide is shown in Figure 52.

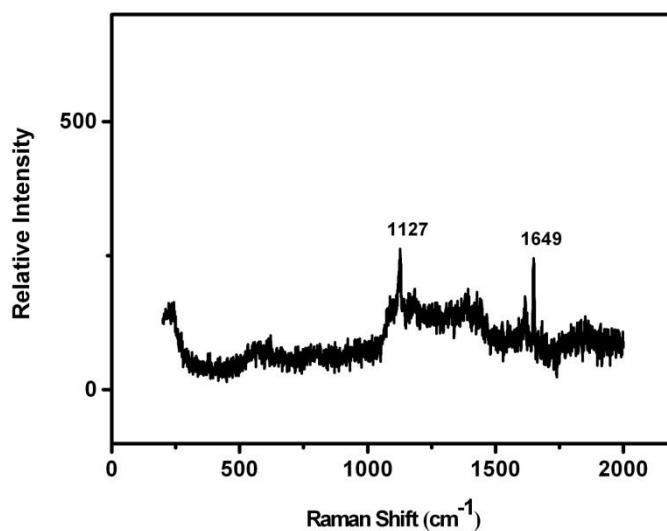


**Figure 52** SERS spectrum of FITC labeled DNA probe solution acquired by using silver colloid in dry condition. Labeling was done electrostatically at room temperature for 4 h.

The concentrations of BCB, CFV, CV and FITC in the DNA solutions labeled with these dyes noncovalently were estimated by comparing SERS intensities of them (Figure 46, Figure 49, Figure 50 and Figure 52) with their standard solutions (Figure



37-40). The results have shown that the magnitude of cationic dyes adsorbed on the DNA were at least order of magnitude more than that of neutral dye FITC. In other words, if the amount of FITC adsorbed on DNA (Figure 52) is considered as a measure of hydrophobic interactions and possible hydrogen bond formations among sugar and amine functional groups of DNA with FITC respectively, contribution of electrostatic interactions is at least ten fold higher than this amount.

### 3.2.5.1.2.1 Zeta Potential Measurements of Unlabelled Oligonucleotides and Electrostatically labeled Oligonucleotides

Zeta potentials of BCB and FITC labeled DNA and sole DNA were measured at room temperature in phosphate buffer solution (pH 7.0). DNA and dye labeled DNA were diluted to a concentration of 8.1  $\mu\text{M}$  in 750  $\mu\text{L}$  phosphate buffer solution (10 mM, pH 7.0). Zeta potential distribution of sole DNA is given in Figure 53.

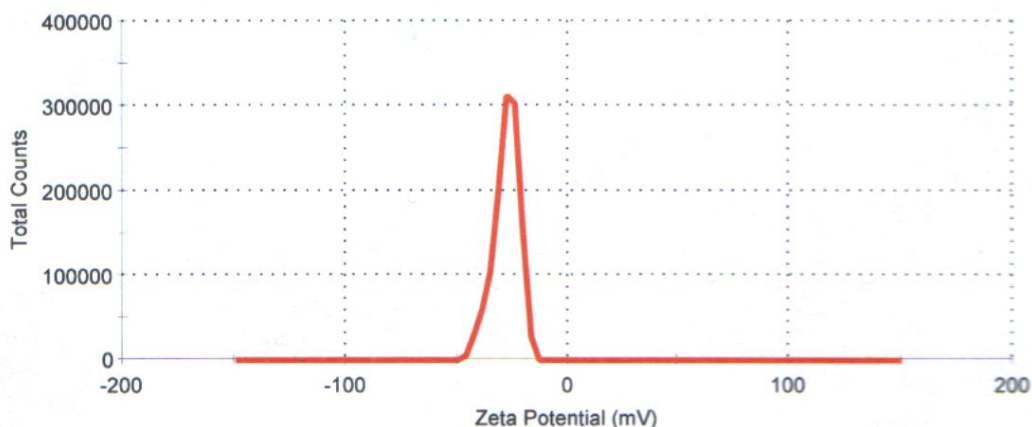


**Figure 53** Zeta potential distribution of DNA.

According to the literature, DNA has a negative zeta potential in a broad pH range due to the negative phosphate backbone (Lomas, et al., 2007). In fact, in our measurements, the zeta potential of DNA in phosphate buffer solution was measured as -41 mV (Figure 53).

On the other hand, BCB labeled DNA displayed a neutral (0.11 mV) zeta potential due to the electrostatic interaction between them. This result was in accordance with our expectations. Because for labeling charge excess of cationic BCB over the anionic DNA was used and excess BCB was removed through column separation. Consequently almost all the negatively charged phosphate groups should have been neutralized by ion pair formation with cationic dye.

The zeta potential value of neutral FITC labeled DNA was measured as - 41 mV, the same as the zeta potential value of unlabeled DNA. SERS measurements of FITC labeled DNA (Figure 52) discussed in section 3.2.5.1.2 have shown that small amount of FITC was adsorbed on DNA. Since there was no change in the zeta potential of DNA, the neutral dye was probably attached through the sugar groups or base groups without shielding the charge of the phosphate groups.

As a summary of these two successive sections we can conclude that covalent labeling frequently reported in literature is meaningless with cationic dyes. Because the signal is produced almost totally due to the noncovalent (mainly electrostatic) interaction of the dyes with the negative backbone of DNA even a covalent attachment process is applied. This fact was proved by SERS measurements and zeta potential measurements. The noncovalent labeling is stable enough to be used in hybridization conditions. Moreover noncovalent labeling is much easier, less time consuming and more economical compared to the covalent labeling. Thus electrostatic labeling was decided to be used in our SERS Gen studies.

### 3.2.5.2 Characterization of SERGen Probes onto the Gold surface

BCB labeled oligonucleotide prepared by electrostatic binding was used as the SERGen probe in the rest of the experiments. Before the hybridization experiments, we checked whether the SERGen probe alone can bind onto the gold surface or not, under the hybridization conditions (Figure 54).

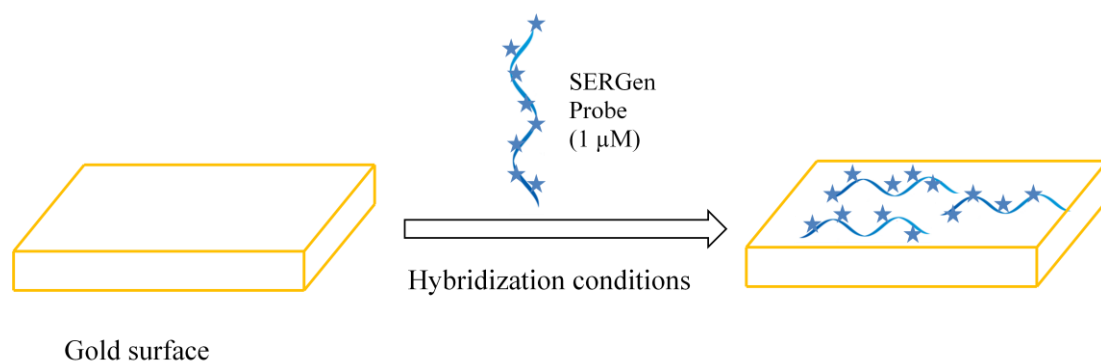


**Figure 54** Schematic representation of immobilization of SERGen probes onto the gold surface under the hybridization conditions: 300  $\mu$ L 10 mM phosphate buffer solution (pH 7) and 150  $\mu$ L 2 M NaCl solution for 90 min. at 25  $^{\circ}$ C.

In our study gold surface was chosen as substrate due to its resistance toward oxidation at hybridization conditions. Besides, gold- sulphur interaction is the easiest way to fix the DNA on the surface. However, the existence of gold nanoparticles on the surface was not enough to generate an electromagnetic field enhancement, therefore direct SERS detection of the SERGen probe after hybridization could not be achieved (Cao, Jin, & Mirkin, 2002). For his reason, silver colloid was added onto the substrate after SERGen probe addition and washing, to acquire SERS spectrum. SERS spectra were recorded from five different points of the substrate in the dried condition, Figure 55. In the figure the numbers are representing the locations at which the SERS measurements were done. The colors are coding the signal obtained from that particular point on the gold surface.

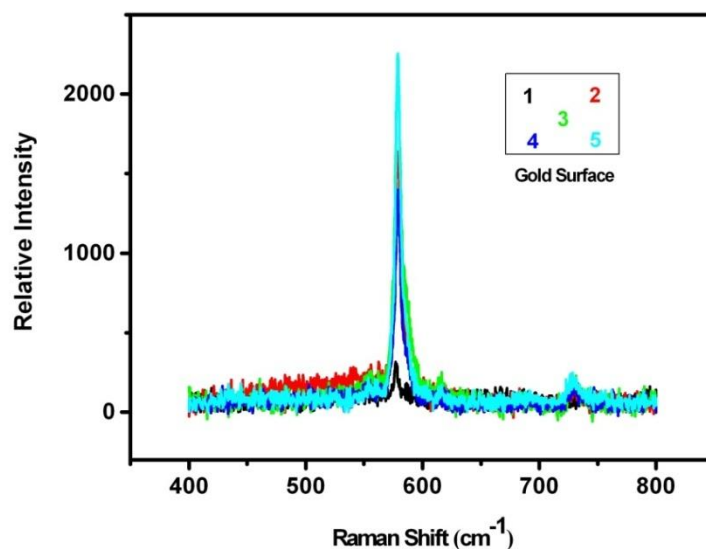


**Figure 55** SERS spectra of only SERGen probe on the gold surface with silver colloid in dry condition. SERGen probe was designed based on the archaea proteasome gene sequence. The numbers are representing the locations at which the SERS measurements were done. The colors are coding the signal obtained from that particular point on the gold surface.

As can be seen from Figure 55, SERS spectra of the only SERGen probe on gold surface revealed characteristic BCB peaks indicating that SERGen probe was attached onto the gold surface. This result is in agreement with the observations of Herne and Tarlov (**Herne & Tarlov, 1997**). Therefore, we decided to use spacer to prevent nonspecific adsorption of DNA onto gold substrate in our experiments. Decanethiol, 11-mercapto-1-undecanol and 10 T chain were used as spacers.

### **3.2.5.3 Characterization of SERGen Probes Attached onto Gold surface under the Hybridization Conditions After the Decanethiol Treatment**

In this experiment, decanethiol was used as a spacer. Firstly 1mM decanethiol solution was added onto the substrate and after 1 hour, the gold surface was rinsed

with sterile water. Then SERGen probe was added and incubated under the hybridization conditions (Figure 56).

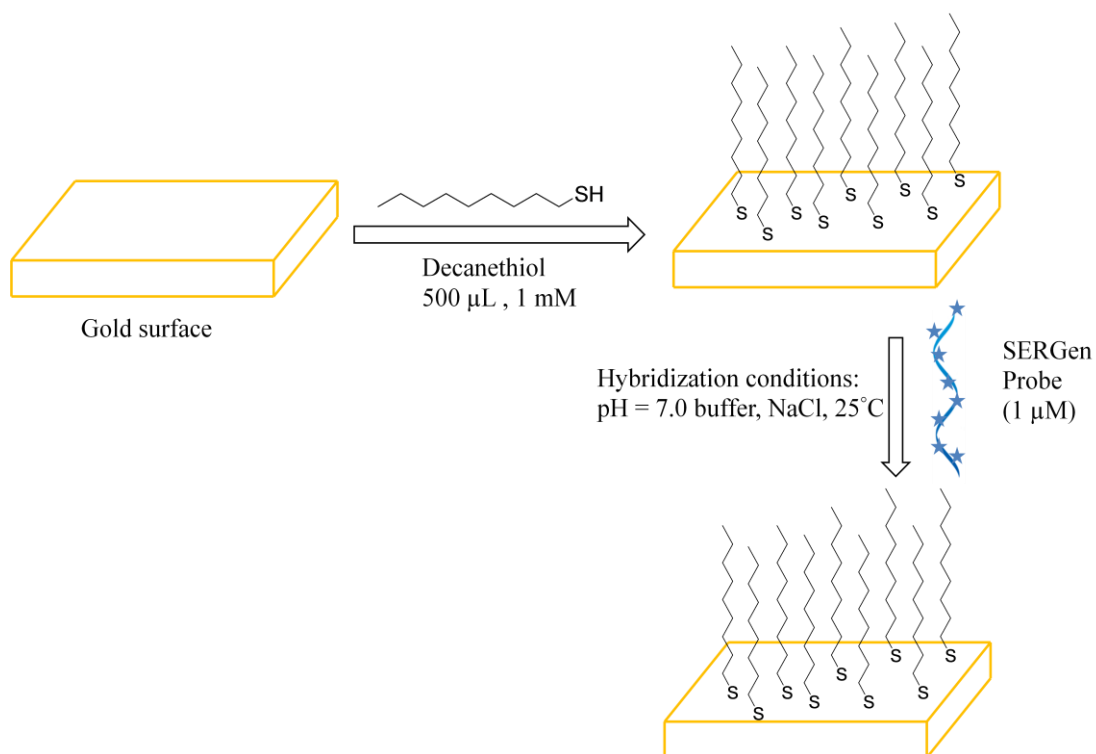


**Figure 56** Schematic representation of expected binding of SERGen probes onto the gold surface after the decanethiol treatment under the hybridization conditions.

Then, to record SERS spectrum in dry conditions silver colloid was added. Although no SERS peak was expected due to covering of decanethiol whole gold surface, still SERS peaks were observed (Figure 57).

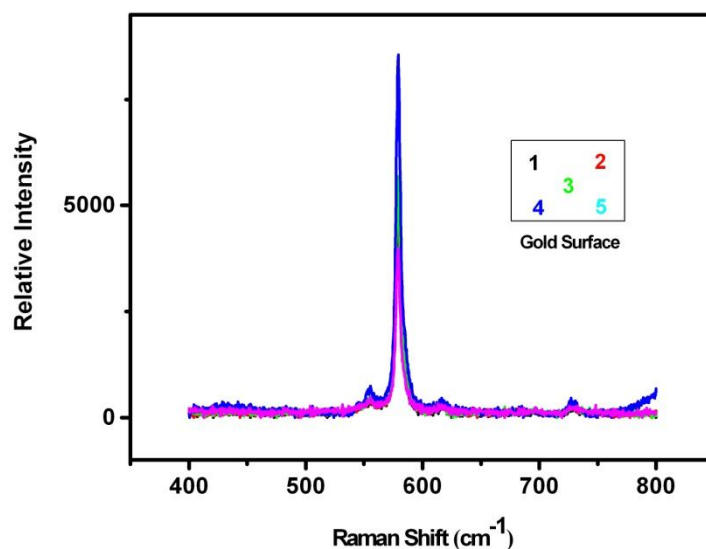


**Figure 57** SERS spectra of SERGen probe on the gold surface with silver colloid in dry condition when decanethiol is used as spacer. SERGen probe was designed using archaea proteasome gene sequence. The numbers are representing the locations at which the SERS measurements were done. The colors are coding the signal obtained from that particular point on the gold surface.

Appearance of SERS peaks of the probe could be explained by a possible hydrophobic interaction between DNA and decanethiol. DNA has a 5-carbon sugar (pentose) and it may be partitioned into the decanethiol through the pentose part. For this reason, SERS peaks were obtained from the different points of surface. To prevent this nonspecific attachment of probe DNA through decanethiol layer, we have tried more vigorous washing following incubation with probe. Washing was made using hybridization buffer solution through mechanical shaking. To determine effective washing time, duration changed from 10 to 30 min. When washing was performed for 20 and 30 min., hybridization buffer solution was renewed every 10 min (Figure 58).

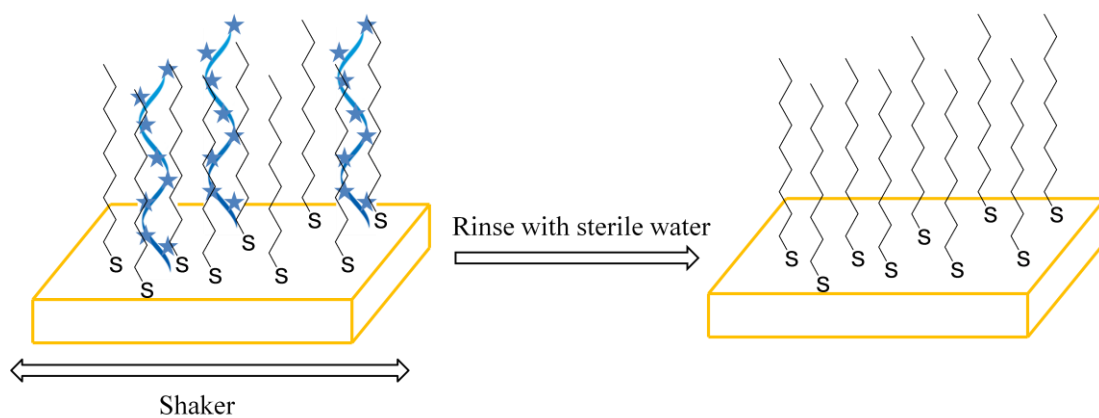


**Figure 58** Schematic representation of SERGen probes onto the gold surface after the decanethiol treatment under the hybridization conditions washing with hybridization buffer in a shaker. SERGen probe was designed using archaea proteasome gene sequence.

SERS spectra of the samples we obtained after 10, 20 and 30 min washings are given in Figure 59. As can be seen from the Figure 10 min washing was enough to remove SERGen probes diffused into the self-assembled monolayer of decanethiol. This result also revealed an effective coverage of gold surface by decanethiol.

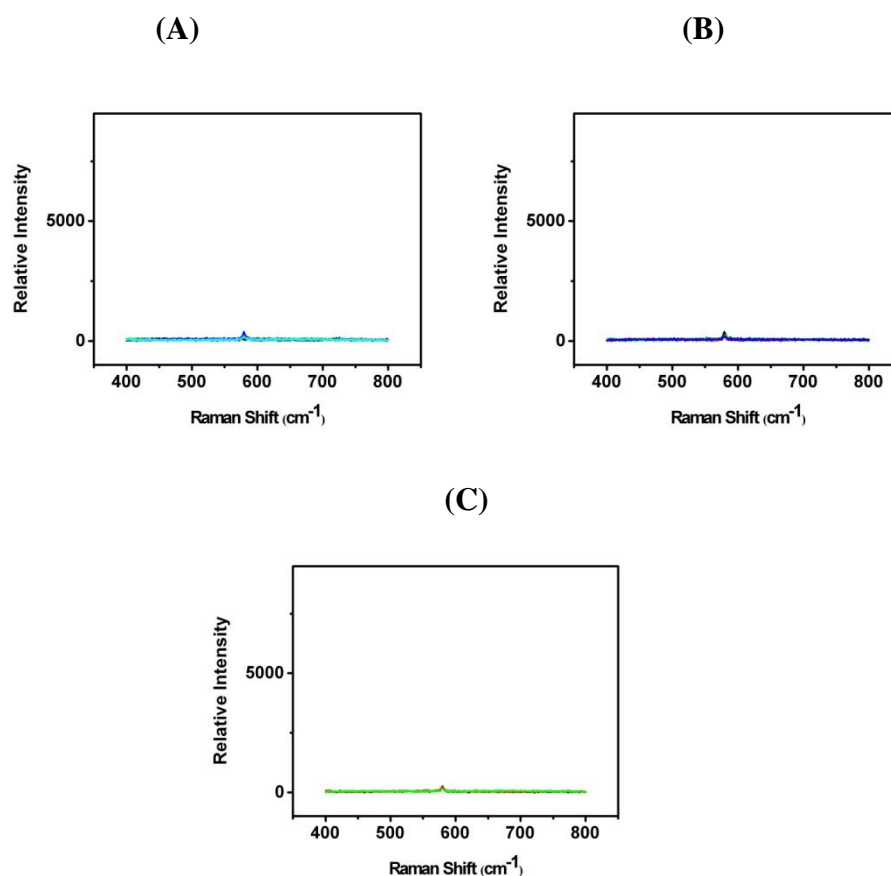


**Figure 59** SERS spectra of SERGen probe on the gold surface with silver colloid in dry condition: A) after 10 min. shake wash, B) after 20 min. shake wash, C) after 30 min. shake wash.

### 3.2.5.4 Hybridization Experiments

In the hybridization experiments, firstly, 5' end thiol modified target sequences were immobilized on the gold surface. High affinity of thiol groups for gold surfaces provides the formation of covalent bonds between the sulfur and gold atoms (Sassolas, Leca-Bouvier, & Blum, 2008).





After incubation of target sequences on the gold surface for binding, the surface was washed with sterile water to remove unbound targets. In surface hybridization, nonspecific oligonucleotide surface interactions, electrostatic forces, and steric issues between adjacent oligonucleotides affect DNA hybridization efficiency and capacity. For instance, nucleotide primary amines on nonhybridized DNA fragments can interact (e.g., covalently (**Huang, Zhou, & Deng, 2000**) or by acid-base adsorption) with the surface, becoming unavailable to hybridization (**Lee, Gong, Harbers, Grainger, Castner, & Gamble, 2006**). To prevent nonspecific adsorption of DNA onto the substrate, we have decided to use spacers (decanethiol, mercaptoundecanol and 10T oligo) in all hybridization experiments. However in order to emphasize the importance of the use of spacer, the first hybridization experiment was carried out in the absence of spacer.

#### **3.2.5.4.1 Hybridization Experiment using The Probe Based on Archaea Proteasome Gene Sequence without Spacer**

In this experiment, hybridization was carried out by the addition of the SERGen probe onto the gold nanoparticle coated surface covered with target DNAs as described in the materials and methods. Expected result of this hybridization experiment was schematically shown in the Figure 60.

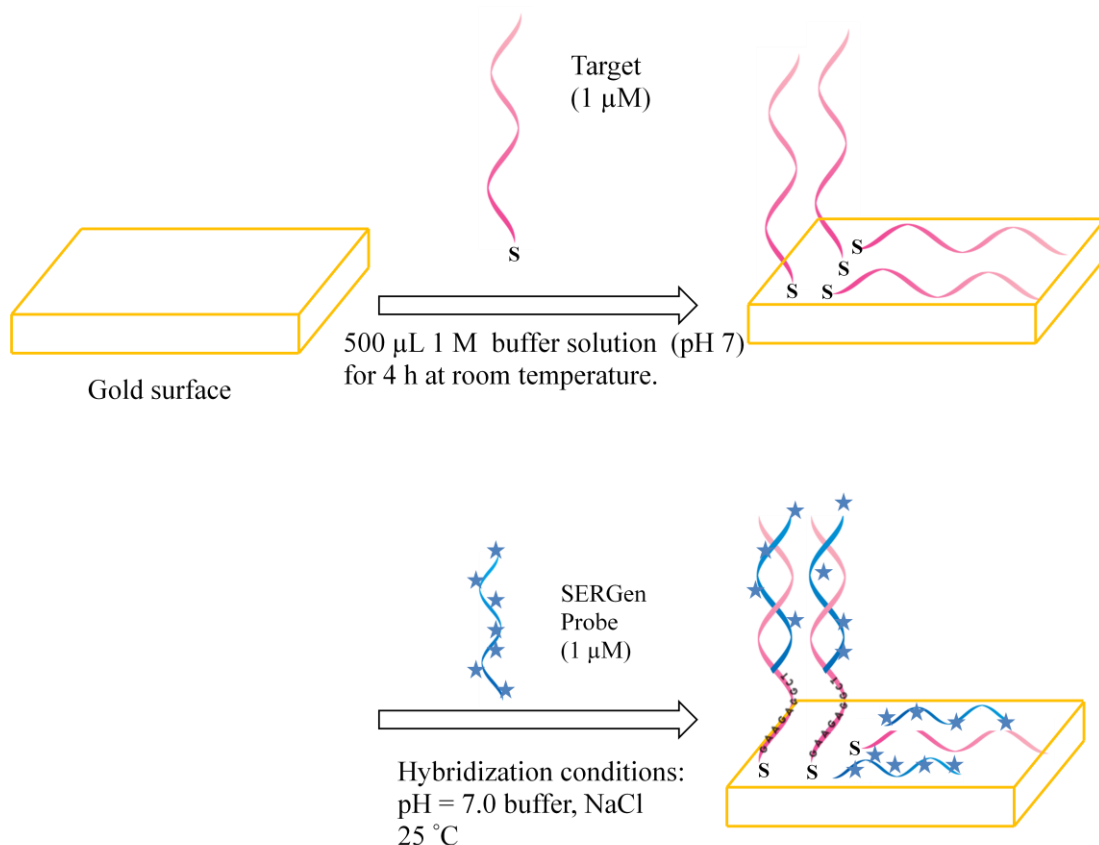


**Figure 60** Schematic representation of hybridization without spacer possible bindings are shown.

SERS result showed that the intensities of the peaks varied from 2500 to 15000 (Figure 61). Our previous results showed that SERGen probe alone can attach onto the gold surface (Figure 55). Heterogeneity of peak intensities could be due to low hybridization efficiency between probe and target and nonspecific adsorption of both target and probe oligonucleotides onto the gold substrate. In other words, these SERS peaks were arised from hybridized SERGen probes as well as nonspecifically adsorbed nonhybridized SERGen probes. As will be discussed later, inconsistency in the SERS measurements on the same gold surface might also be attributed to heterogeneities of the gold surface preparation.

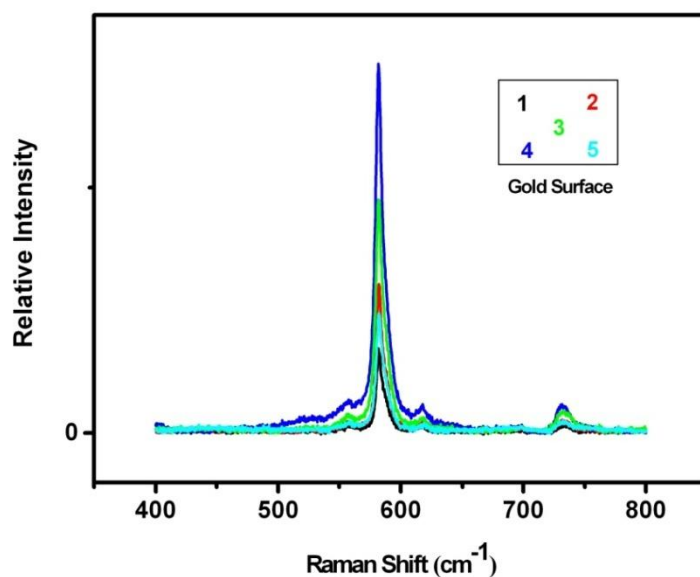


**Figure 61** SERS spectra of BCB-labeled DNA after the hybridization onto the gold surface with silver colloid in dry condition in the absence of a spacer. SERGen probe was designed using archaea proteasome gene sequence. The numbers are representing the locations at which the SERS measurements were done. The colors are coding the signal obtained from that particular point on the gold surface (See Appendix 1).

#### 3.2.5.4.2 Hybridization Experiments using Archaea Proteasome Gene Based Probe in the Presence of the Spacer decanethiol

Hybridization experiment with spacer was done as described in section 2.3.2.5.4 (Figure 62). Incubation time of the spacer is an important parameter. For thiolated oligonucleotides, longer spacer treatment is expected to cause the replacement of DNA by the spacer. For nonthiolated oligonucleotides, on the other hand, almost all strands are expected to be displaced by spacer. Steel *et al.* (Steel, Levicky, Herne, &

**Tarlov, 2000**) have suggested one hour incubation as an optimum time. Hence 1 hour incubation time was adopted in our experiments.

SERS spectra were recorded in dry condition. As can be seen from Figure 63, the intensity of the peaks from the different points of the surface gave similar results. This result showed that these SERS peaks are produced because of the hybridized SERGen probes. Since, when gold surface was exposed to the decanethiol before addition of SERGen probe, no SERS peak was observed due to the complete coverage of the whole surface by decanethiol (Figure 59). In conclusion, in the mixed monolayer on the gold surface created by using thiolated DNA targets and decanethiol, only hybridized SERGen probes, which are complementary to the DNA targets, were detected by SERS measurements.

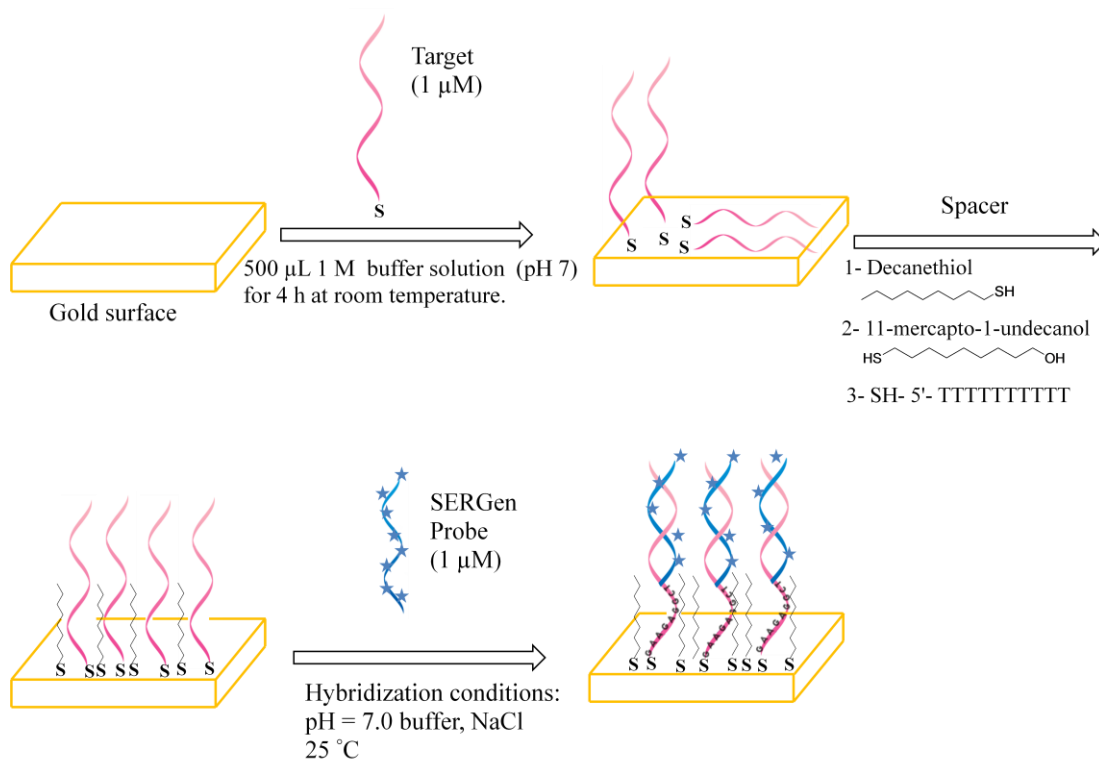


**Figure 62** Schematic representation of hybridization with various spacers (i.e., decanethiol, mercaptoundecanol and 10T oligo).

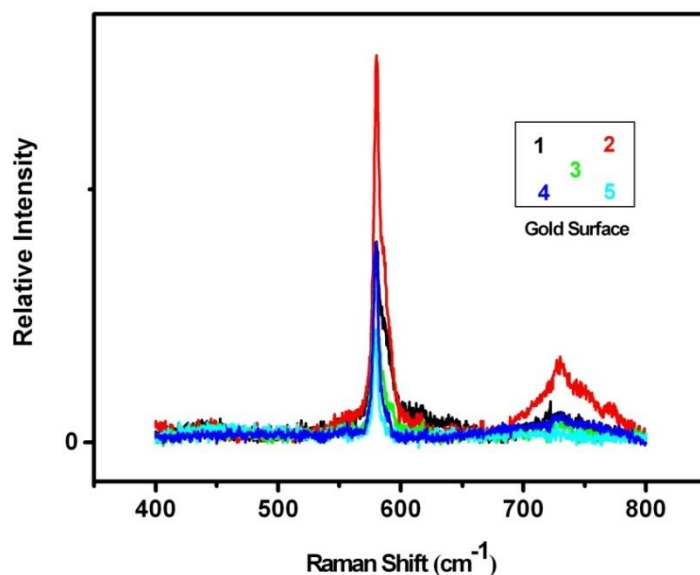


**Figure 63** SERS spectra of BCB-labeled DNA after hybridization onto the gold surface with silver colloid in dry condition when decanethiol was used as spacer. SERGen probe was designed using archaea proteasome gene sequence. The numbers are representing the locations at which the SERS measurements were done. The colors are coding the signal obtained from that particular point on the gold surface (See Appendix 2).

As can be seen from Figure 62, target and probe sequences are not in the same length. Target sequence contains nine bases more than probe sequence. These bases act as spacer to move part of target DNA, which will hybridize with probe, away from the surface and lessens the steric hindrance which would otherwise interfere with the probe/target hybridization (Lytton-Jean & Mirkin, 2005). We suggest that decanethiol is almost at the same length as the target DNA (9 bp) and is not long enough to interfere with the hybridization reactions on the substrate.

DNA targets are short oligonucleotides (12-40 mer) able to hybridized with specific probe fragments. The sizes of the oligos we used in our experiments were also within this range. It has been reported that the surface coverage by such oligos is more effective and they tend to remain vertical, since attachment onto surface is mainly from their thiol groups at the 5' ends (Sassolas, Leca-Bouvier, & Blum, 2008). When the length of DNA exceeds 24 mer, surface coverage starts to decrease owing to the large number of adsorptive nucleotide-gold interactions (Figure 64).



**Figure 64** Schematic representation of thiol modified short and long oligonucleotides behavior onto the gold surface (Steel, Levicky, Herne, & Tarlov, 2000).

To further confirm that SERS signal obtained in the hybridization experiment is due to specific base pairing between target and probe sequences we have run a control experiment. It was performed like standart hybridization experiment but as a probe the same sequence as the immobilized target without the thiol attachment at the 5' end (Figure 65). In this experiment the spacer was decanethiol. As can be seen from the SERS spectra no BCB signal was detected (Figure 66). This result confirmed that hybridized SERGen probe was detected in the hybridization experiment.

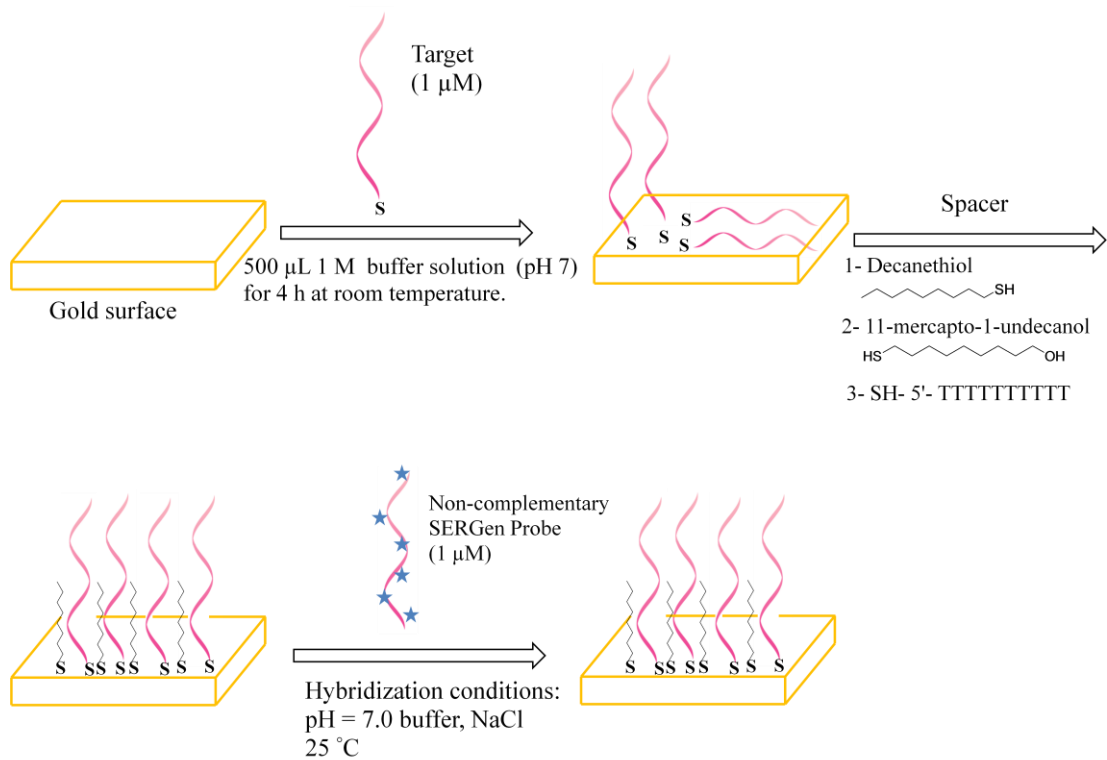


**Figure 65** Schematic representation of control hybridization experiment by use of a non-complementary SERGen probe with spacer. Spacer used in this experiment was decanethiol.

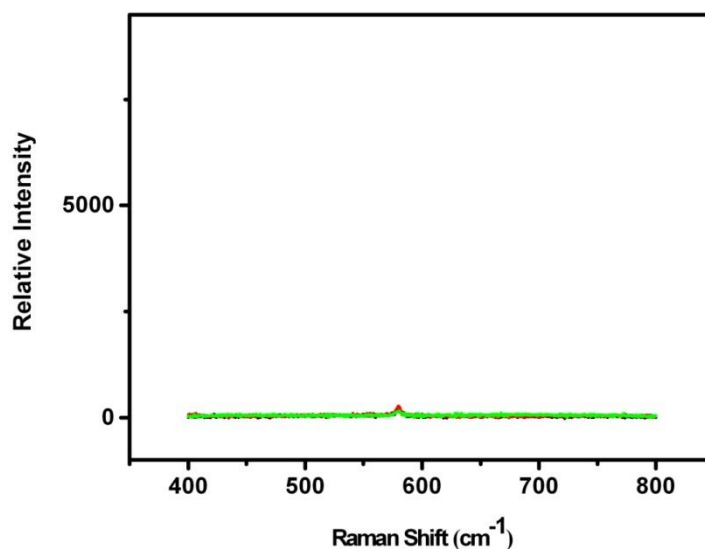


**Figure 66** SERS spectra of BCB-labeled DNA after the hybridization control experiment onto the gold surface with silver colloid in dry condition. SERGen probe was designed using archaea proteasome gene sequence having same sequence as the target DNA. Spacer used in this experiment was decanethiol.

#### **3.2.5.4.3 Hybridization Experiments using Archaea Proteasome Gene Sequence Based Probe with Other Spacers (11-Mercapto-1- undecanol and 10 T oligo)**

Hybridization and hybridization control experiments were carried out using mercaptoundecanol and 10 T spacers in the same way as those experiments where decanethiol was used as spacer.

SERS spectra obtained from both hybridization and hybridization control experiments were similar to results obtained with decanethiol when mercaptoundecanol was used as a spacer. As can be seen from the SERS spectra of hybridization experiment (Figure 67), the intensity of the peaks from the different points of the surface were similar. We confirmed that these SERS peaks referred to the hybridized SERGen probes. No BCB signal was observed in the SERS spectrum



in the control hybridization experiment performed using non-complementary probe, as described before (Figure 68). Thus we confirmed that the SERS peaks obtained in the test hybridization experiment was due to hybridized SERGen probes.

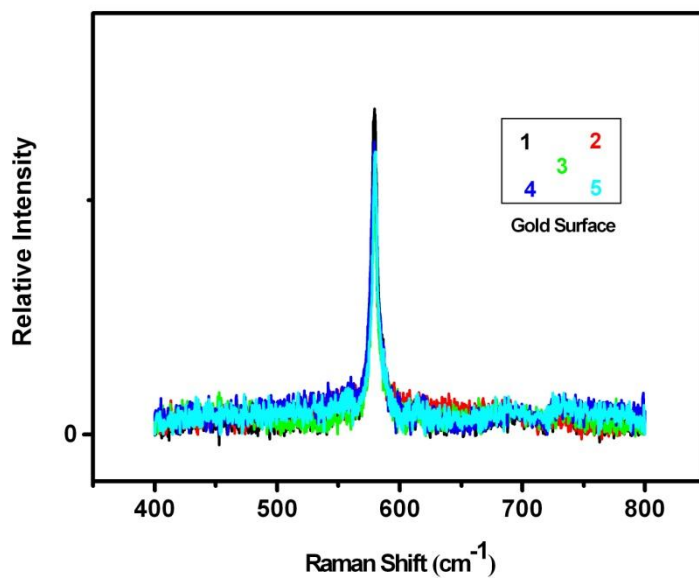


**Figure 67** SERS spectra of BCB-labeled DNA after hybridization onto the gold surface with silver colloid in dry condition. SERGen probe was designed using archaea proteasome gene sequence. The numbers are representing the locations at which the SERS measurements were done. The colors are coding the signal obtained from that particular point on the gold surface. Spacer used in this experiment was 11-mercapto-1-undecanol (See Appendix 3).

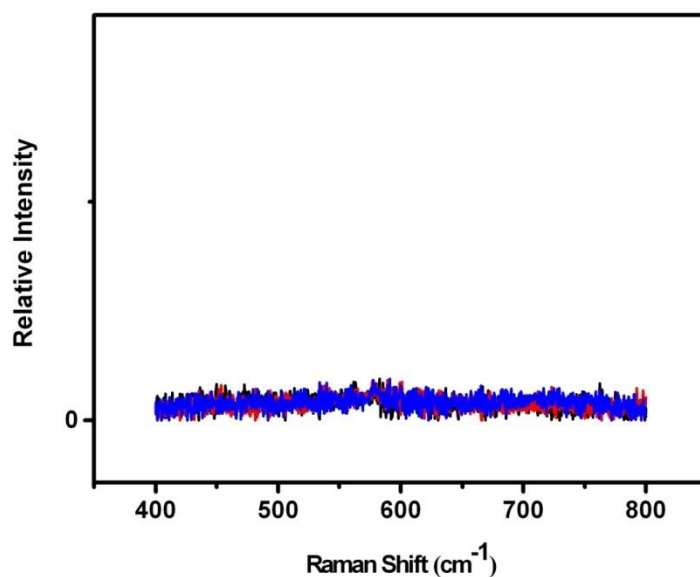


**Figure 68** SERS spectra of BCB-labeled DNA after the hybridization control experiment onto the gold surface with silver colloid in dry condition. SERGen probe was designed using archaea proteasome gene sequence having same sequence as the target DNA. Spacer used in this experiment was 11-mercapto-1-undecanol.

SERS spectra obtained from both hybridization and hybridization control experiments using 10 T as a spacer gave different results from experiments where decanethiol and 11-mercapto-1-undecanol used as spacers. Hybridization was performed as described before except for concentration of 10T spacer. The concentration of 10T solution used in this experiment was 10  $\mu$ M instead of 1 mM as used for other spacers, because it is quite expensive. The SERS spectra of both test hybridization (Figure 69) and control hybridization experiments (Figure 70) were similar to the spectrum obtained from hybridization experiment without spacer (Figure 61). In other words, SERS peaks were arised from hybridized SERGen probes as well as nonspecifically adsorbed nonhybridized SERGen probes probably due to inadequate surface coverage or blockage by 10T spacer under experimental conditions (Figure 71, 72).

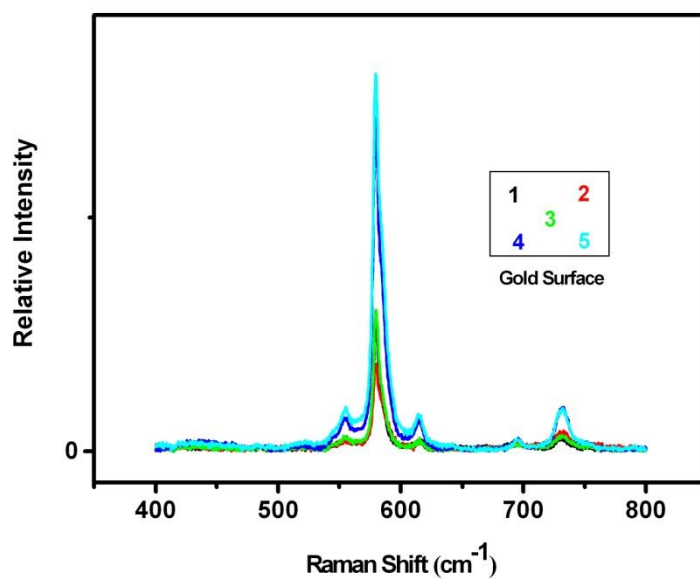


**Figure 69** SERS spectra of BCB-labeled DNA after hybridization onto the gold surface with silver colloid in dry condition. SERGen probe was designed using archaea proteasome gene sequence. The numbers are representing the locations at which the SERS measurements were done. The colors are coding the signal obtained from that particular point on the gold surface. Spacer used in this experiment was 10T (See Appendix 4).

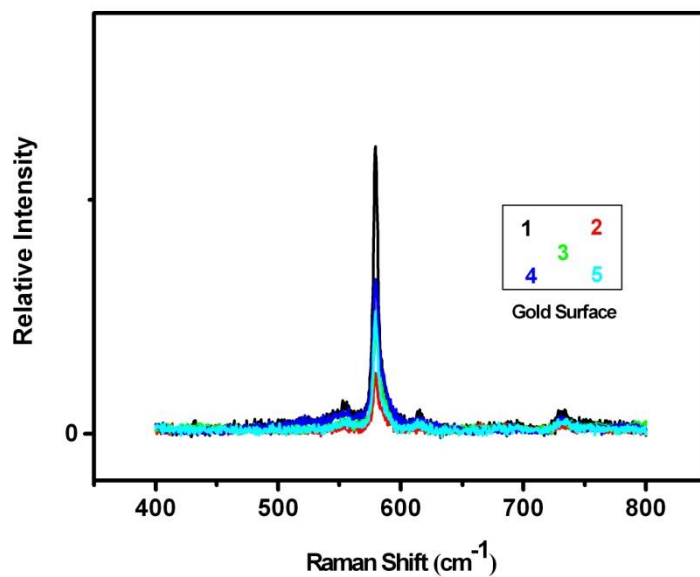


**Figure 70** SERS spectrum of BCB-labeled DNA obtained in the control hybridization experiment onto the gold surface with silver colloid in dry condition. SERGen probe was designed using archaea proteasome gene sequence having same sequence as the target DNA. The numbers are representing the locations at which the SERS measurements were done. The colors are coding the signal obtained from that particular point on the gold surface. Spacer used in this experiment was 10T (See Appendix 5).

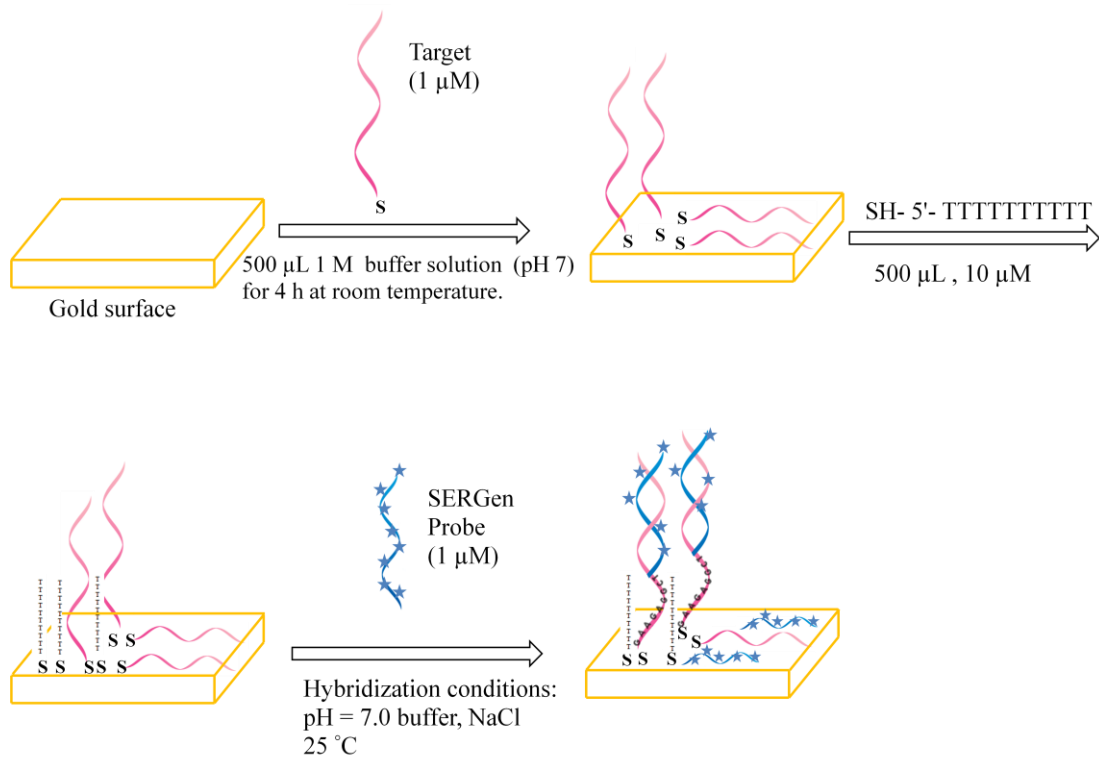


**Figure 71** Schematic representation of test hybridization using 10T as spacer.

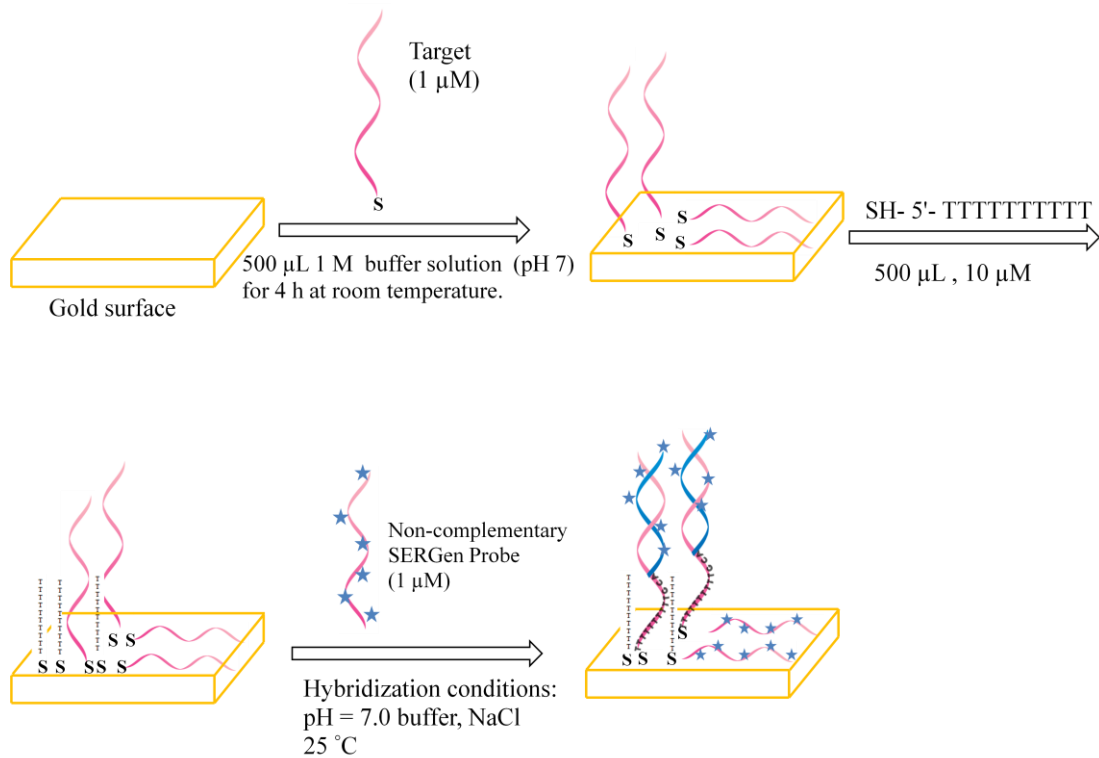


**Figure 72** Schematic representation of control hybridization experiment using 10T as spacer.

#### **3.2.5.4.4 Hybridization Experiments using Human Proteasome Gene Sequence with Based Target DNA with 10 T oligo**

In this experiment as target DNA we used human proteasome based oligo nucleotide with 10 T residues at its 5' end: SH- 5'- TTTTTTTTTT GCA GTG GAT TCT CGG GCC. The SERGen probe was complementary to the target sequence above the oligo T. The reason for the preference of oligo T extension or spacer is in the previous studies it was found that dT has a much lower binding affinity to the gold nanoparticle surface than the other deoxynucleosides, dG, dC, and dA (**Storhoff, Elghanian, Mirkin, & Letsinger, 2002**)

Using human proteasome gene sequence hybridization (Figure 73) and hybridization control (Figure 74) experiments were done like former hybridization. As explained previously, SERS peaks were arised from hybridized SERGen probes as well as nonspecifically adsorbed nonhybridized SERGen probes probably due to inadequate surface coverage.

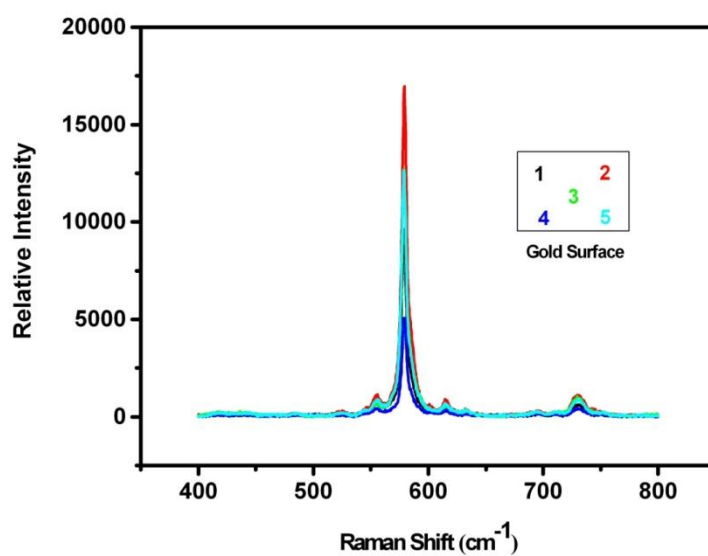


**Figure 73** SERS spectra of BCB-labeled DNA after hybridization onto the gold surface with silver colloid in dry condition. SERGen probe was designed using human proteasome gene sequence. The numbers are representing the locations at which the SERS measurements were done. The colors are coding the signal obtained from that particular point on the gold surface. Spacer used in this experiment was 10T (See Appendix 6).

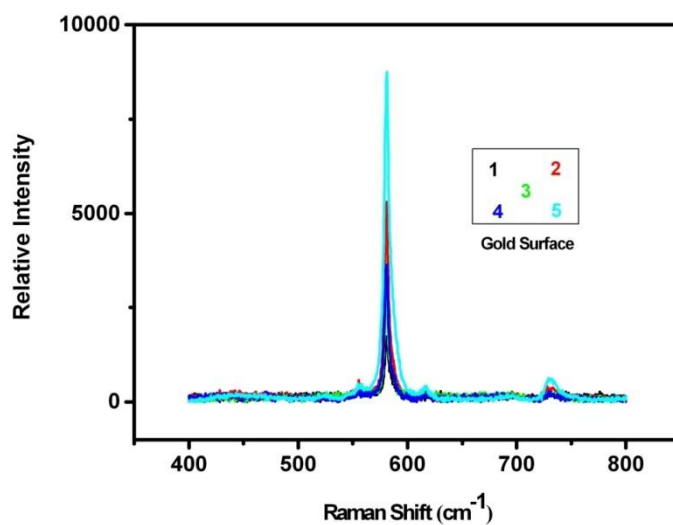


**Figure 74** SERS spectra of BCB-labeled DNA in the control hybridization experiment onto the gold surface with silver colloid in dry condition. SERGen probe was designed using human proteasome gene sequence. The numbers are representing the locations at which the SERS measurements were done. The colors are coding the signal obtained from that particular point on the gold surface. Spacer used in this experiment was 10T (See Appendix 7).

An experiment was done with a smaller gold surface than previous experiments to increase amount of 10 T. However, SERS spectrum obtained from small gold substrate was the same SERS spectrum obtained from normal gold substrate (Figure 75). This indicates that low efficiency of surface coverage by 10T spacer is not due to its low concentration. As the same concentration as that of the other spacers still it did not provide sufficient surface blockage. For this reason in the following hybridization experiments decanethiol and / or 11-mercapto-1-undecanol was used as spacer.



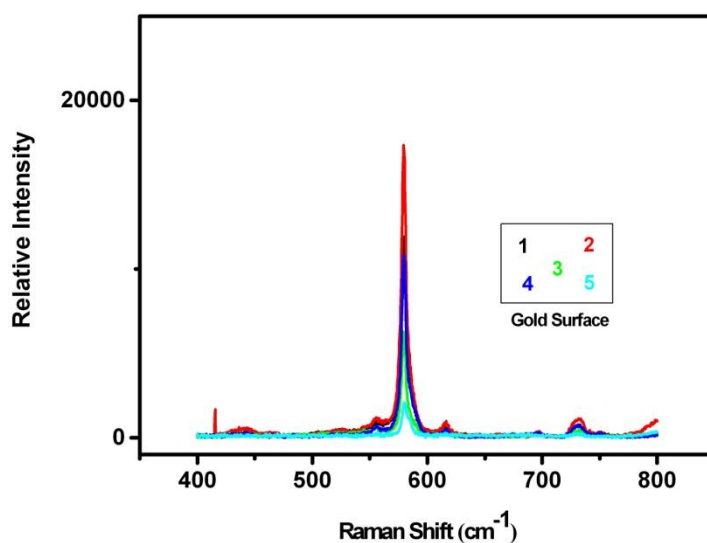


**Figure 75** SERS spectra of BCB-labeled DNA after hybridization onto the gold surface with silver colloid in dry condition. SERGen probe was designed using human proteasome gene sequence. The numbers are representing the locations at which the SERS measurements were done. The colors are coding the signal obtained from that particular point on the gold surface. Spacer used in this experiment was 10T (See Appendix 8).

#### 3.2.5.4.5 Hybridization Experiments using Target and Probe Oligos Based on Human Proteasome Gene Sequence

In these experiments decanethiol and mercapto undecanol were used as spacers. Hybridization and hybridization control experiments were performed using these spacers as described before. SERS results of both test hybridization (Figure 76, 78) and control hybridization experiments (Figure 77, 79) results were in good agreement with those obtained with oligonucleotides based on archaea proteasome gene sequence.

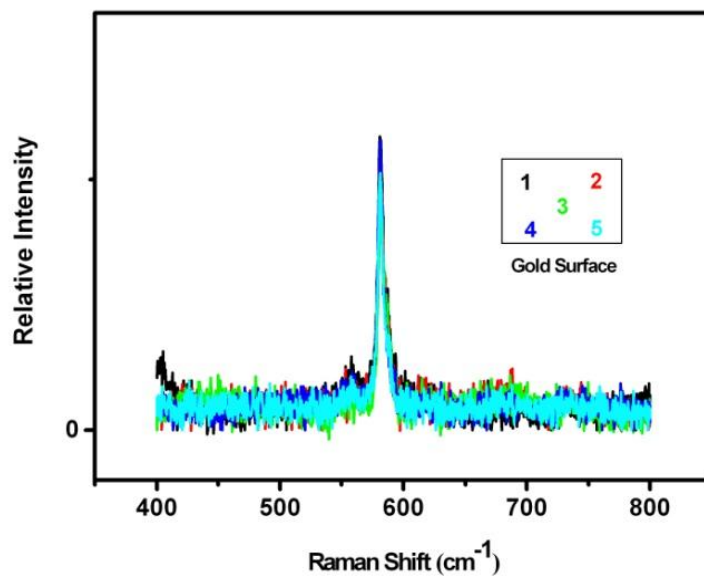


**Figure 76** SERS spectra of BCB-labeled DNA after hybridization onto the gold surface with silver colloid in dry condition. SERGen probe was designed using human proteasome gene sequence. The numbers are representing the locations at which the SERS measurements were done. The colors are coding the signal obtained from that particular point on the gold surface. Spacer used in this experiment was decanethiol (See Appendix 9).

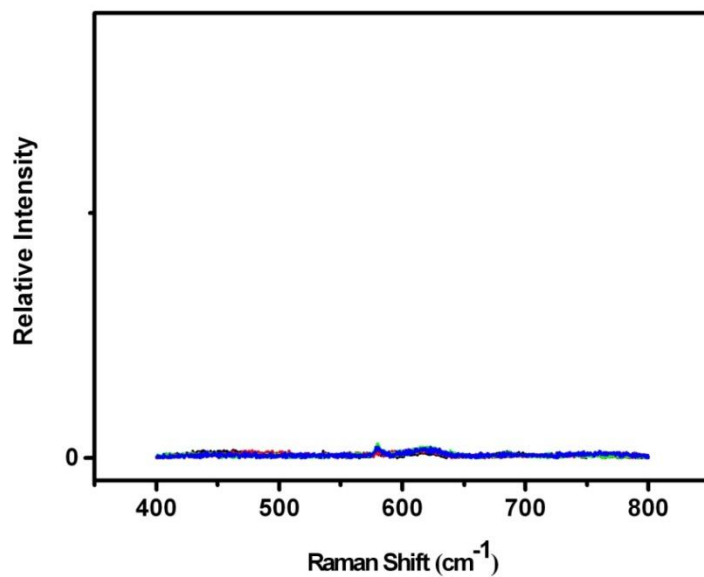


**Figure 77** SERS spectra of BCB-labeled DNA in the control hybridization experiment onto the gold surface with silver colloid in dry condition. SERGen probe was designed using human proteasome gene sequence. Spacer used in this experiment was decanethiol.

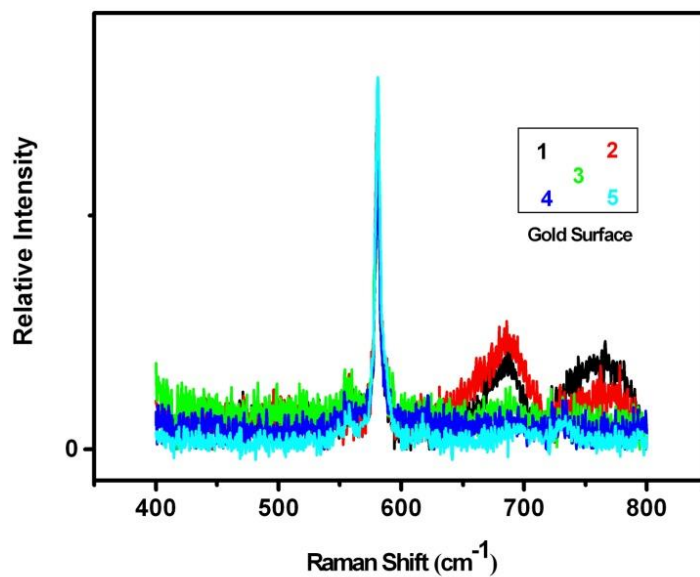


**Figure 78** SERS spectra of BCB-labeled DNA after hybridization onto the gold surface with silver colloid in dry condition. SERGen probe was designed using human proteasome gene sequence. The numbers are representing the locations at which the SERS measurements were done. The colors are coding the signal obtained from that particular point on the gold surface. Spacer used in this experiment was 11-mercapto-1-undecanol (See Appendix 10).

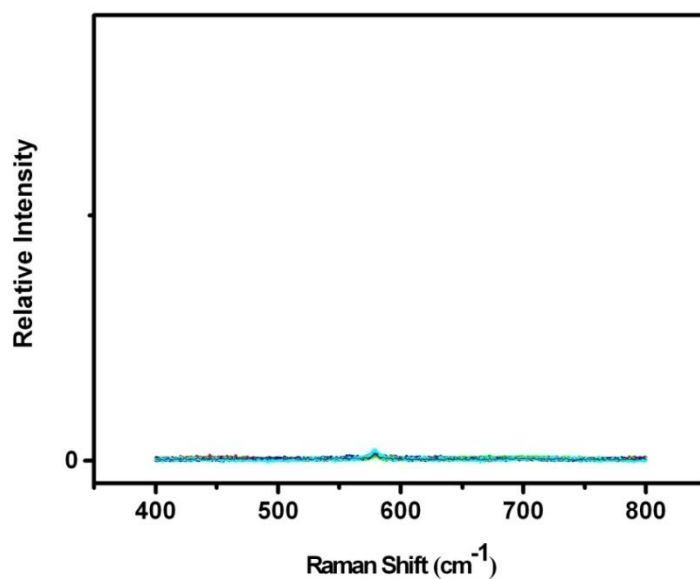


**Figure 79** SERS spectra of BCB-labeled DNA in the control hybridization experiment onto the gold surface with silver colloid in dry condition. SERGen probe was designed using human proteasome gene sequence. Spacer used in this experiment was 11-mercapto-1-undecanol.

A hybridization experiment was performed on gold film instead of gold substrate using mercapto undecanol as a spacer as described before. Three different experiments were done at the same time (Figure 80 A, B,C). SERS intensity of peaks were similar to each other obtained from each film surface.

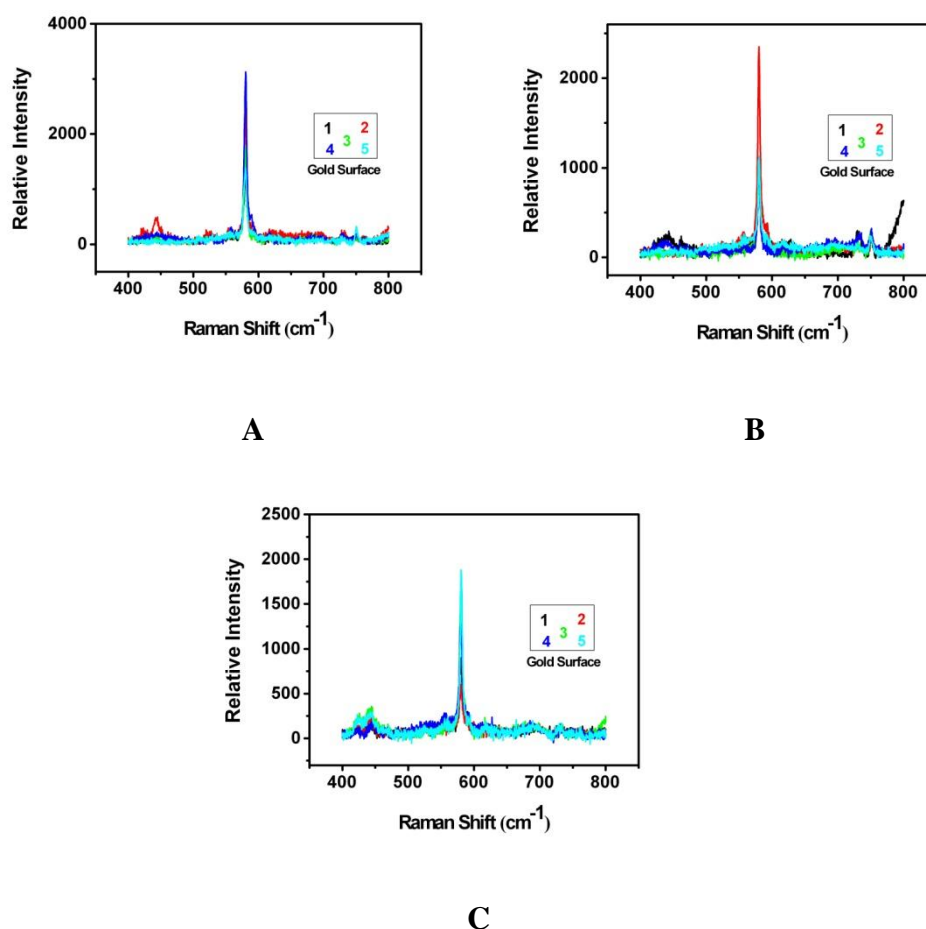


**Figure 80** SERS spectra of three BCB-labeled DNA after hybridization onto the gold film with silver colloid in dry condition (A, B, C). SERGen probe was designed using human proteasome gene sequence. The numbers are representing the locations at which the SERS measurements were done. The colors are coding the signal obtained from that particular point on the gold film. Spacer used in this experiment was 11-mercapto-1-undecanol (See Appendix 11-13).

### 3.2.5.4.6 Effect of Pre-Heating of Oligo Probe on Hybridization

A control experiment was run to see if there is secondary structure formation of probe DNA that might affect hybridization. Before preparation of SERGen probe electrostatically, first, oligonucleotide probe was heated at 100°C for 5 min., then placed on the ice for 2 min. and then was linked BCB. Also, target DNA was heated and cooled in the same manner. By heating at boiling temperature the hydrogen bonds between and within the DNA molecules were removed and thus oligonucleotides were rendered single stranded (Barhoumi, Zhang, Tam, & Halas, 2008). Hybridization experiment was performed as described before. The average SERS intensity measured was around 20000 au at 580 nm and that was very similar to SERS intensities measured in the previous experiments. This result showed that preheating did not have any detectable effect on hybridization (Figure 81).

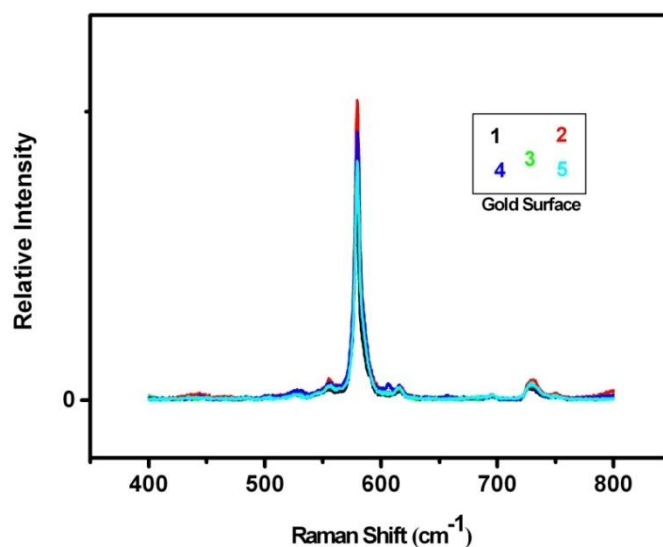


**Figure 81** SERS spectra of BCB-labeled DNA after hybridization onto the gold surface with silver colloid in dry condition. SERGen probe was designed using human proteasome gene sequence. The numbers are representing the locations at which the SERS measurements were done. The colors are coding the signal obtained from that particular point on the gold surface. Spacer used in this experiment was 11-mercapto-1-undecanol (See Appendix 14).

### 3.2.5.5 The Effect of Different Temperatures on Hybridization

Hybridization experiments were performed at different temperatures i.e, 25, 35, 45, 55 and 65 °C to find out if annealing temperature effects on hybridization. Human proteasome specific oligonucleotides and as a spacer 11-mercapto-1-undecanol were used in these experiments (Figure 82).

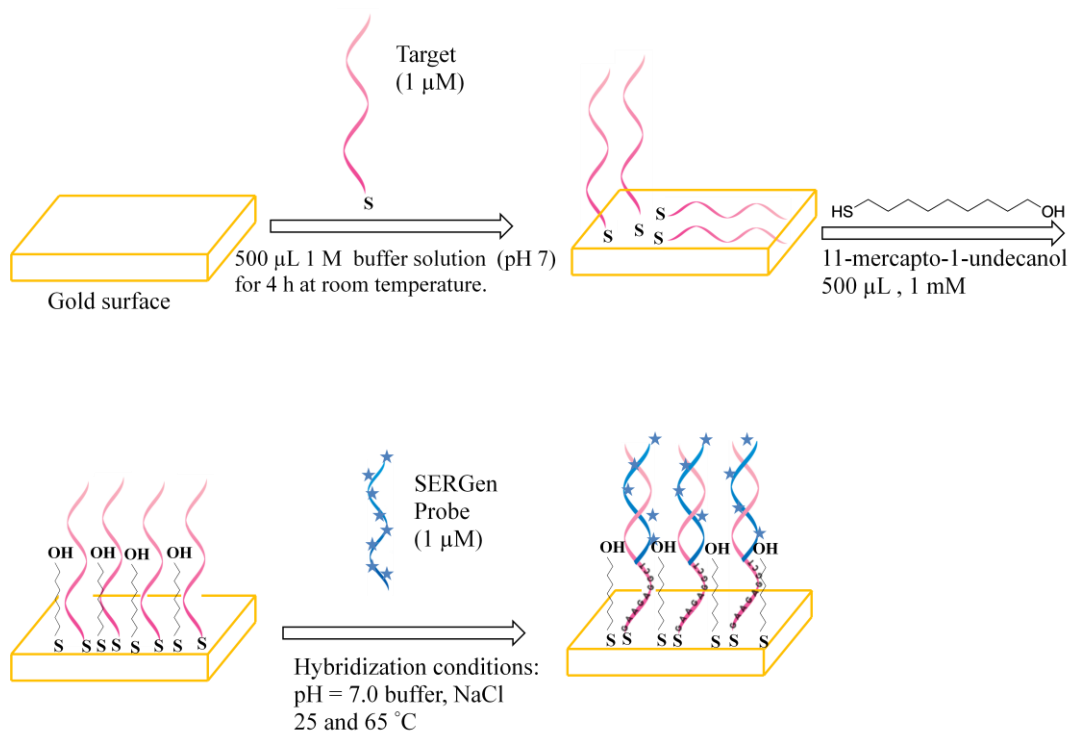
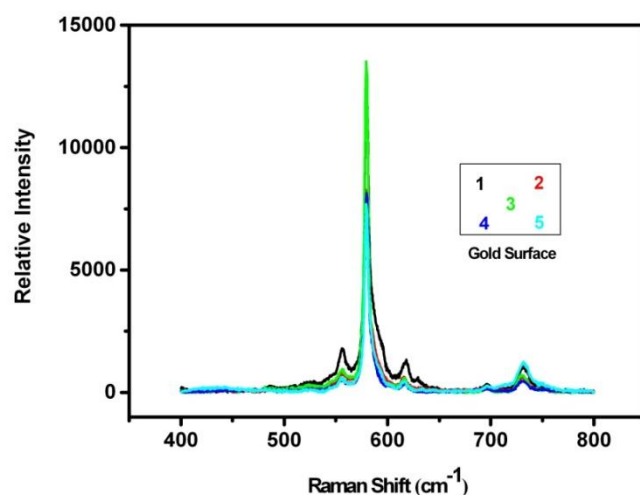


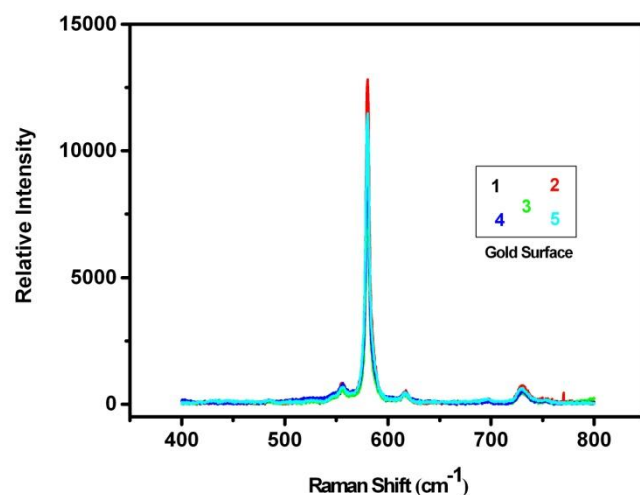
**Figure 82** Schematic representation of hybridization at different annealing temperatures.

SERS spectra were recorded in dry condition. For all the hybridization temperatures, the intensity of the peaks from the different points of the surface gave similar results (Figure 83-85).



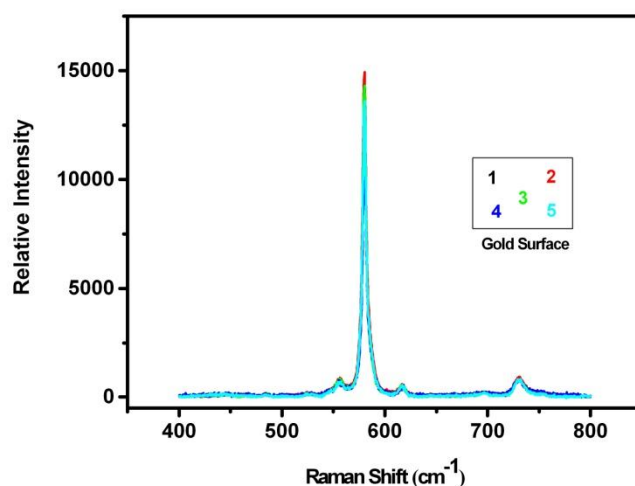


**A**

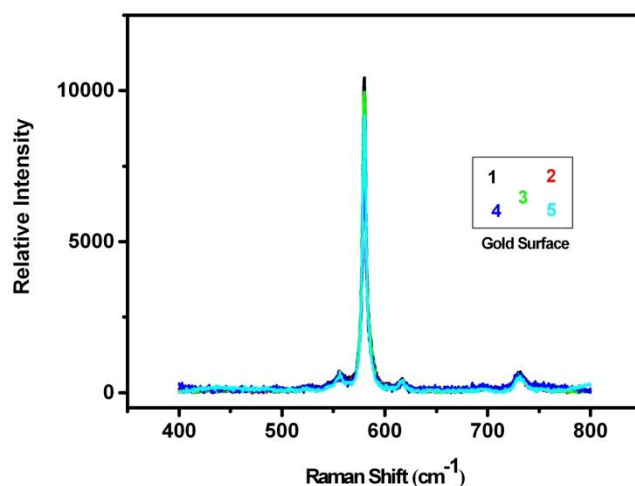


**B**

**Figure 83** SERS spectra of BCB-labeled DNA after the hybridization at A) 25 °C B) 35 °C onto the gold surface with silver colloid in dry condition. SERGen probe was designed using human proteasome gene sequence. The numbers are representing the locations at which the SERS measurements were done. The colors are coding the signal obtained from that particular point on the gold surface. Spacer used in this experiment was 11-mercapto-1-undecanol (See Appendix 15, 16).



A



B

**Figure 84** SERS spectra of BCB-labeled DNA after the hybridization at A) 45 °C B) 55 °C onto the gold surface with silver colloid in dry condition. SERGen probe was designed using human proteasome gene sequence. The numbers are representing the locations at which the SERS measurements were done. The colors are coding the signal obtained from that particular point on the gold surface. Spacer used in this experiment was 11-mercapto-1-undecanol (See Appendix 17, 18).

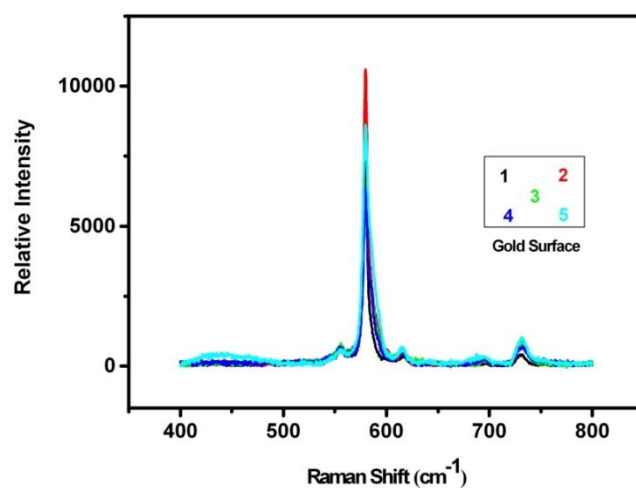


**Figure 85** SERS spectra of BCB-labeled DNA after the hybridization at 65 °C onto the gold surface with silver colloid in dry condition. SERGen probe was designed using human proteasome gene sequence. The numbers are representing the locations at which the SERS measurements were done. The colors are coding the signal obtained from that particular point on the gold surface. Spacer used in this experiment was 11-mercapto-1-undecanol (See Appendix 19).

### 3.2.5.6 Hybridization of with Probes Containing Single and Double Base Mismatches

In these experiments we aimed at, detection of single-base and double-base pair mismatches at discrete locations in archaea and human proteasome specific probes by performing hybridization at different temperatures. SERGen probes were prepared containing single-base and double-base mismatches were prepared as described in the material and methods. Hybridization experiments were performed as described before (Figure 86).

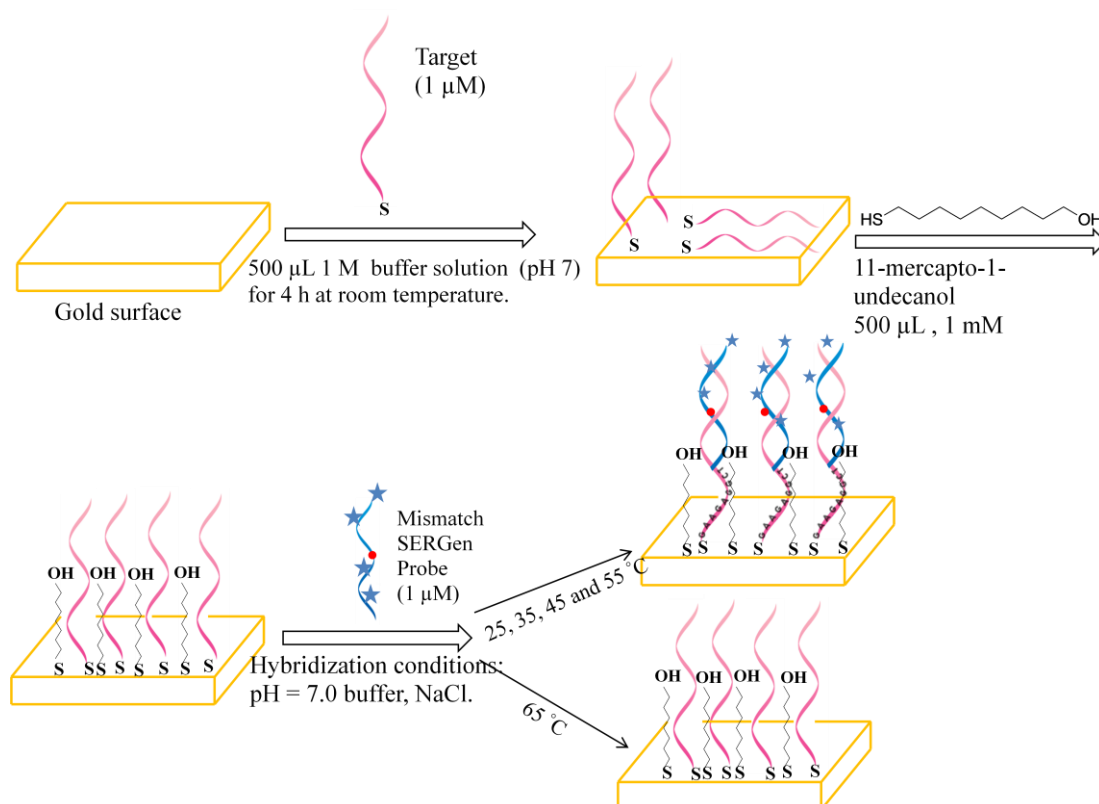
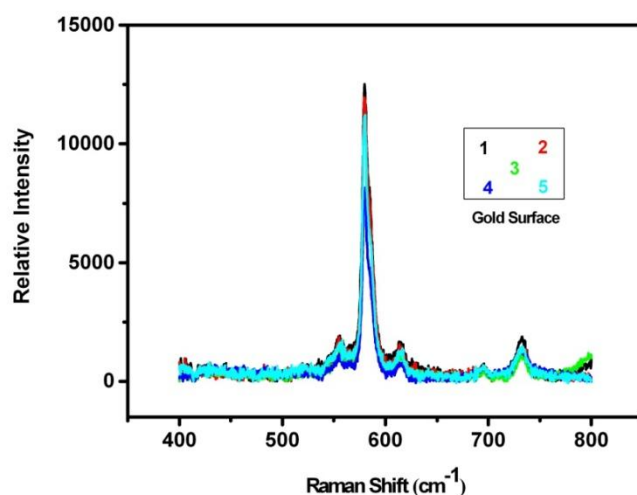


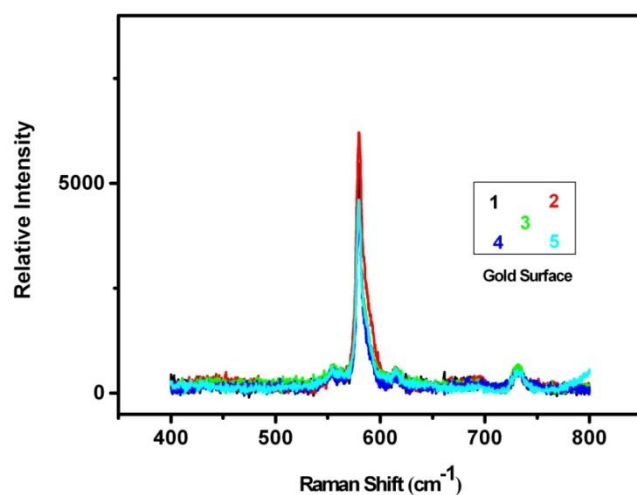
**Figure 86** Schematic representation of hybridization mismatch experiments. Spacer was 11-mercapto-1-undecanol.

### **3.2.5.6.1 SERS Results of Hybridization with of Archaea Proteasome Gene Specific Single-Mismatch Probe**

SERS spectra were recorded in dry condition at all the hybridization temperatures between 25 and 65 °C, the intensity of the peaks obtained at different points of the surface were quite similar. The peak intensity is expected to decrease with increasing hybridization temperature. Because at high temperatures, double strand DNA denatures i.e. splits into single strands, and when it is cooled slowly strands rehybridize. Single mismatched sequences would have lower melting temperatures than fully complementary strands. For this reason, mismatched duplexes will separate at lower temperatures than fully complementary (non mutant) duplexes. As can be seen from the Figures (Figure 87-89), intensity of the peak decreased with increasing hybridization temperature and at 65 °C (Figure 89) an insignificant peak was observed. Therefore, under the experimental conditions it is possible to detect single nucleotide mutations by disappearance of SERS peak at 65 °C hybridization temperature. Average peak intensities observed at 580 nm for all temperatures are given in Table 5.

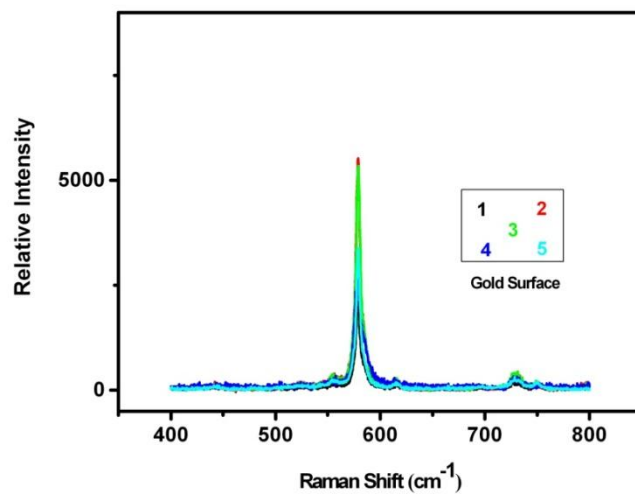


A

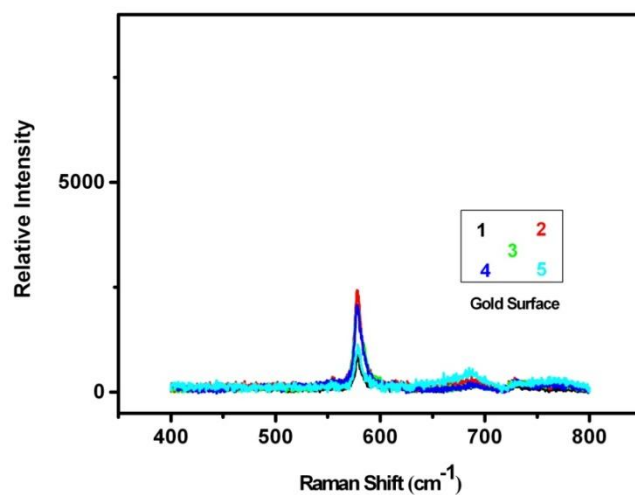


B

**Figure 87** SERS spectra of BCB-labeled DNA after the hybridization at A) 25 °C B) 35 °C onto the gold surface with silver colloid in dry condition. SERGen probe was designed using archaea proteasome gene sequence. The numbers are representing the locations at which the SERS measurements were done. The colors are coding the signal obtained from that particular point on the gold surface. Spacer used in this experiment was 11-mercapto-1-undecanol (See Appendix 20, 21).



A



B

**Figure 88** SERS spectra of BCB-labeled DNA after the hybridization at A) 45 °C B) 55 °C onto the gold surface with silver colloid in dry condition. SERGen probe was designed using archaea proteasome gene sequence. The numbers are representing the locations at which the SERS measurements were done. The colors are coding the signal obtained from that particular point on the gold surface. Spacer used in this experiment was 11-mercapto-1-undecanol (See Appendix 22, 23).

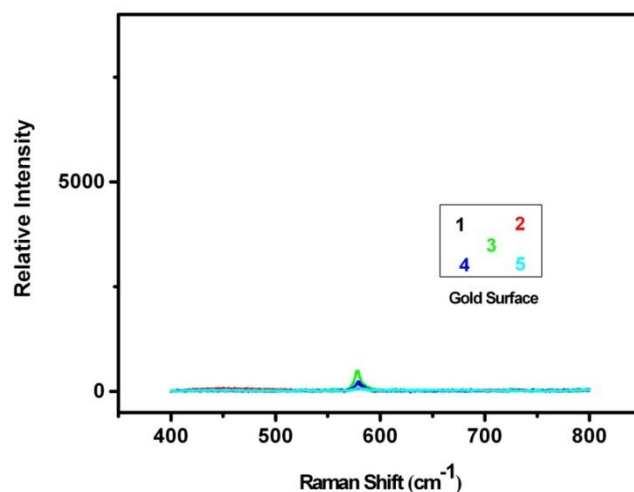


**Figure 89** SERS spectra of BCB-labeled DNA after the hybridization at 65 °C onto the gold surface with silver colloid in dry condition. SERGen probe was designed using archaea proteasome gene sequence. The numbers are representing the locations at which the SERS measurements were done. The colors are coding the signal obtained from that particular point on the gold surface. Spacer used in this experiment was 11-mercapto-1-undecanol (See Appendix 24).

**Table 5** Average peak intensities observed at 580 nm for all temperatures

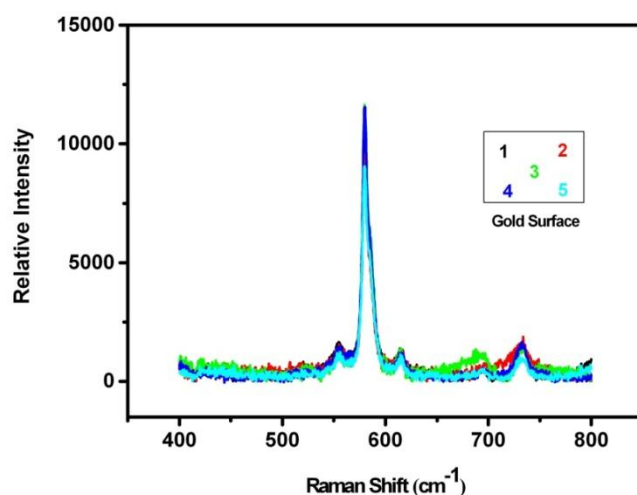
Temperature (°C)	Average Intensity at 580 nm
25	10294 (± 2221)
35	5032 (± 798)
45	3705 (± 1518)
55	1711 (± 659)
65	220 (±163)

**Note:** Five measurements were performed on each substrate and average value was calculated.

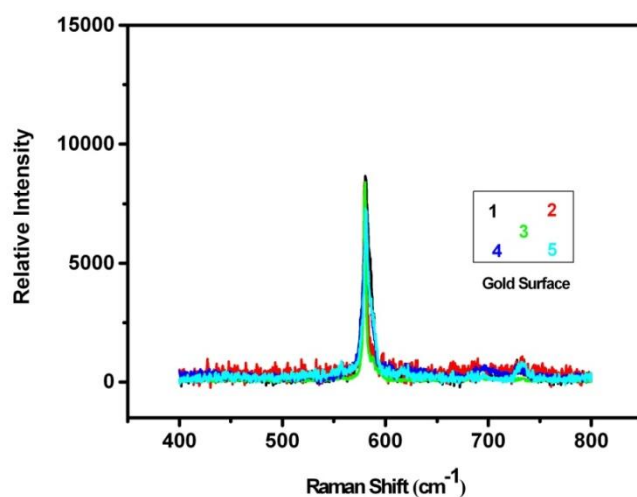


### **3.2.5.6.2 SERS Results of Hybridization with of Human Proteasome Gene Specific Single-Mismatch Probe**

SERS spectra were recorded in dry condition at all the hybridization temperatures between 25 and 65 °C, the intensity of the peaks obtained at different points of the surface were quite similar. SERS results of the experiments carried out with archaea and human proteasome specific probes were in agreement with each other. As can be seen from the Figures (Figure 90-92), intensity of the peak decreased with increasing hybridization temperature and at 65 °C (Figure 92) an insignificant peak was observed. Therefore, under the experimental conditions it is possible to detect single nucleotide mutations by disappearance of SERS peak at 65°C hybridization temperature. Average peak intensities observed at 580 nm for all temperatures are given in Table 6.

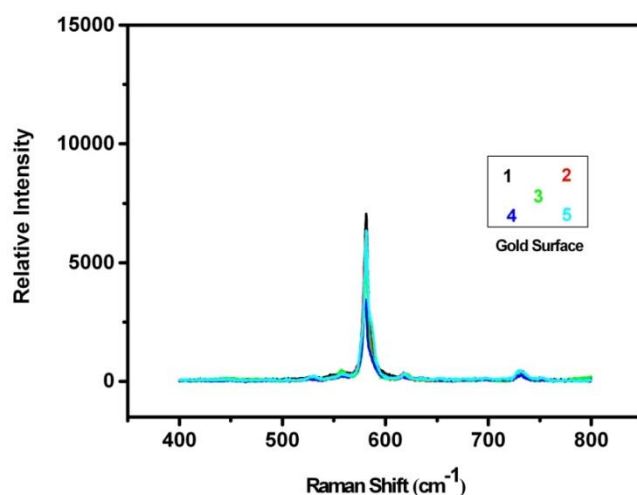


A

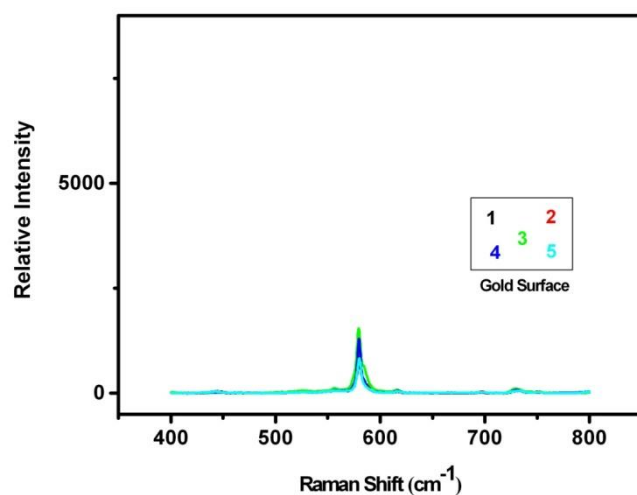


B

**Figure 90** SERS spectra of BCB-labeled DNA after the hybridization at A) 25 °C B) 35 °C onto the gold surface with silver colloid in dry condition. SERGen probe was designed using human proteasome gene sequence. The numbers are representing the locations at which the SERS measurements were done. The colors are coding the signal obtained from that particular point on the gold surface. Spacer used in this experiment was 11-mercapto-1-undecanol (See Appendix 25, 26).



**A**



**B**

**Figure 91** SERS spectra of BCB-labeled DNA after the hybridization at A) 45 °C B) 55 °C onto the gold surface with silver colloid in dry condition. SERGen probe was designed using human proteasome gene sequence. The numbers are representing the locations at which the SERS measurements were done. The colors are coding the signal obtained from that particular point on the gold surface. Spacer used in this experiment was 11-mercapto-1-undecanol (See Appendix 27, 28).

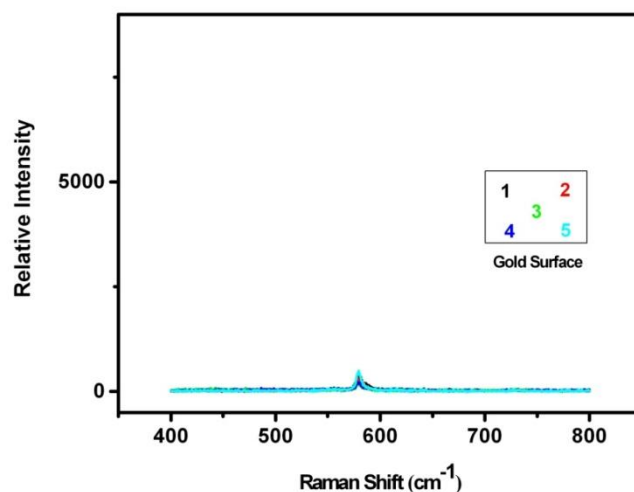


**Figure 92** SERS spectra of BCB-labeled DNA after the hybridization at 65 °C onto the gold surface with silver colloid in dry condition. SERGen probe was designed using human proteasome gene sequence. The numbers are representing the locations at which the SERS measurements were done. The colors are coding the signal obtained from that particular point on the gold surface. Spacer used in this experiment was 11-mercapto-1-undecanol (See Appendix 29).

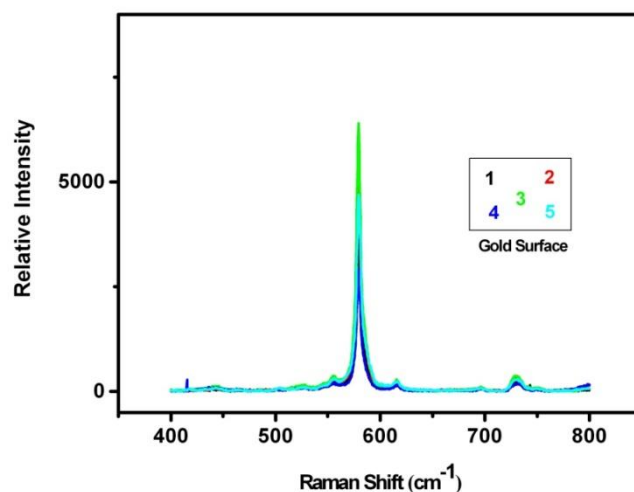
**Table 6** Average peak intensities observed at 580 nm for all temperatures

Temperature (°C)	Average Intensity at 580 nm
25	10382 ( $\pm$ 1155)
35	7921 ( $\pm$ 688)
45	5668 ( $\pm$ 1412)
55	1064 ( $\pm$ 337)
65	315( $\pm$ 133)

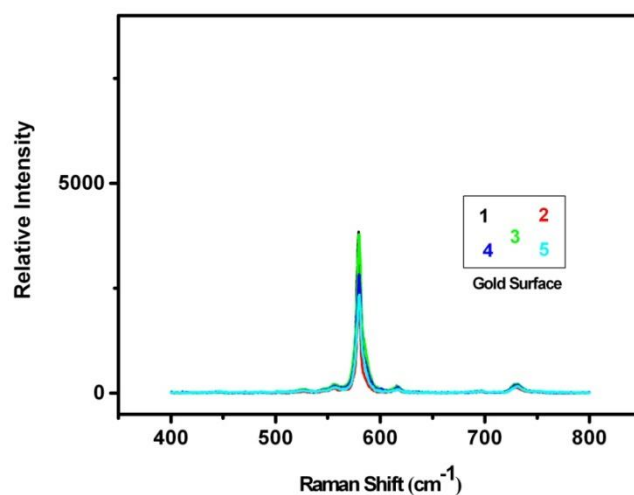
**Note:** Five measurements were performed on each substrate and average value was calculated.

### **3.2.5.6.3 SERS Results of Hybridization with of Human Proteasome Gene Specific Double-Mismatch Probe**

SERS spectra were recorded in dry condition at all the hybridization temperatures between 25 and 65 °C, the intensity of the peaks obtained at different points of the surface were quite similar. Duplexes with double nucleotide substitutions would have lower melting temperatures than duplexes with single nucleotide mismatched. Therefore, at 55 °C (Figure 94 B) significant decline in the peak density was observed than the one obtained with single nucleotide mismatch probe. Average peak intensities observed at 580 nm for all temperatures are given in Table 7.

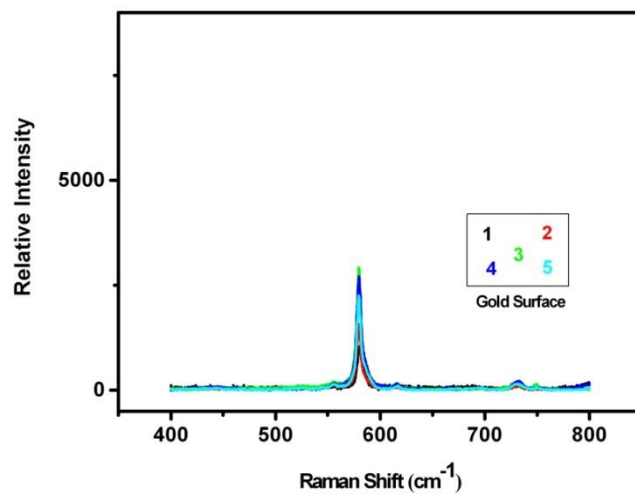


A

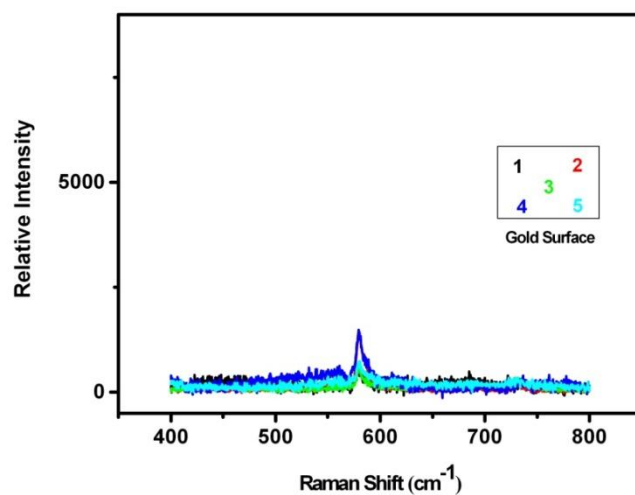


B

**Figure 93** SERS spectra of BCB-labeled DNA after the hybridization at A) 25 °C B) 35 °C onto the gold surface with silver colloid in dry condition. SERGen probe was designed using human proteasome gene sequence (double base mismatch). The numbers are representing the locations at which the SERS measurements were done. The colors are coding the signal obtained from that particular point on the gold surface. Spacer used in this experiment was 11-mercapto-1-undecanol (See Appendix 30, 31).



A



B

**Figure 94** SERS spectra of BCB-labeled DNA after the hybridization at A) 45 °C B) 55 °C onto the gold surface with silver colloid in dry condition. SERGen probe was designed using human proteasome gene sequence. The numbers are representing the locations at which the SERS measurements were done. The colors are coding the signal obtained from that particular point on the gold surface. Spacer used in this experiment was 11-mercapto-1-undecanol (See Appendix 32, 33).

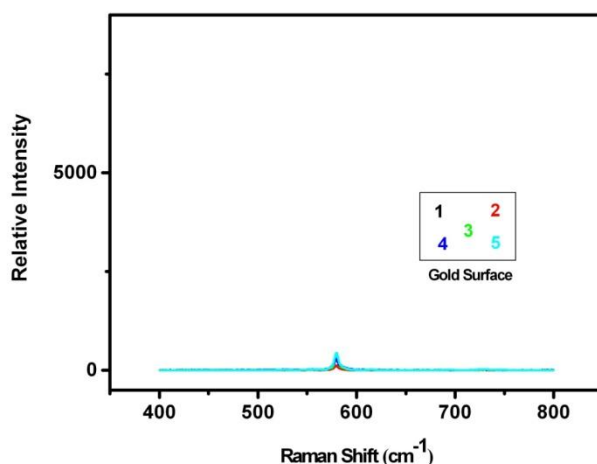


**Figure 95** SERS spectra of BCB-labeled DNA after the hybridization at 65 °C onto the gold surface with silver colloid in dry condition. SERGen probe was designed using human proteasome gene sequence. The numbers are representing the locations at which the SERS measurements were done. The colors are coding the signal obtained from that particular point on the gold surface. Spacer used in this experiment was 11-mercapto-1-undecanol (See Appendix 34).

**Table 7** Average peak intensities observed at 580 nm for all temperatures

Temperature (°C)	Average Intensity at 580 nm
25	4692 ( $\pm$ 1438)
35	3003 ( $\pm$ 753)
45	2127 ( $\pm$ 786)
55	949 ( $\pm$ 447)
65	313 ( $\pm$ 124)

**Note:** Five measurements were performed on each substrate and average value was calculated.



### 3.2.5.7 Quantitative Study Results for Human Proteasome Gene Sequence

To investigate if there is a correlation between the SERS signal intensity and SERGen probe concentration in the hybridization experiments, target concentration was kept constant at 5  $\mu\text{M}$  and SERGen probes were prepared as 0.8, 1.6, 2.4 and 4.8  $\mu\text{M}$ . To minimize the errors in the preparation of SERGen probes, three separate 3  $\mu\text{M}$  SERGen probes were prepared at the same time and after passing through separately from different spin columns, the eluents from 3 columns were combined. Target concentration was kept constant at 5  $\mu\text{M}$  on the gold surfaces and 5  $\mu\text{L}$  (0.8  $\mu\text{M}$ ), 10  $\mu\text{L}$  (1.6  $\mu\text{M}$ ), 15  $\mu\text{L}$  (2.4  $\mu\text{M}$ ) and 30  $\mu\text{L}$  (4.8  $\mu\text{M}$ ) SERGen probes were added used for hybridization on different gold substrates. Hybridization experiments were done at 55  $^{\circ}\text{C}$  as explained before. Oligonucleotides specific for the human proteasome gene sequences were used for this study.

SERS intensity values at 580 nm for different concentrations of SERGen probes are given in Table 8.

**Table 8** SERS intensity at 580 nm for different concentrations of SERGen probes.

Probe Volume ( $\mu\text{M}$ )	Intensity at 580 nm
0.8	4621
1.6	10509
2.4	13223
4.8	25980

**Note:** Five measurements were performed on each substrate and average value was calculated.

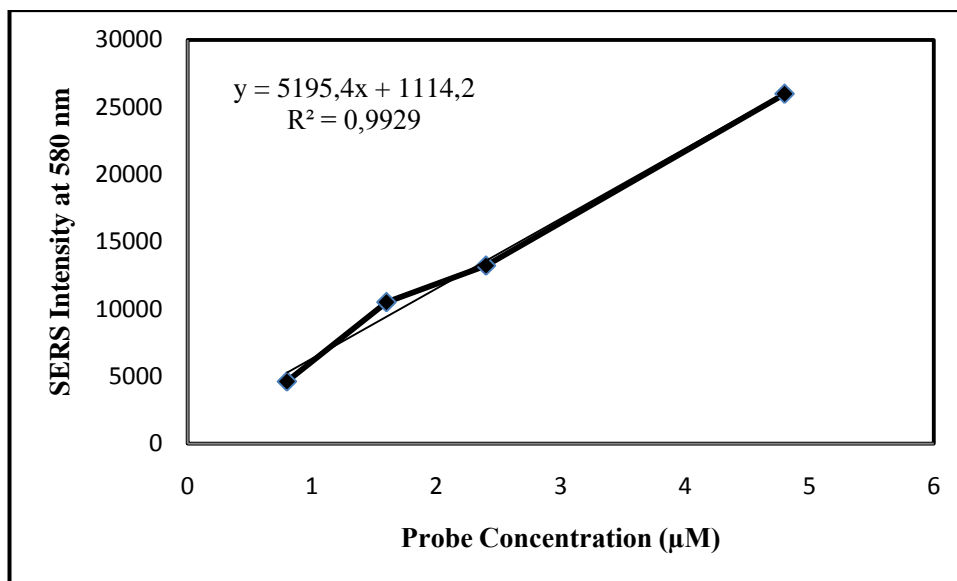


**Figure 96** The graph of SERGen probes concentrations to SERS intensities at 580 nm.

Increased intensity was observed with increasing probe volumes. The graph of probe volume versus SERS intensity at 580 nm was drawn. A linear correlation between increasing concentrations of oligo probe and increased peak intensities were observed. The correlation coefficient was  $y = 831.27x + 1114.2$  and  $R^2 = 0.9929$  (Figure 96). As can be seen from the Table 8, when the probe volume was increased 5 in two (10 µL), three (15 µL) and six times (30 µL), 2, 3 and 6-fold increase in intensity was observed respectively. This result might imply that SERS/hybridization system we developed is suitable for quantification of the hybridized DNA and thus could be well adapted for application using clinical samples.

## CHAPTER 4

### CONCLUSIONS

In this study, a new type of SERS active substrate has been developed. PVA-AgNO<sub>3</sub> solution was prepared by mixing silver nitrate with solution of PVA and films were prepared from this solution. Silver ions in PVA matrix were reduced both chemically and electrochemically. In the chemical reduction, FeSO<sub>4</sub>·7H<sub>2</sub>O reduced the silver ions in PVA matrix and SERS active polymer coating was obtained. In the electrochemical reduction, indium tin oxide glass (ITO) coated by PVA-Ag substrate was dipped into the electrochemical cell and potential was applied to reduce silver ion to metallic silver. The performances of SERS-active substrates obtained through both chemical and electrochemical reduction were evaluated with benzoic acid (BA) to make comparison between two substrates. Lower concentration solution of BA (10<sup>-6</sup> M) was obtained with the electrochemically reduced PVA-Ag substrate than that of the PVA-Ag substrate prepared by chemical reduction. However, the PVA-Ag substrate prepared by electrochemical reduction was not homogeneous. Therefore, biologically important compounds frequently used in SERS studies, p-amino benzoic acid (PABA), pyridine and dopamine, were examined using SERS-active substrates obtained through chemical reduction. As a conclusion, the PVA-Ag substrate prepared by chemical reduction was better.

Specific proteasome gene sequences were detected both label free spectrophotometric method and surface-enhanced Raman scattering (SERS) method based on label detection.

In spectrophotometric method, firstly, archaea proteasome gene probe and complementary target gene sequences were attached to the gold nanoparticles separately. Then, the target and probe oligonucleotide-modified gold solutions were mixed for hybridization and the shift in the surface plasmon absorption band of gold nanoparticles were followed. After thiolated DNA adsorption on gold nanoparticles, only a modest shift in the surface plasmon band from 520 to 525 nm was observed. On the other hand, hybridization induced the formation of a polymeric network of DNA-gold nanoparticles with a concomitant red-to-purple color change and a shift in the surface plasmon band from 520 to 557 nm was observed. To show thermally dissociation of gold probe/target polynucleotide aggregate(s), the temperature was increased from 25 °C to 75 °C and 25 °C to 100 °C. The particles were reversibly dissociated inducing a blue shift in the surface plasmon absorbance to 525 nm. Moreover, sharper plasmon band was obtained from polynucleotide aggregates heated to 100 °C compared to that of 75 °C due to the more complete dissociation of the aggregates.

In SERS method, first SERGen probes were designed using specific proteasome gene sequences. Brilliant cresyl blue (BCB), cresyl fast violet (CFV), crystal violet (CV) and fluorescein isothiocyanate (FITC) were used as Raman active labels. Labeling was done covalently and noncovalently. Zeta potential measurements showed that the signal was produced almost totally due to the noncovalent (mainly electrostatic) interaction of the dyes with the negative backbone of DNA even a covalent attachment process was applied.

The SERS spectra of SERGen probes were measured utilizing silver nanoparticles as substrate either in wet or dry conditions. Reproducibility of intensity in dry conditions was better than in wet conditions.

Spacers are used to prevent nonspecific adsorption of DNA onto gold substrate. Consequently, decanethiol, 11-mercapto-1-undecanol and 10 T chain were used as spacers. When decanethiol and 11-mercapto-1-undecanol were used as spacers, adequate surface coverage was obtained. Variations in SERS intensity were observed on gold substrate. These variations in intensity were reduced using decanethiol and

11-mercapto-1-undecanol as spacers. In addition, when experiments were performed with special care to produce an homogenous substrate surface, variation was even minimized.

Hybridization experiments were performed at different temperatures i.e, 25 and 65 °C to find out if annealing temperature effects on hybridization. For all the hybridization temperatures, the intensity of the peaks from the different points of the surface gave similar results.

Single and double base mismatches of proteasome gene sequences were detected using SERS method. Single and double mismatched sequences would have lower melting temperatures than fully complementary strands. In the experiment, intensity of the peak decreased with increasing temperature and SERS peak disappeared at 65 °C hybridization temperature.

To investigate if there is a correlation between the SERS signal intensity and SERGen probe concentration in the hybridization experiments, a quantitative study was performed. The result might imply that SERS/hybridization system we developed is suitable for quantification of the hybridized DNA and thus could be well adapted for application using clinical samples.

## REFERENCES

- Adams, J. (2004). The proteasome: a suitable antineoplastic target. *Nat. Rev. Cancer* , 4, 349–360.
- Albrecht, M. G., & Creighton, J. A. (1977). Anomalously Intense Raman Spectra of Pyridine at a Silver Electrode. *J. Am. Chem. Soc.* , 99, 5215-5217.
- Asher, G., Bercovich, Z., Tsvetkov, P., Shaul, Y., & Kahana, C. (2005). 20S Proteasomal Degradation of Ornithine Decarboxylase Is Regulated by NQO1. *Mol. Cell* , 17, 645–655.
- Badr, Y., & Mahmoud, M. (2006). Enhancement of the Optical Properties of Poly Vinyl Alcohol by Doping with Silver Nanoparticles. *J. Appl. Polymer Sci.* , 99, 3608–3614.
- Badr, Y., & Mahmoud, M. (2006). Manifestation of the silver nanoparticles incorporated into the poly vinyl alcohol matrices. *J. Mater. Sci.* , 41, 3947–3953.
- Barhoumi, A., Zhang, D., Tam, F., & Halas, N. J. (2008). Surface-enhanced Raman spectroscopy of DNA. *J. Am. Chem. Soc.* , 130, 5523–5529.
- Bell, S. E., & Spence, S. J. (2001). Disposable, stable media for reproducible surface-enhanced Raman spectroscopy. *Analyst* , 126, 1–3.
- Bell, S. E., Fido, L. A., Sirimuthu, N. M., Speers, S. J., Peters, K. L., & Cosbey, S. H. (2007). Screening Tablets for DOB Using Surface-Enhanced Raman Spectroscopy. *J. Forensic Sci.* , 52, 1063-1067.
- Bowerman, B., & Kurz, T. (2006). Degrade to create: developmental requirements for ubiquitin-mediated proteolysis during early *C. elegans* embryogenesis. *Development* , 133, 773-784.
- Brolo, A. G., Irish, D. E., & Lipkowsky, J. (1997). Surface-Enhanced Raman Spectra of Pyridine and Pyrazine Adsorbed on a Au(210). *J. Phys. Chem. B* , 101, 3906-3909.
- Campion, A., & Kambhampati, P. (1998). Surface-enhanced Raman scattering. *Chem. Soc. Rev.* , 27, 241-250.

Cao, Y., Jin, R., & Mirkin, C. A. (2002). Nanoparticles with Raman Spectroscopic Fingerprints for DNA and RNA Detection. *Science* , 297, 1536–1540.

Chou, K.-S., & Ren, C.-Y. (2000). Synthesis of nanosized silver particles by chemical reduction method. *Mater. Chem. Phys.* , 64 , 241–246.

Chourpa, I., Lei, F. H., Dubois, P., Manfait, M., & Sockalingum, G. D. (2008). Intracellular applications of analytical SERS spectroscopy and multispectral imaging. *Chem. Soc. Rev.* , 37, 993-1000.

Chu, B. C., & Orgel, L. E. (1983). Derivatization of unprotected polynucleotides. *Nucl. Acids Res.* , 11, 6513-6529.

Ciechanover, A. (2005). Intracellular protein degradation: from a vague idea thru the lysosome and the ubiquitin-proteasome system and onto human diseases and drug targeting. *Cell Death Differ.* , 12, 1178-1190.

Ciechanover, A., Orian, A., & Schwartz, A. L. (2000). The Ubiquitin-Mediated Proteolytic Pathway: Mode of Action and Clinical Implications. *J. Cell. Biochem. Suppl.* , 34, 40–51.

Collins, G. A., & Tansey, W. P. (2006). The proteasome: a utility tool for transcription? *Curr. Opin. Genet. Dev.* , 16, 197–202.

Creighton, J. A., & Eadon, D. G. (1991). Ultraviolet-Visible Absorption Spectra of the Colloidal Metallic Elements. *J. Chem. Soc. Faraday Trans.* , 87, 3881-3891.

Dahlmann, B. (2007). Role of proteasomes in disease. *BMC Biochem.* , 8.

Darnell, J., Lodish, H., & Baltimore, D. (1990). *Molecular Cell Biology, 2nd Ed.* New York: Scientific American Book.

Doering, W. E., Piotti, M. E., Natan, M. J., & Freeman, R. G. (2007). SERS as a Foundation for Nanoscale, Optically Detected Biological Labels. *Adv. Mater.* , 19, 3100–3108.

Dollish, F., Fateley, W., & Bentley, F. (1974). *Characteristic Raman Frequencies of Organic Compounds.* Toronto, Canada.

Ferraro, J. R., Nakamoto, K., & Brown, C. W. (2003). *Introductory Raman spectroscopy.* Amsterdam ; Boston : Academic Press.

Fleischmann, M., Hendra, P., & McQuilla, A. (1974). Raman-spectra of pyridine adsorbed at a silver electrode. *Chem. Phys. Lett.* , 26, 163-166.

Gaddy, G., Korchev, A., McLain, J., & Slaten, B. (2004). Light-Induced Formation of Silver Particles and Clusters in Crosslinked PVA/PAA Films. *J. Phys. Chem. B* , 108, 14850-14857.

- Gaddy, G., McLain, J., Steigerwalt, E., Broughton, R., Slaten, B., & Mills, G. (2001). Photogeneration of Silver Particles in PVA Fibers and Films. *J. Cluster Sci.* , 12,, 457-471.
- Giesfeldt, K. S., Connatser, R. M., De Jesu' s, M. A., Dutta, P., & Sepaniak, M. J. (2005). Gold-polymer nanocomposites: studies of their optical properties and their potential as SERS substrates. *J. Raman . Spectrosc.* , 36, 1134–1142.
- Grabar, K., Freeman, R., Hommer, M., & Natan, M. J. (1995). Preparation and Characterization of Au colloid Monolayers. *Anal. Chem.* , 735-743.
- Green, M., Liu, F.-M., Cohen, L., Köllensperger, P., & Cass, T. (2006). SERS platforms for high density DNA arrays. *Faraday Discuss.* , 132, 269–280.
- Haynes, C. L., McFarland, A. D., & Van Duyne, R. P. (2005). Surface-Enhanced Raman Spectroscopy. *Anal. Chem.* , 338A-346A.
- Hering, K., Cialla, D., Ackermann, K., Dörfer, T., Möller, R., Schneidewind, H., et al. (2008). SERS: a versatile tool in chemical and biochemical diagnostics. *Anal. Bioanal. Chem.* , 390, 113–124.
- Herne, T. M., & Tarlov, M. J. (1997). Characterization of DNA Probes Immobilized on Gold Surfaces. *J. Am. Chem. Soc.* , 119, 8916-8920.
- Hershko, A. (2005). The ubiquitin system for protein degradation and some of its roles in the control of the cell division cycle. *Cell Death Differ.* , 12, 1191-1197.
- Hirai, H., Nakao, Y., & Toshima, N. (1979). Preparation of colloidal transition-metals in polymers by reduction with alcohols or ethers. *J. Macromol. Sci-Chem.* , 727-750.
- Ho, W. S., & Dalrymple, D. (1994). Facilitated transport of olefins in Ag+-containing polymer membranes. *J. Membr. Sci.* , 13-25.
- Huang, E., Zhou, F., & Deng, L. (2000). Studies of Surface Coverage and Orientation of DNA Molecules Immobilized onto Preformed Alkanethiol Self-Assembled Monolayers. *Langmuir* , 16, 3272-3280.
- Huang, X., Neretina, S., & El-Sayed, M. A. (2009). Gold Nanorods: From Synthesis and Properties to Biological and Biomedical Applications. *Adv. Mater.* , 21, 4880–4910.
- Hudson, S. D., & Chumanov, G. (2009). Bioanalytical applications of SERS (surface-enhanced Raman spectroscopy). *Anal. Bioanal. Chem.* , 394, 679–686.



- Ibrahim, A., Oldham, P. B., Stokes, D. L., & Vo-Dinh, T. (1996). Determination of Enhancement Factors for Surface-Enhanced FT-Raman Spectroscopy on Gold and Silver Surfaces. *J. Raman Spectrosc.* , 27, 887-891.
- Isola, N. R., Stokes, D. L., & Vo-Dinh, T. (1998). Surface-Enhanced Raman Gene Probe for HIV Detection. *Anal. Chem.* , 70, 1352-1356.
- Jeanmaire, D. L., & Van Duyne, R. P. (1977). Surface raman spectroelectrochemistry: Part I. Heterocyclic, aromatic, and aliphatic amines adsorbed on the anodized silver electrode. *J. Electroanal. Chem. Interfacial Electrochem.* , 84, 1-20.
- Jennings, C., Aroca, R., Hor, A.-M., & Loutfy, R. (1984). Surface-Enhanced Raman Scattering from Copper and Zinc Phthalocyanine Complexes by Silver and Indium Island Films. *Anal. Chem.* , 56 , 2033-2035.
- Karabıçak, S., Kaya, M., Vo-Dinh, T., & Volkan, M. (2008). Silver Nanoparticle-Doped Polyvinyl Alcohol Coating as a Medium for Surface-Enhanced Raman Scattering Analysis. *J. Nanosci. Nanotech.* , 8, 955–960.
- Keller, J. N., Hanni, K. B., & Markesbery, W. R. (2000). Impaired Proteasome Function in Alzheimer's Disease. *J. Neurochem.* , 75, 436-439.
- Khanna, P., Singh, N., Charan, S., Subbarao, V.V.V.S., & Gokhale, R. (2005). Synthesis and characterization of Ag/PVA nanocomposite by chemical reduction method. *Mater. Chem. Phys.* , 93 , 117–121.
- Kloetzel, P.-M. (2001). Antigen processing by the proteasome. *Nat. Rev. Mol. Cell Bio.* , 2, 179-188.
- Kneipp, K., Kneipp, H., & Kneipp, J. (2006). Surface-Enhanced Raman Scattering in Local Optical Fields of Silver and Gold Nanoaggregates-From Single-Molecule Raman Spectroscopy to Ultrasensitive Probing in Live Cells. *Acc. Chem. Res.* , 39, 443-450.
- Kneipp, K., Kneipp, H., Itzkan, I., & Dasari, R. R. (2002). Surface-enhanced Raman scattering and biophysics. *J. Phys.: Condens. Matter* , 14 , R597–R624.
- Kneipp, K., Kneipp, H., Itzkan, I., Dasari, R. R., & Feld, M. S. (1999). Ultrasensitive Chemical Analysis by Raman Spectroscopy. *Chem. Rev.* , 99, 2957-2975.
- Kneipp, K., Kneipp, H., Itzkan, I., Dasari, R., & Feld, M. (2002). Surface-enhanced Raman scattering and biophysics. *Journal of Physics: Condensed Matter* , R597-R62.
- Krkljes, A., Nedeljkovic, J., & Kacarevic-Popovic, Z. (2007). Fabrication of Ag-PVA hydrogel nanocomposite by  $\gamma$ -irradiation. *Polymer Bull.* , 271–279.

- Kudelski, A. (2008). Analytical applications of Raman spectroscopy. *Talanta* , 76, 1–8.
- Kurokawa, Y., & Imaib, Y. (1991). Surface-enhanced Raman scattering (SERS) using polymer (cellulose acetate and Nafion) membranes impregnated with fine silver particles. *J. Membr. Sci.* , 55, 227-233.
- Laserna, J., Torres, E., & Winefordner, J. (1987). Studies of sample preparation for surface-enhanced Raman spectrometry on silver hydrosols. *Anal. Chim. Acta* , 200, 469-480.
- Lee, C.-Y., Gong, P., Harbers, G. M., Grainger, D., Castner, D. G., & Gamble, L. J. (2006). Surface Coverage and Structure of Mixed DNA/Alkylthiol Monolayers on Gold: Characterization by XPS, NEXAFS, and Fluorescence Intensity Measurements. *Anal. Chem.* , 78 , 3316-3325.
- Lee, P. C., & Meisel, D. J. (1982). Adsorption and Surface-Enhanced Raman of Dyes on Silver and Gold Sols. *J. Phys. Chem.* , 3391-3395.
- Li, Y.-S., Wang, Y., & Cheng, J. (2001). Interaction Effects on Surface-Enhanced Raman Scattering Activities in Silver Sols. *Vib. Spectrosc.* , 27, 65-74.
- Liang, E., Engert, C., & Kiefer, W. (1993). Surface-enhanced Raman spectroscopy of p-aminobenzoic acid with excitation in the visible and near infrared spectral region. *Vib. Spectrosc.* , 6, 79-85.
- Lin, W.-C., & Yang, M.-C. (2005). Novel Silver/Poly(vinyl alcohol) Nanocomposites for Surface-Enhanced Raman Scattering-Active Substrates. *Macromol. Rapid Commun.* , 26, 1942–1947.
- Link, S., & El-Sayed, M. A. (2003). Optical Properties and Ultrafast Dynamics of Metallic Nanocrystals. *Annu. Rev. Phys. Chem.* , 54, 331-366.
- Link, S., & El-Sayed, M. A. (1999). Spectral Properties and Relaxation Dynamics of Surface Plasmon Electronic Oscillations in Gold and Silver Nanodots and Nanorods. *J. Phys. Chem. B* , 103, 8410-8426.
- Liu, Y.-C., Yu, C.-C., & Hsu, T.-C. (2008). Effect of TiO<sub>2</sub> Nanoparticles on the Improved Performances on Electrochemically Prepared Surface-Enhanced Raman Scattering-Active Silver Substrates. *J. Phys. Chem. C* , 112, 16022–16027.
- Lomas, H., Canton, I., MacNeil, S., Du, J., Armes, S. P., Ryan, A. J., et al. (2007). Biomimetic pH Sensitive Polymersomes for Efficient DNA Encapsulation and Delivery. *Adv. Mater.* , 19, 4238–4243.

- Lytton-Jean, A. K., & Mirkin, C. A. (2005). A Thermodynamic Investigation into the Binding Properties of DNA Functionalized Gold Nanoparticle Probes and Molecular Fluorophore Probes. *J. Am. Chem. Soc.* , *127*, 12754-12755.
- Mbhele, Z., Salemane, M., Sittert, C. v., Djokovic, V., & Luyt, A. (2003). Fabrication and Characterization of Silver-Polyvinyl Alcohol Nanocomposites. *Chem. Mater.* , *15*, 5019-5024.
- Moskovits, M. (1985). Surface-enhanced Spectroscopy. *Rev. Mod. Phys.* , *57*, 783-826.
- Naujokat, C., & Hoffmann, S. (2002). Role and Function of the 26S Proteasome in Proliferation and Apoptosis. *Lab. Invest.* , *82*, 965-980.
- Nawrocki, S. T., Carew, J. S., Pino, M. S., Highshaw, R. A., Dunner, K. J., Huang, P., et al. (2005). Bortezomib sensitizes pancreatic cancer cells to endoplasmic reticulum stress-mediated apoptosis. *Cancer Res.* , *65*, 11658–11666.
- Otto, A. (1982). *Springer Chem. Phys.* , *21*, 186–195.
- Papandreou, C. N., & Logothetis, C. J. (2004). Bortezomib as a potential treatment for prostate cancer. *Cancer Res.* , *64*, 5036–5043.
- Park, S. Y., Lee, J.-S., Georganopoulou, D., & Mirkin, C. A. (2006). Structures of DNA-Linked Nanoparticle Aggregates. *J. Phys. Chem. B* , *110*, 12673-12681.
- Paul, S. (2008). Dysfunction of the ubiquitin–proteasome system in multiple disease conditions: therapeutic approaches. *BioEssays* , *30*, 1172–1184.
- Peters, J. M., Franke, W. W., & Kleinschmidt, J. A. (1994). Distinct 19 S and 20 S subcomplexes of the 26 S proteasome and their distribution in the nucleus and the cytoplasm. *J. Biol. Chem.* , *269* , 7709–18.
- Ren, B., Liu, G.-K., Lian, X.-B., Yang, Z.-L., & Tian, Z.-Q. (2007). Raman spectroscopy on transition metals. *Anal. Bioanal. Chem.* , *388*, 29–45.
- Richardson, P. G., Mitsiades, C., Hideshima, T., & Anderson, K. C. (2006). Bortezomib: proteasome inhibition as an effective anticancer therapy. *Annu. Rev. Med.* , *57*, 33–47.
- Rose, I. (2005). Ubiquitin at Fox Chase. *Cell Death Differ.* , *12*, 1198-1201.
- Saito, H. (1993). Behaviour of the 1025 cm<sup>-1</sup> Band of SERS Spectra Due to Pyridine on a Silver Electrode in Aqueous Halide Media. *J. Raman Spectrosc.* , *24*, 191-197.
- Sakai, N., Sawada, M. T., & Sawada, H. (2004). Non-traditional roles of ubiquitin–proteasome system in fertilization and gametogenesis. *Int. J. Biochem. Cell Biol.* , *36*, 776–784.

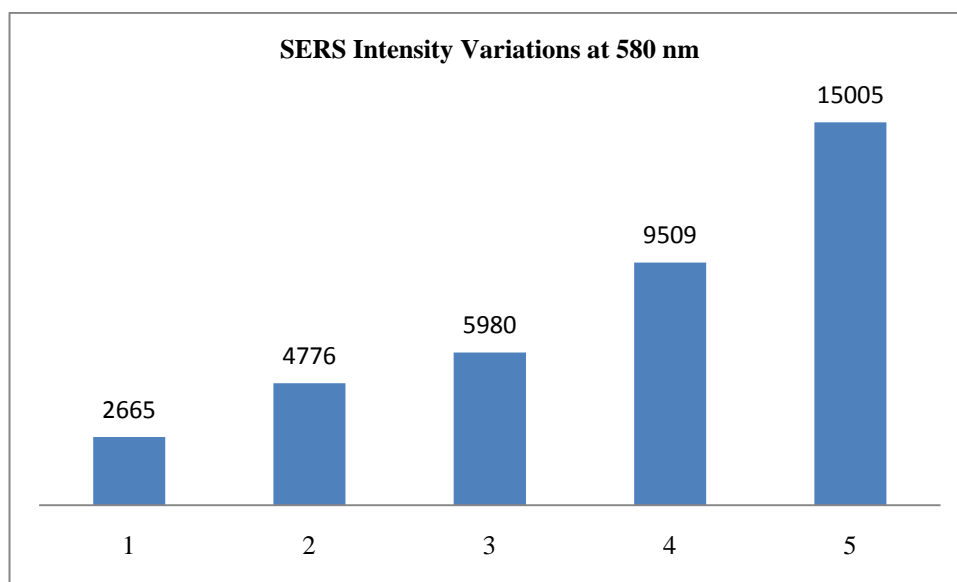
- Salama, S., Stong, J. D., Neilands, J. B., & Spiro, T. G. (1978). Electronic and Resonance Raman Spectra of Iron( 111) Complexes of Enterobactin, Catechol, and N-Methyl-2,3-dihydroxybenzamide . *Biochemistry* , 17 , 3781-3785.
- Sassolas, A., Leca-Bouvier, B. D., & Blum, L. J. (2008). DNA Biosensors and Microarrays. *Chem. Rev.* , 108, 109-139.
- Sauer, G., Nickel, U., & Schneider, S. (2000). Preparation of SERS-active silver film electrodes via electrocrystallization of silver. *J. Raman Spectrosc.* , 31, 359-363.
- Steel, A. B., Levicky, R. L., Herne, T. M., & Tarlov, M. J. (2000). Immobilization of Nucleic Acids at Solid Surfaces: Effect of Oligonucleotide Length on Layer Assembly. *Biophys. J.* , 79 , 975–981.
- Stokes, R. J., Macaskill, A., Lundahl, P. J., Smith, W. E., Faulds, K., & Graham, D. (2007). Quantitative Enhanced Raman Scattering of Labeled DNA from Gold and Silver Nanoparticles. *Small* , 3, 1593 – 1601.
- Storhoff, J. J., Elghanian, R., Mirkin, C. A., & Letsinger, R. L. (2002). Sequence-Dependent Stability of DNA-Modified Gold Nanoparticles. *Langmuir* , 18, 6666-6670.
- Storhoff, J. J., Elghanian, R., Mucic, R. C., Mirkin, C. A., & Letsinger, R. L. (1998). One-Pot Colorimetric Differentiation of Polynucleotides with Single Base Imperfections Using Gold Nanoparticle Probes. *J. Am. Chem. Soc.* , 1959-1964.
- Strehl, B., Seifert, U., Krüger, E., Heink, S., Kuckelkorn, U., & Kloetzel, P.-M. (2005). Interferon- $\gamma$ , the functional plasticity of the ubiquitin–proteasome system, and MHC class I antigen processing. *Immunol. Rev.* , 207, 19–30.
- Suh, J. S., DiLella, D., & Moskovits, M. (1983). Surface-Enhanced Raman Spectroscopy of Colloidal Metal Systems: A Two-Dimensional Phase Equilibrium in p -Aminobenzoic Acid Adsorbed on Silver. *J. Phys. Chem.* , 87 , 1540-1544.
- Taylor, C., & Jobin, C. (2005). Ubiquitin Protein Modification and Signal Transduction: Implications for Inflammatory Bowel Diseases. *Inflamm. Bowel Dis.* , 11, 1097-1107.
- Temperini, M. L., Sala, D., Lacconi, I., Gioda, A. S., Macagno, V. A., & Arvia, A. J. (1988). Correlation between SERS of Pyridine and Electrochemical Response of Silver Electrodes in Halide-Free Alkaline Solutions. *Langmuir* , 4, 1032-1039.
- Thompson, D. G., Enright, A., Faulds, K., Smith, W. E., & Graham, D. (2008). Ultrasensitive DNA Detection Using Oligonucleotide-Silver Nanoparticle Conjugates. *Anal. Chem.* , 80, 2805-2810.

- Tian, Z.-Q., Yang, Z.-L., Ren, B., & Wu, D.-Y. (2006). SERS from transition metals and excited by ultraviolet light. *Top. Appl. Phys.* , 103, 125-146.
- Tourwe', E., & Hubin, A. (2006). Preparation of SERS-active electrodes via ex situ electrocrystallization of silver in a halide free electrolyte. *Vib. Spectrosc.* , 41, 59–67.
- Törnblom, M., & Henriksson, U. (1997). Effect of solubilization of aliphatic hydrocarbons on size and shape of rodlike C16TABr micelles studied by 2H NMR relaxation. *J. Phys. Chem. B* , 101, 6028-6035.
- Tsukamoto, S., & Yokosawa, H. (2006). Natural Products Inhibiting the Ubiquitin-Proteasome Proteolytic Pathway, A Target for Drug Development. *Curr. Med. Chem.* , 13, 745–754.
- Vij, N. (2011). The case for therapeutic proteostasis modulators. *Expert Opin. Ther. Targets* , 3, 233-236.
- Vo-Dinh, T. (2003). *Biomedical Photonics Handbook*. CRC Presss, Boca Raton, FL.
- Vo-Dinh, T. (2008). Nanobiosensing using plasmonic nanoprobos. *IEEE J. Sel. Top. Quant. Electron.* , 14, 198–205.
- Vo-Dinh, T., Allain, L. R., & Stokes, D. L. (2002). Cancer gene detection using surface-enhanced Raman scattering (SERS). *J. Raman Spectrosc.* , 33, 511–516.
- Vo-Dinh, T., Stokes, D. L., Griffin, G. D., Volkan, M., Kim, U. J., & Simon, M. I. (1999). Surface-enhanced Raman Scattering (SERS) Method and Instrumentation for Genomics and Biomedical Analysis. *J. Raman Spectrosc.* , 30, 785–793.
- Volkan, M., Stokes, D. L., & Vo-Dinh, T. (1999). A New Surface-Enhanced Raman Scattering Substrate Based on Silver Nanoparticles in Sol–Gel. *J. Raman Spectrosc.* , 30, 1057–1065.
- Wang, C.-C. (2008). Surfaced-Enhanced Raman Scattering-Active Substrates Prepared through a Combination of Argon Plasma and Electrochemical Techniques. *J. Phys. Chem. C* , 112, 5573-5578.
- Wang, C.-C., & Chen, J.-S. (2008). Improved surfaced-enhanced Raman scattering based on electrochemically roughened silver substrates modified through argon plasma treatment. *Electrochim. Acta* , 53, 5615–5620.
- Wang, J., & Maldonado, M. A. (2006). The Ubiquitin-Proteasome System and Its Role in Inflammatory and Autoimmune Diseases. *Cell. Mol. Immunol.* , 3, 255-261.
- Wang, K., & Li, Y.-S. (1997). Silver doping of polycarbonate films for surface-enhanced Raman scattering. *Vib. Spectrosc.* , 14 , 183-188.

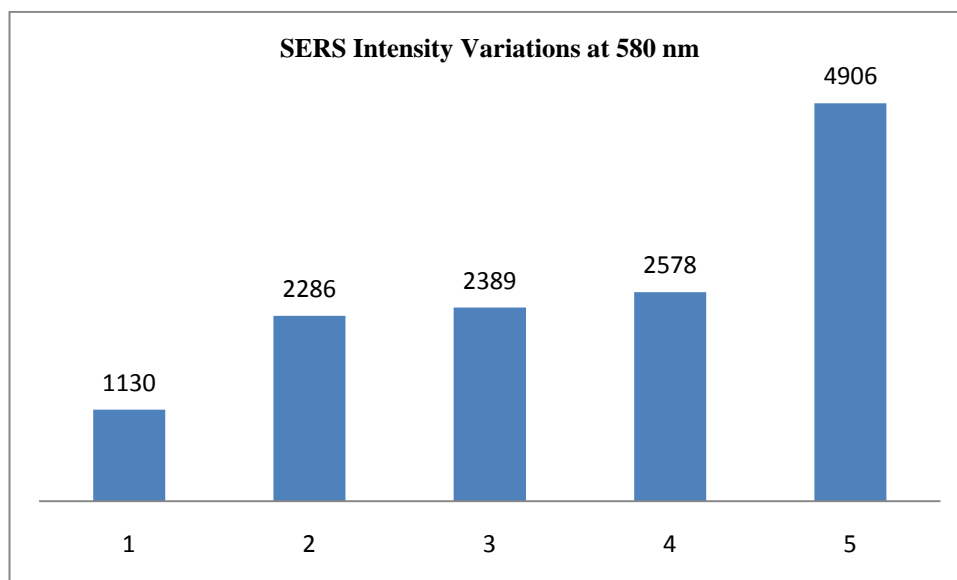
- Wang, Y. T., Zhao, F. L., Li, K. A., & Tong, S. Y. (2000). Molecular spectroscopy study of the reaction of nucleic acids with brilliant cresol blue. *Spectrochim. Acta , Part A* (56 ), 1827–1833.
- Wang, Z., Tang, X., & Ding, Z. (2005). Raman and photoluminescence spectroscopy study of benzoic acid at high pressures. *J. Phys. Chem. Sol. , 66*, 895–901.
- Watson, J., & Crick, F. H. (1953). Molecular Structure of Nucleic Acids. *Nature , 248*, 737-738.
- Wikipedia. (2010). *Wikipedia-Catecholamine*. 12 2010 tarihinde Wikipedia: <http://en.wikipedia.org/wiki/Catecholamine> adresinden alındı
- Wood, E., Sutton, C., Beezer, A. E., Creighton, J. A., Davis, A. F., & Mitchell, J. C. (1997). Surface-enhanced Raman scattering (SERS) study of membrane transport processes. *Int. J. Pharm. , 154* , 115-118.
- Yen, C.-C. (1996). Studies on the Preparation and Properties of Conductive Polymers. IX. Using Photographic Developer to Prepare Metallized Conductive Polymer Films. *J. Appl. Polymer Sci. , 60*, 605-608.
- Yonzon, C. R., Stuart, D. A., Zhang, X., McFarland, A. D., Haynes, C. L., & Van Duyne, R. P. (2005). Towards advanced chemical and biological nanosensors—An overview. *Talanta , 67*, 438–448.
- Yu, D.-G., Lin, W.-C., Lin, C.-H., Chang, L.-M., & Yang, M.-C. (2007). An in situ reduction method for preparing silver/poly(vinyl alcohol) nanocomposite as surface-enhanced Raman scattering (SERS)-active substrates. *Mater. Chem. Phys. , 101* , 93–98.
- Zhang, H., Liu, F., He, T., & Xin, H. (1995). Time dependent UV-absorption spectra and surface enhanced Raman scattering of pyridine in AgCl sol. *Spectrochim. Acta A , 1903-1908*.
- Zhao, N., Shi, F., Wang, Z., & Zhang, X. (2005). Combining Layer-by-Layer Assembly with Electrodeposition of Silver Aggregates for Fabricating Superhydrophobic Surfaces. *Langmuir , 21*, 4713-4716.
- Zhou, Q., Li, X., Fan, Q., Zhang, X., & Zheng, J. (2006). Charge Transfer between Metal Nanoparticles Interconnected with a Functionalized Molecule Probed by Surface-Enhanced Raman Spectroscopy. *Angew. Chem. , 118*, 4074 –4077.

## APPENDIX

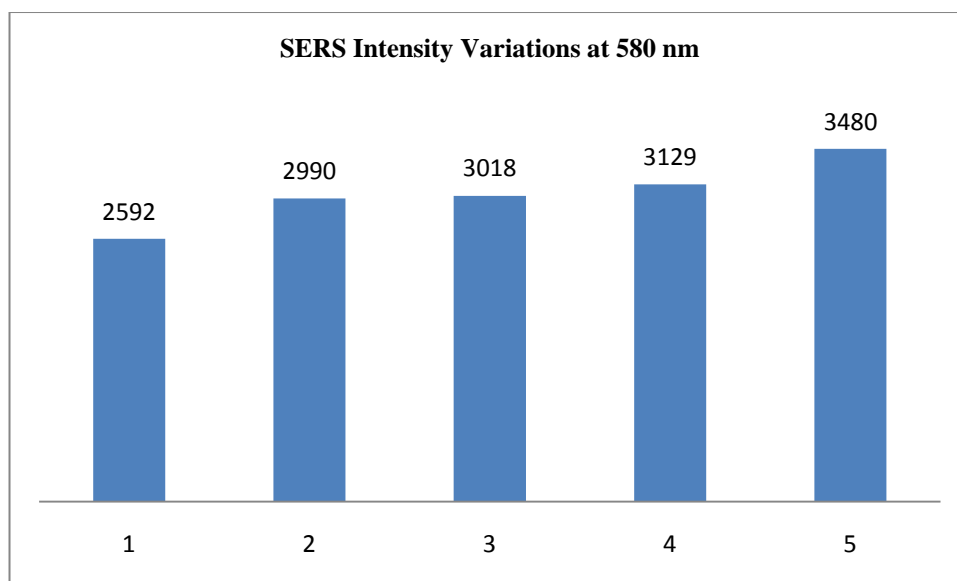
### 1. Figure 61



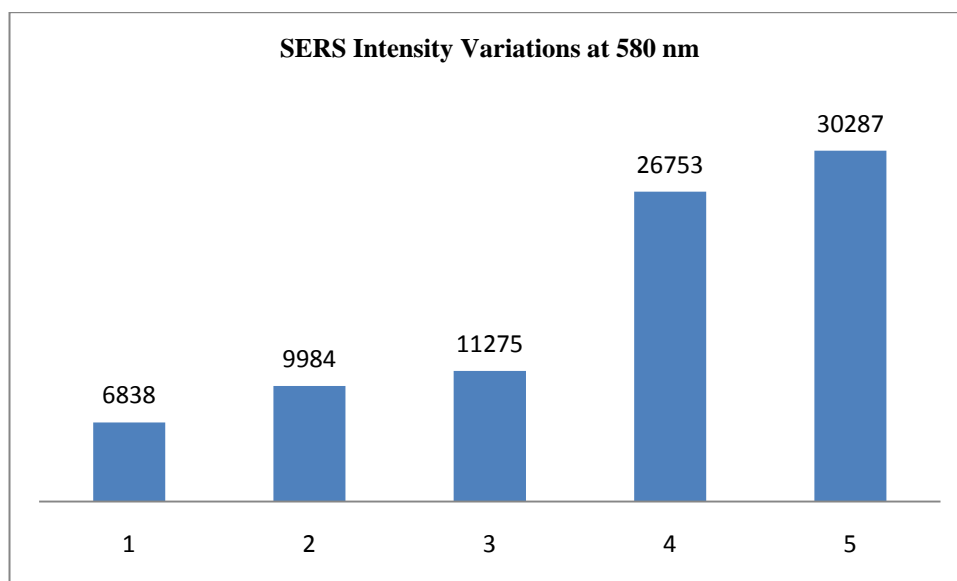
### 2. Figure 63



3. Figure 67

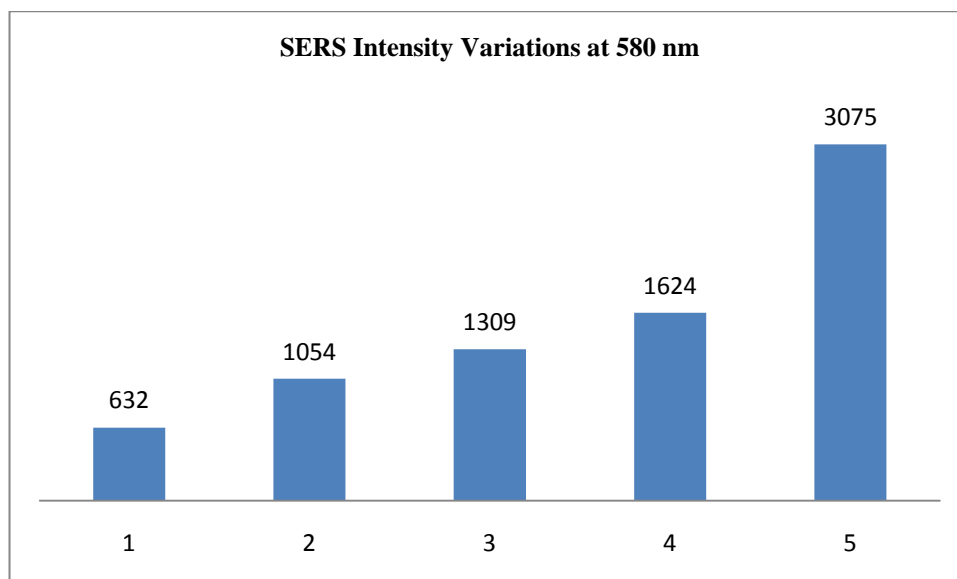


4. Figure 69

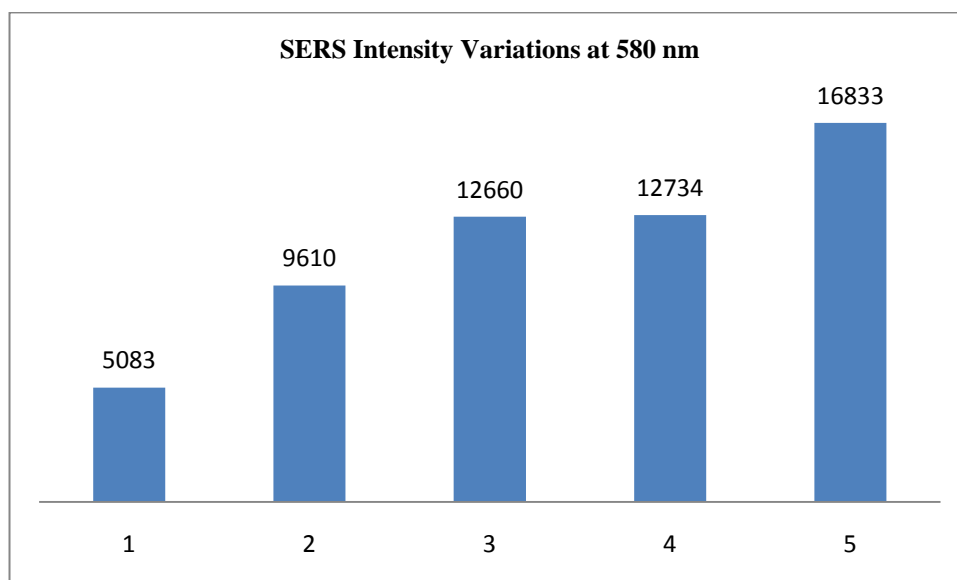




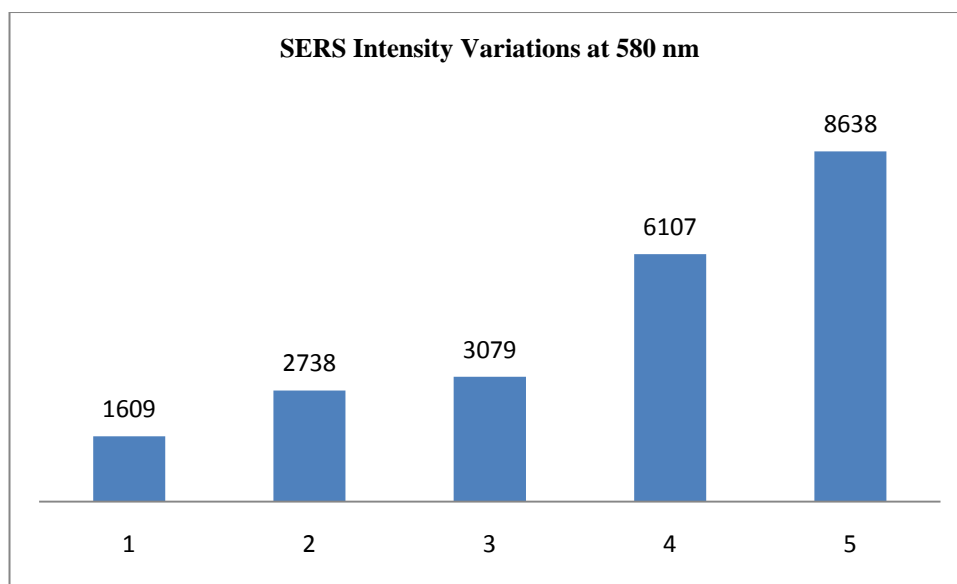
5. Figure 70



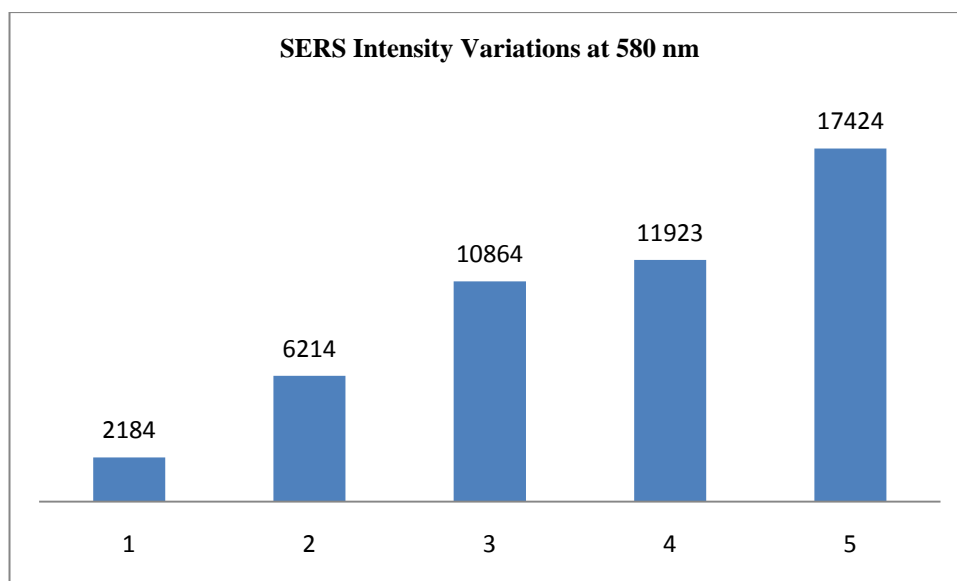
6. Figure 73



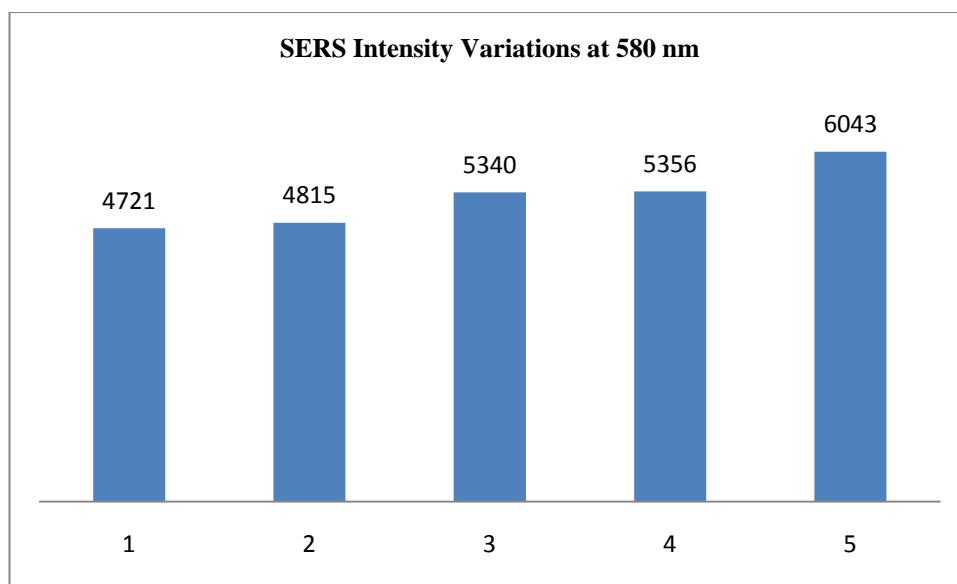
7. Figure 74



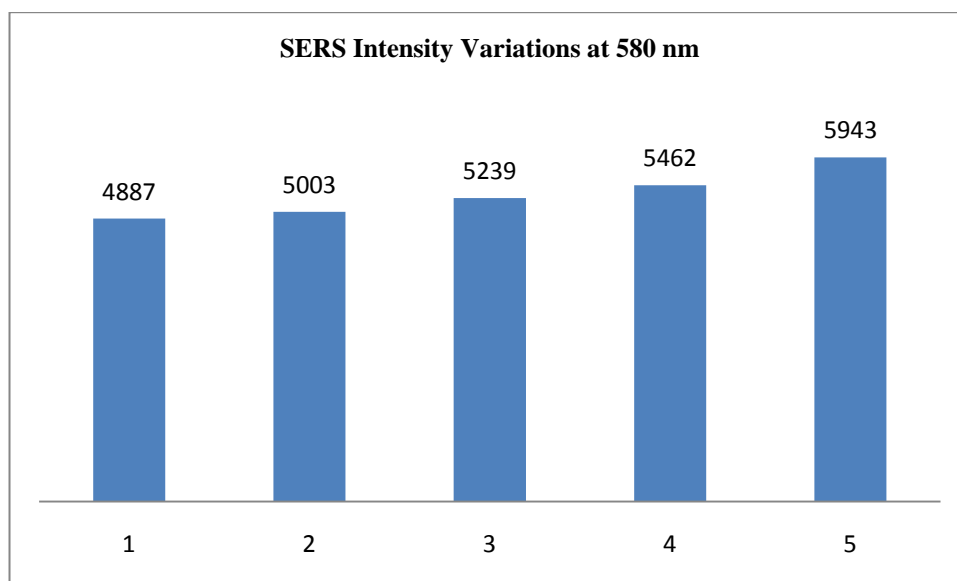
8. Figure 75



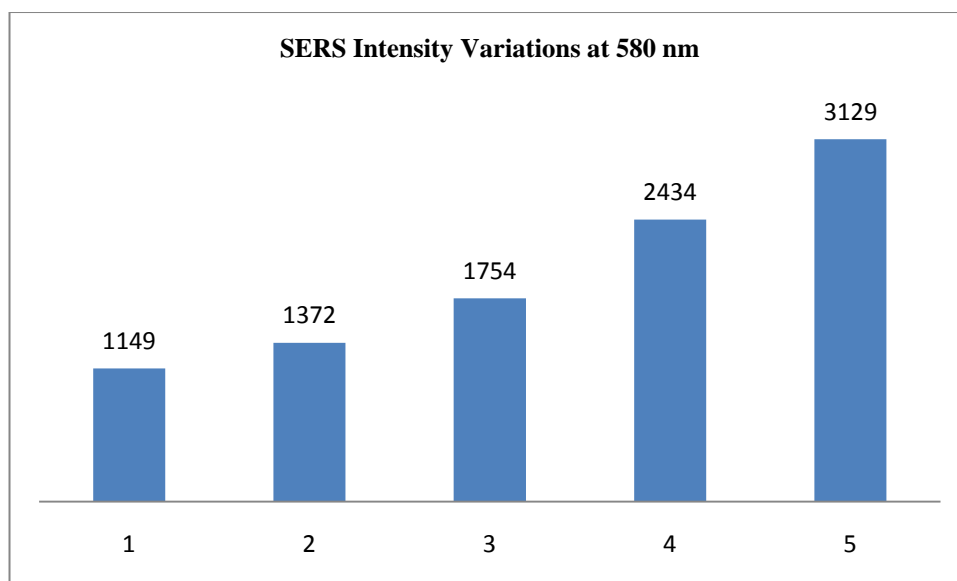
9. Figure 76



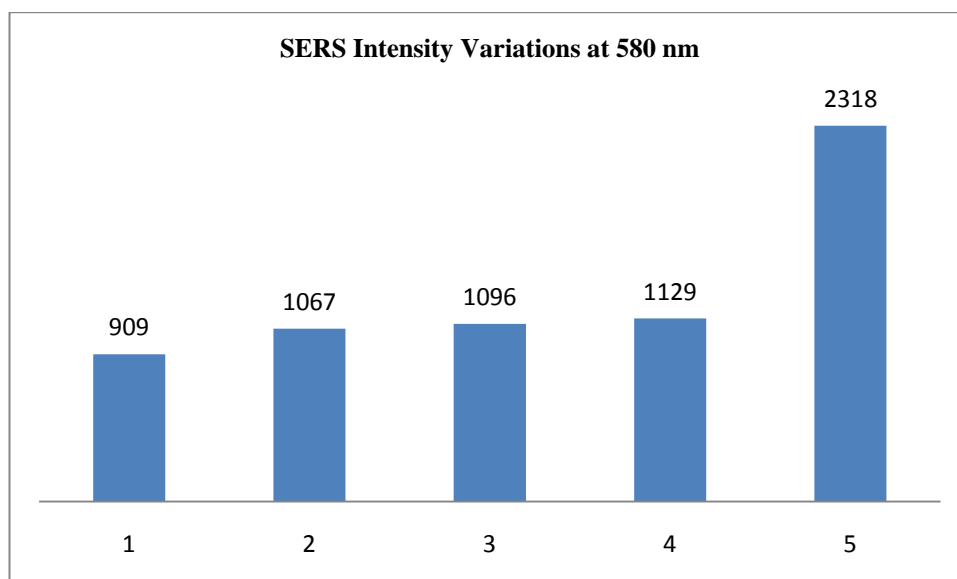
10. Figure 78



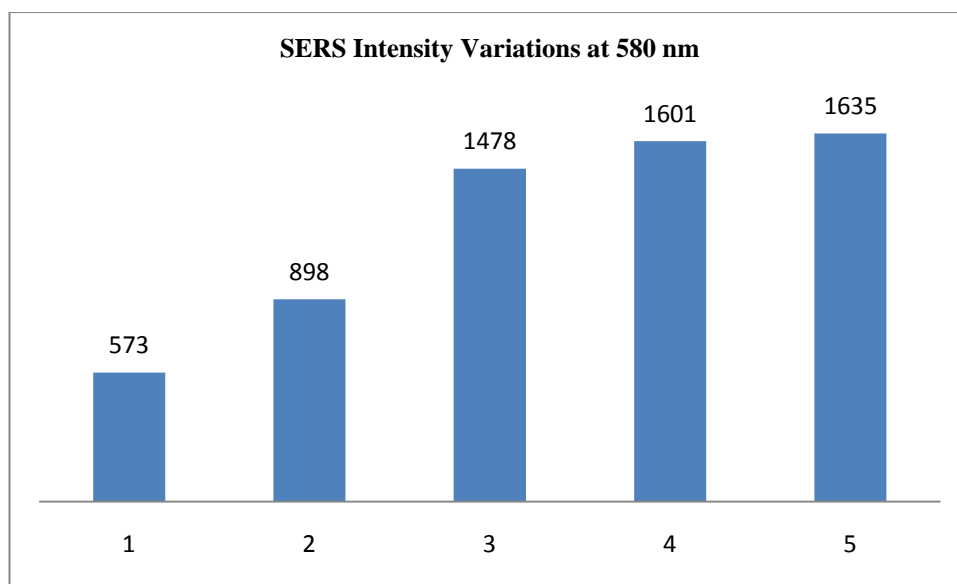
11. Figure 80 A



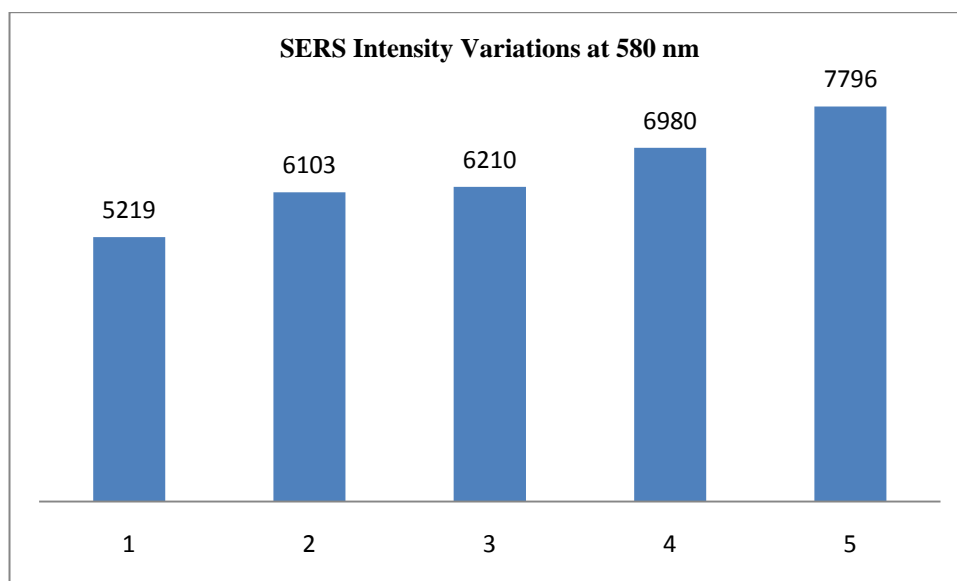
12. Figure 80 B



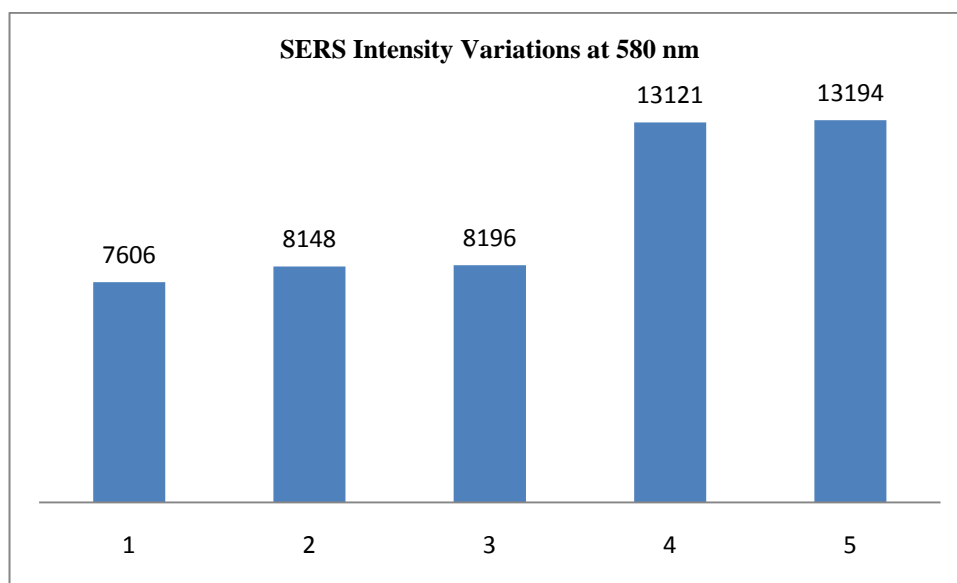
13. Figure 80 C



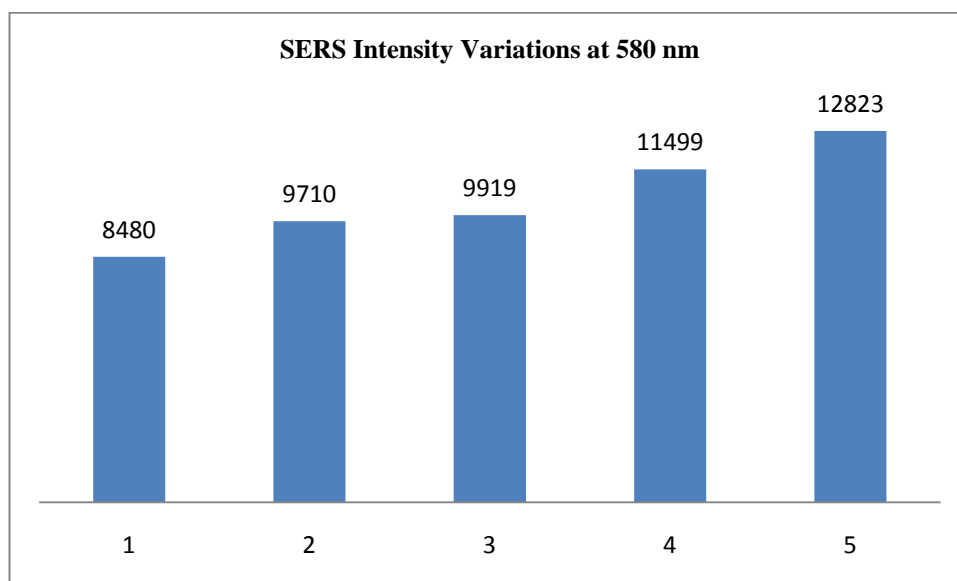
14. Figure 81



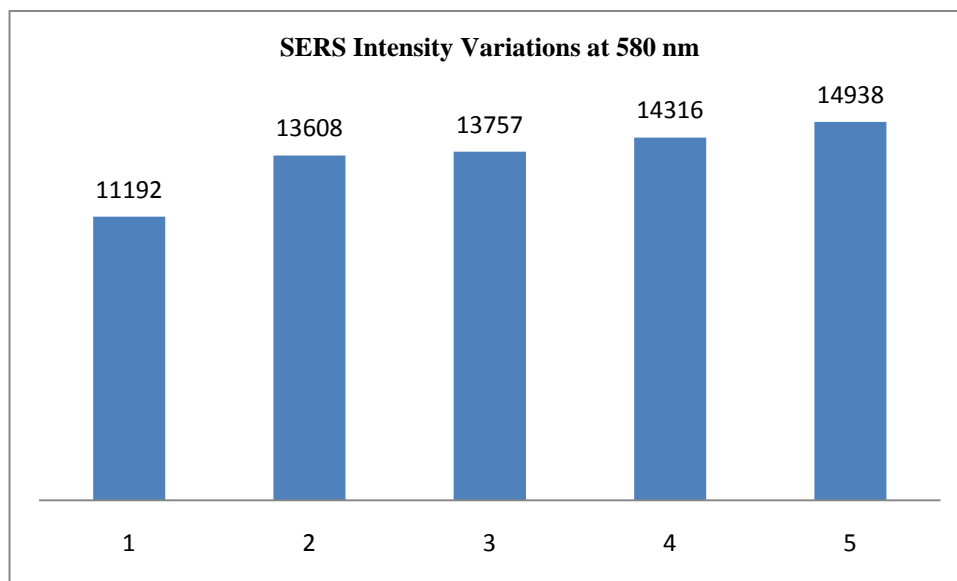
15. Figure 83 A



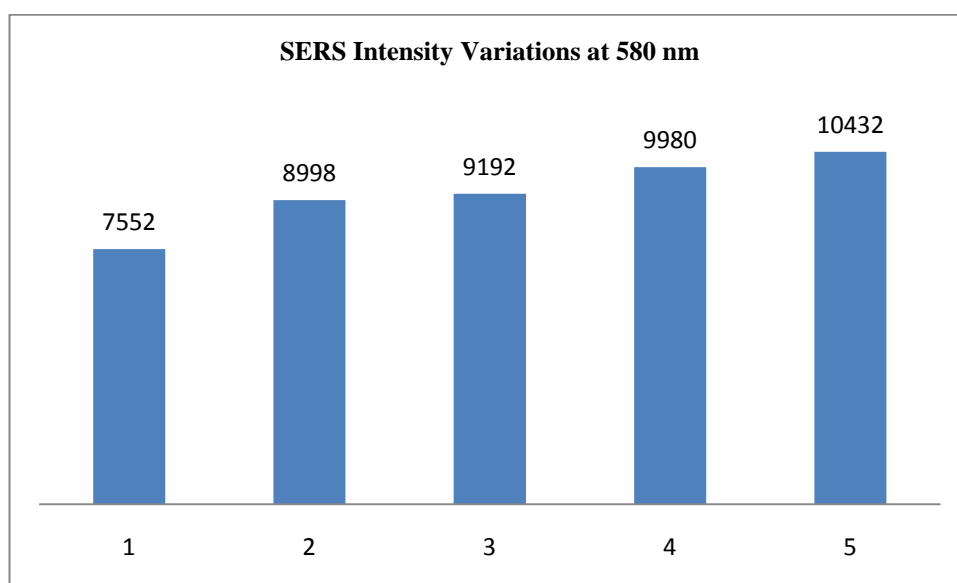
16. Figure 83 B



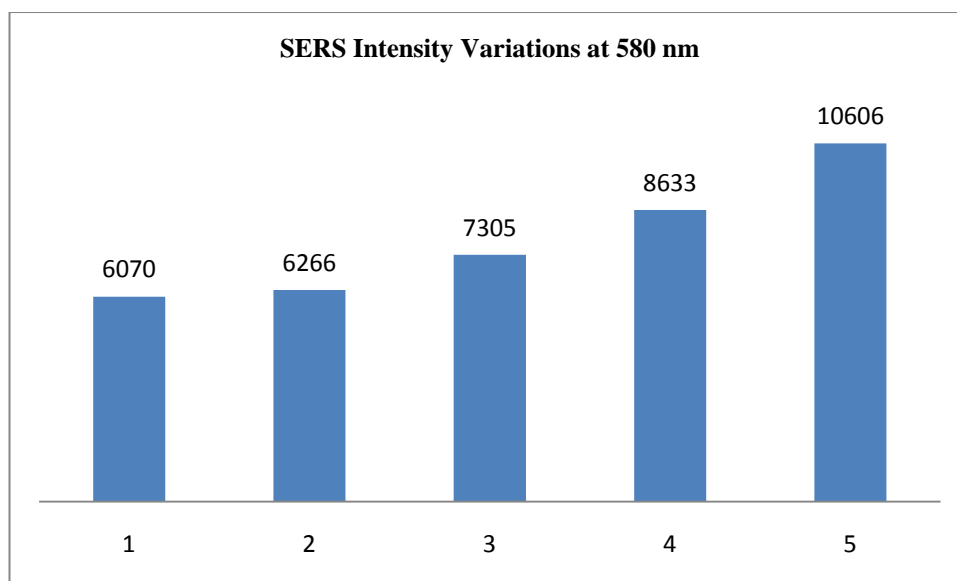
17. Figure 84 A



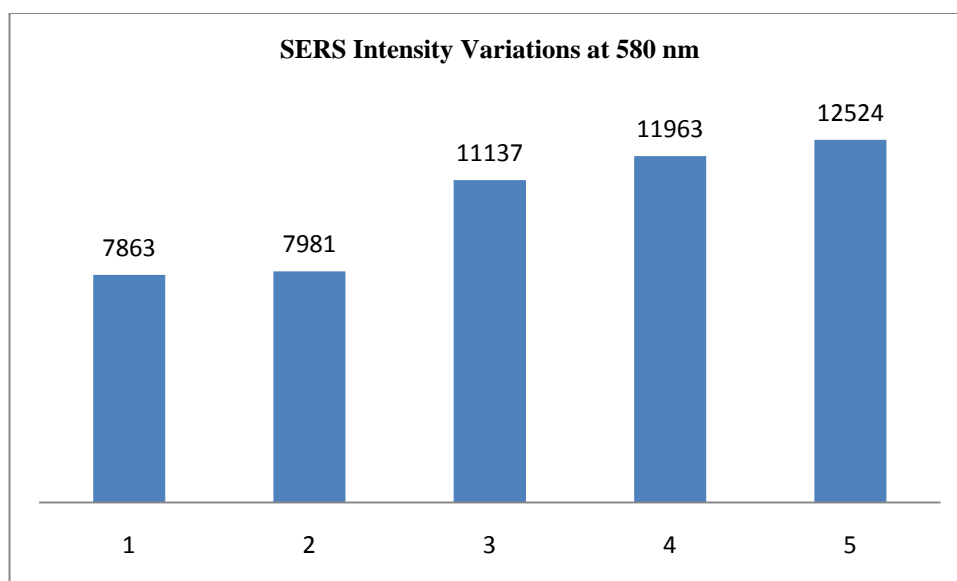
18. Figure 84 B



19. Figure 85

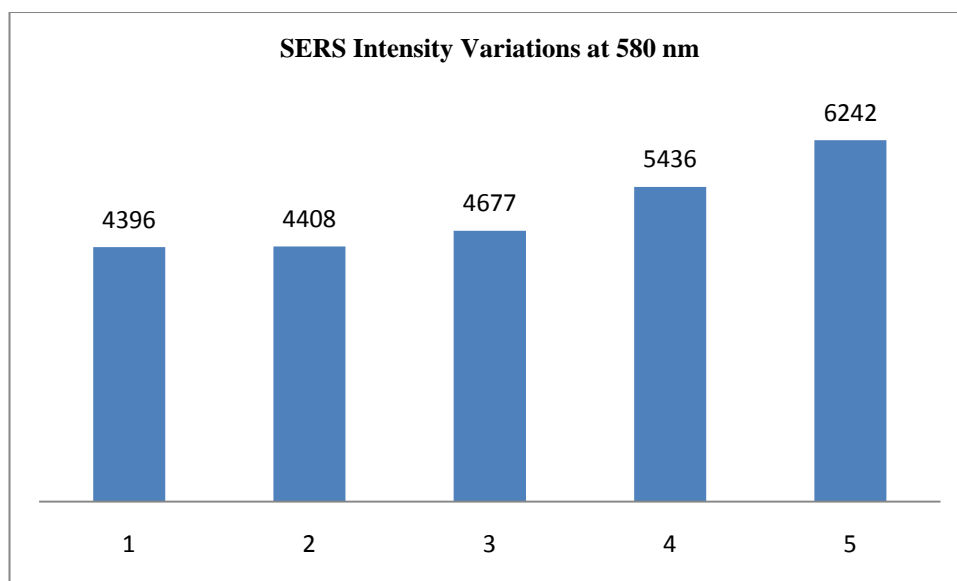


20. Figure 87 A

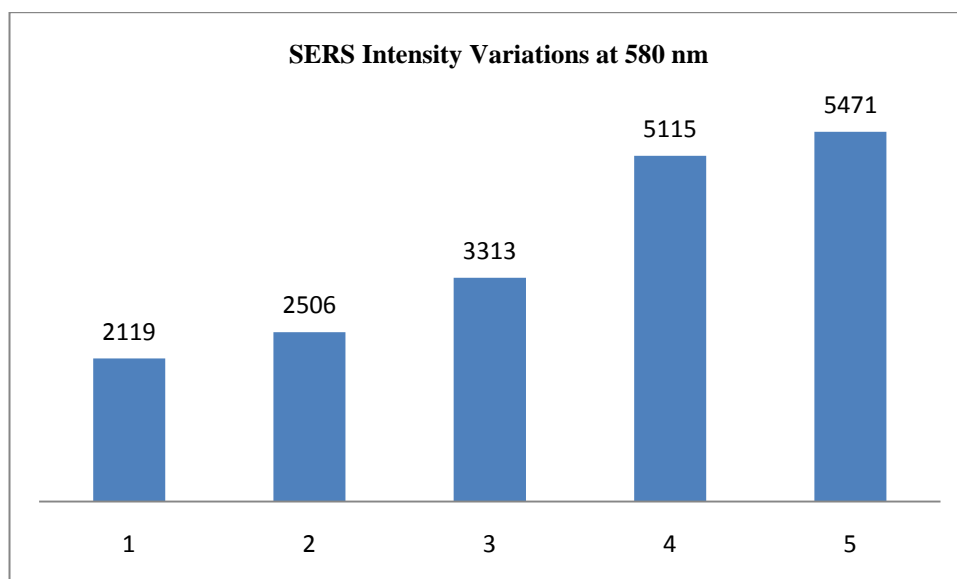




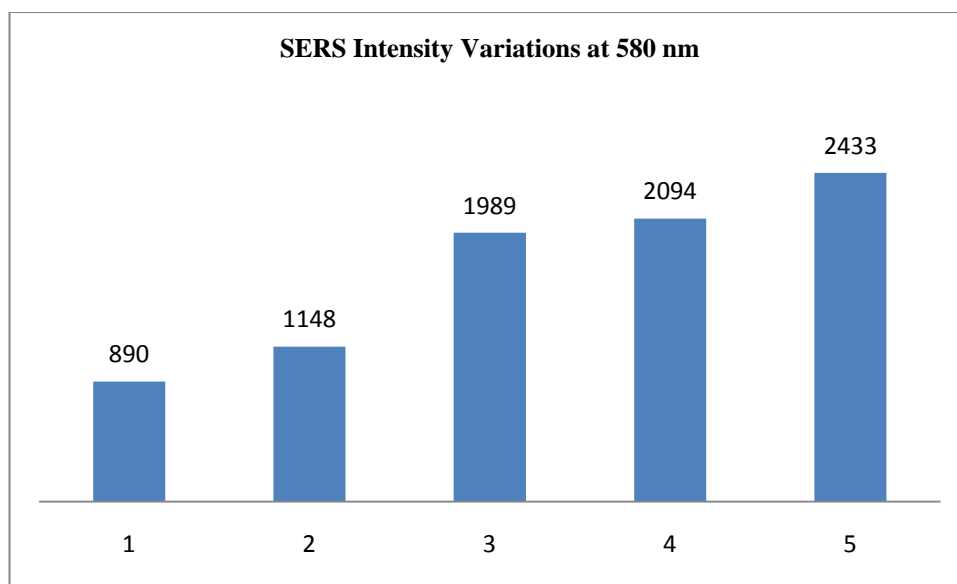
21. Figure 87 B



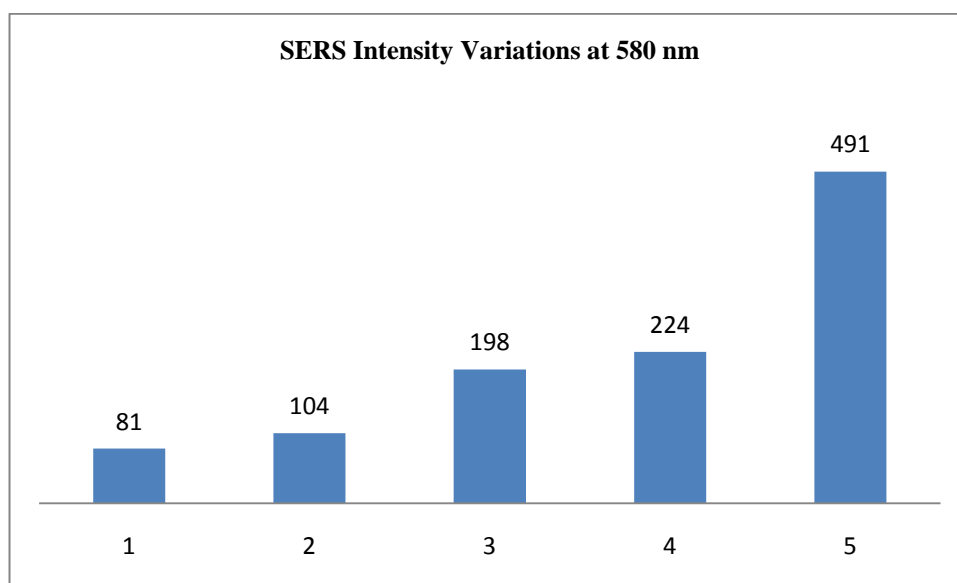
22. Figure 88 A



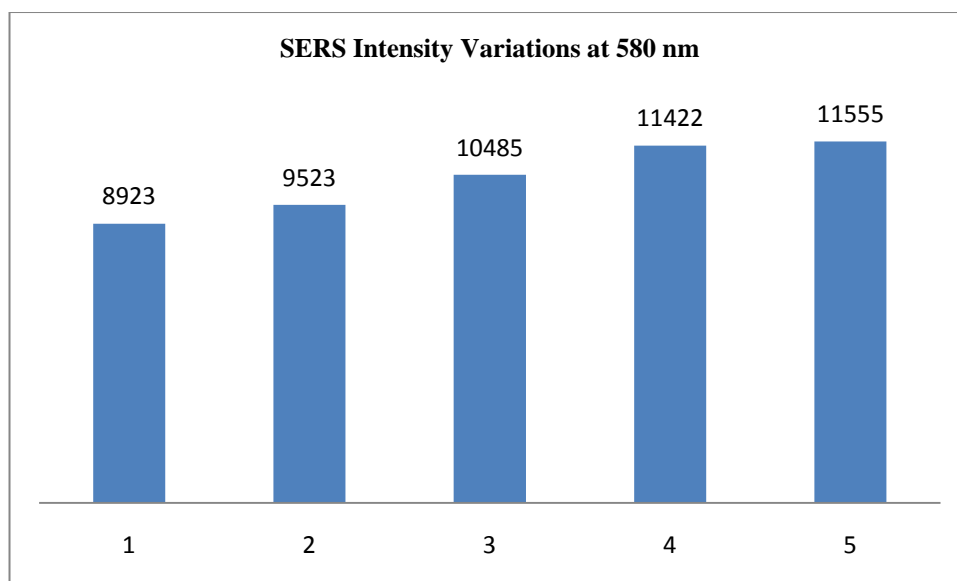
23. Figure 88 B



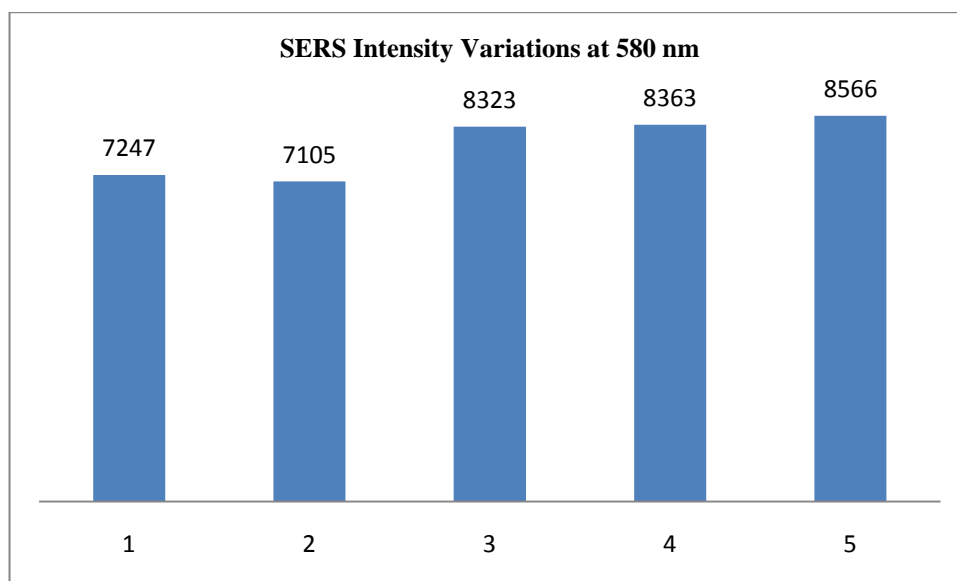
24. Figure 89



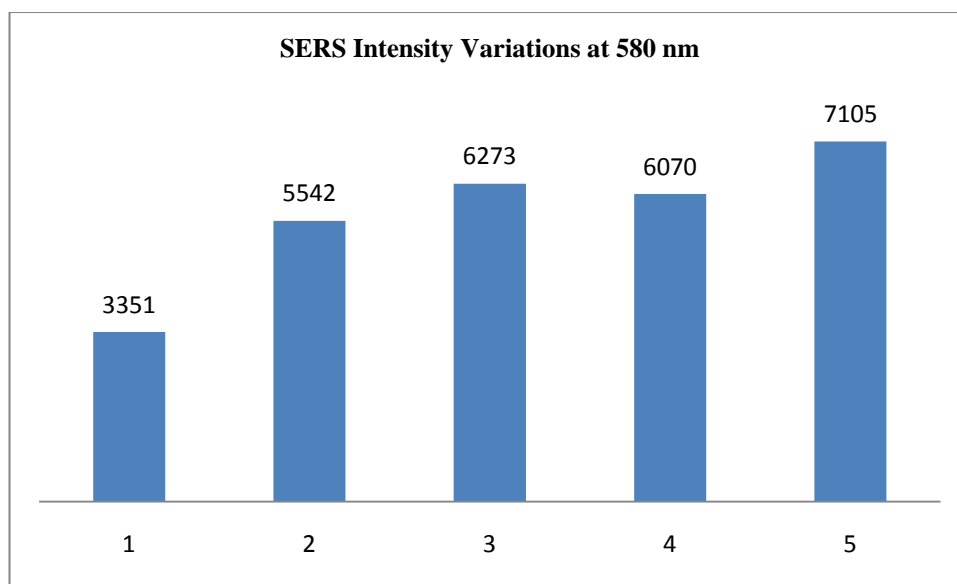
25. Figure 90 A



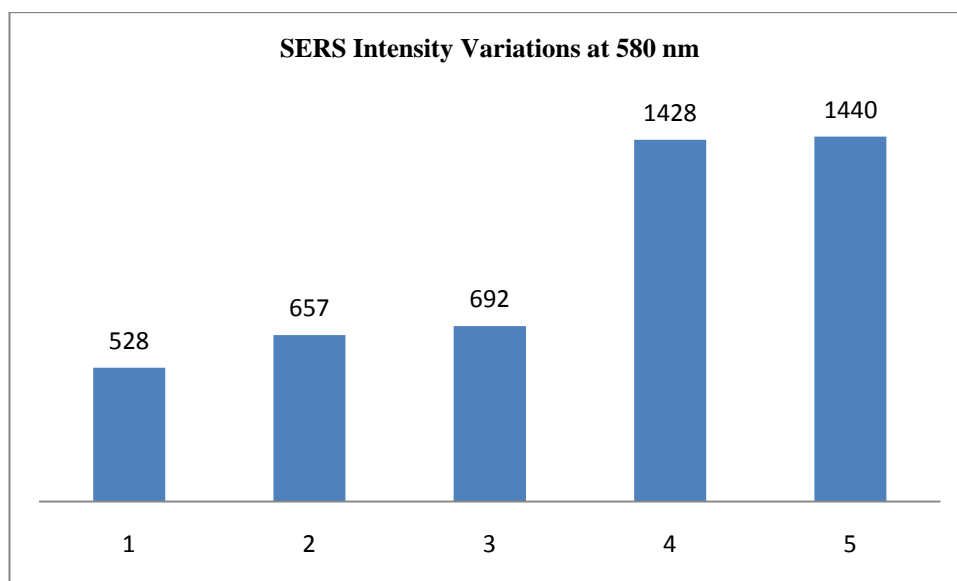
26. Figure 90 B



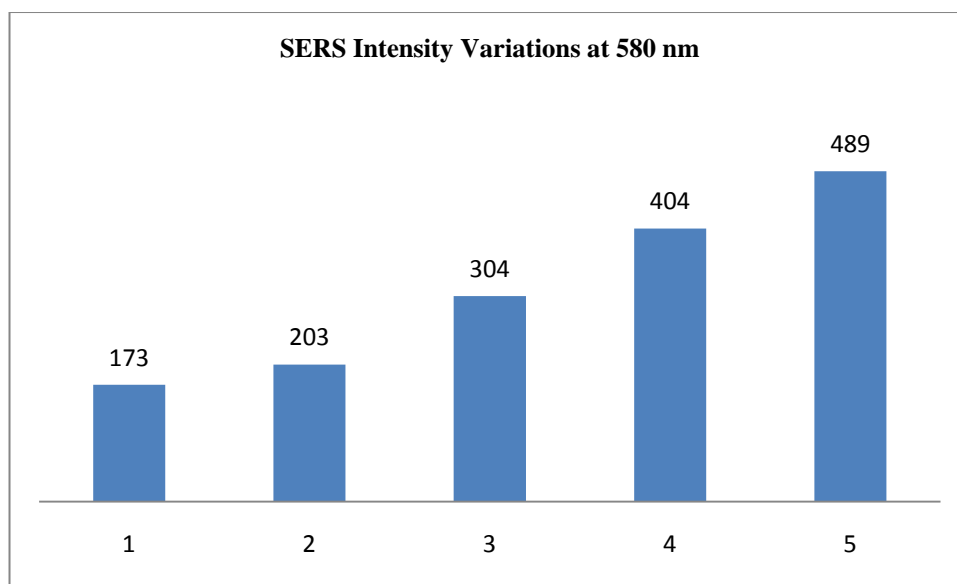
27. Figure 91 A



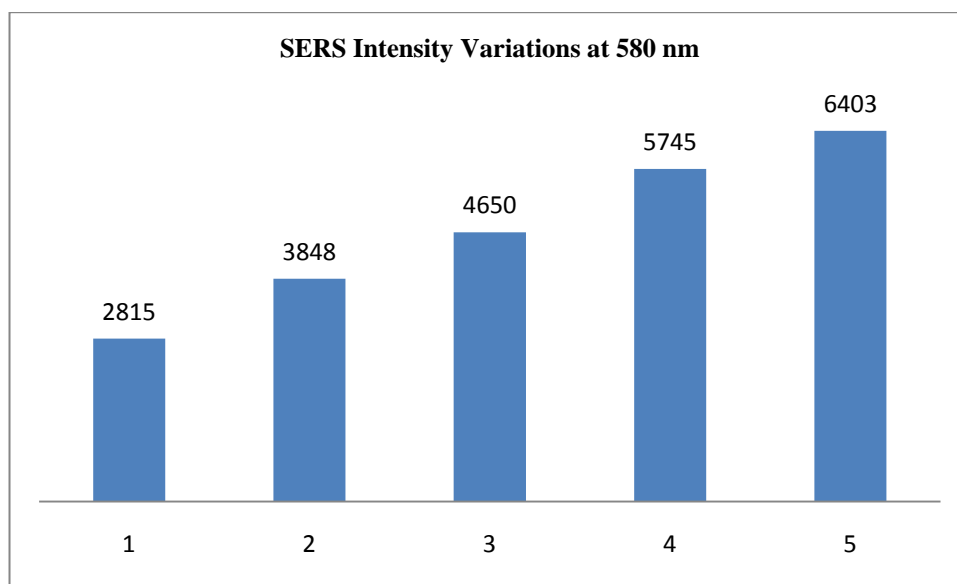
28. Figure 91 B



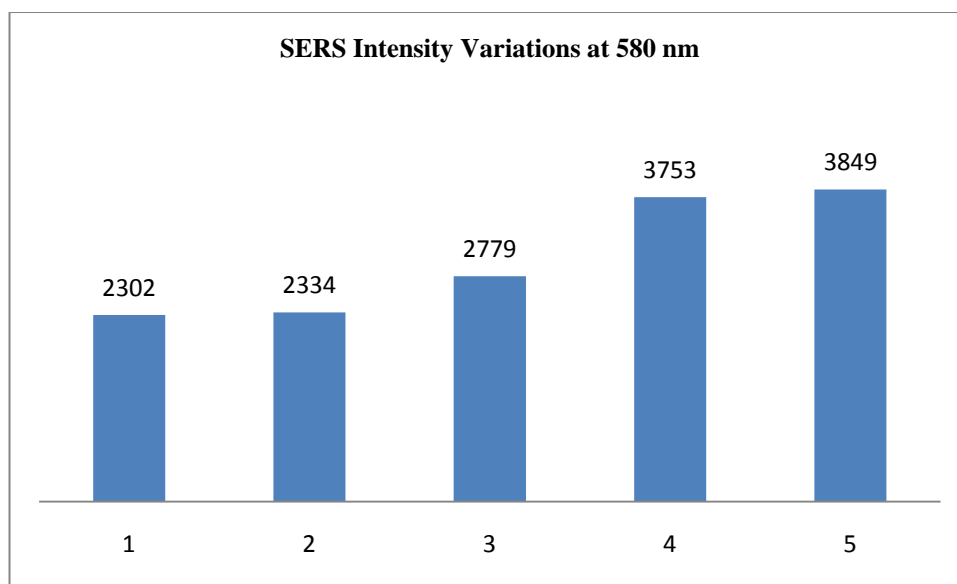
29. Figure 92



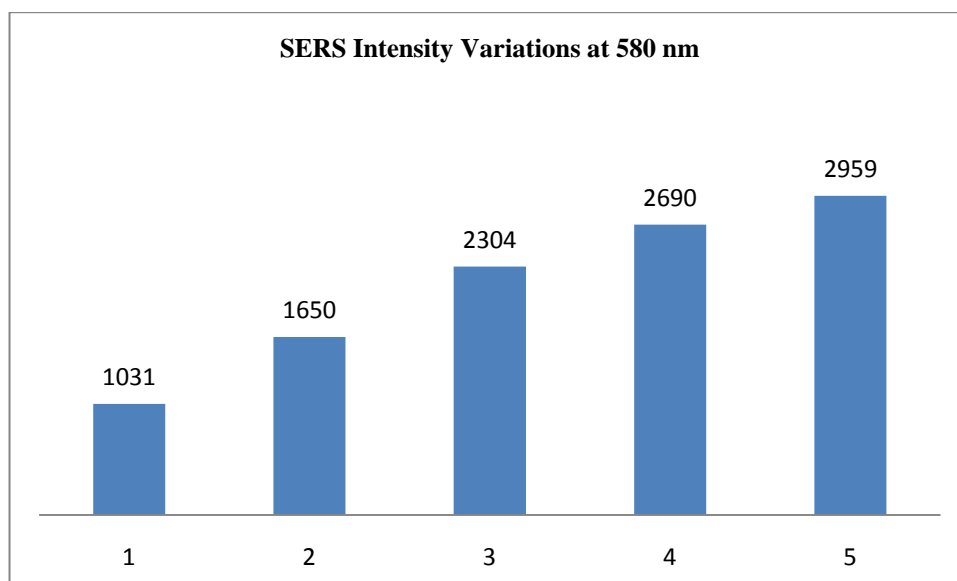
30. Figure 93 A



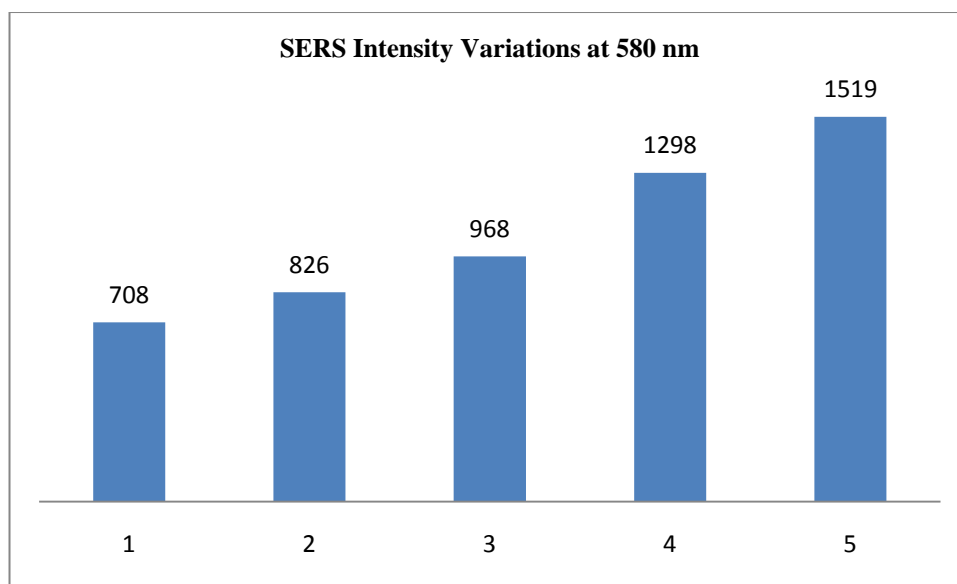
31. Figure 93 B



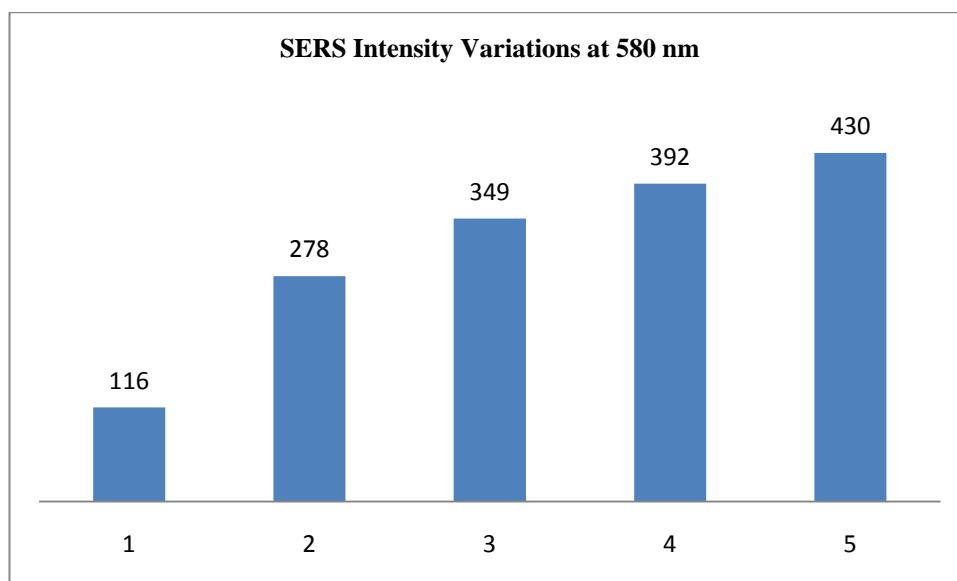
32. Figure 94 A



33. Figure 94 B



34. Figure 95



## VITA

### PERSONAL INFORMATION

Surname, Name: Karabıçak, Seher

Nationality: Turkish

Date and Place of Birth: 3 July 1980, Afyonkarahisar

Marial Status: Single

Phone: 90 3122103245

Fax: 90 3122103200

e-mail: [seherkarabicak@gmail.com](mailto:seherkarabicak@gmail.com)

### EDUCATION

Degree	Institution	Year of Graduation
MS	METU CHEMISTRY	2004
BS	ANADOLU UNIVERSITY	2000
High School	Süleyman Çakır High School, ESKİŞEHİR	1996

### WORK EXPERIENCE

Year	Place	Enrollment
2009-Present	MTA	Chemist
2006-2009	METU Department of Chemistry	Research Assistant

### FOREIGN LANGUAGES

English

### PUBLICATION

1. Karabıçak S., Kaya M., Vo-Dinh T. and Volkan M., "Silver Nanoparticle-Doped Polyvinyl Alcohol Coating as a Medium for Surface-enhanced Raman Scattering Analysis", Journal of Nanoscience and Nanotechnology, 8, 955 (2008)